Energy

SOLAR

DOE/CS/30569-30
(DE84010813)

PERFORMANCE EVALUATION OF AN ACTIVE SOLAR COOLING SYSTEM UTILIZING LOW COST PLASTIC COLLECTORS AND AN EVAPORATIVELY-COOLED ABSORPTION CHILLER

Final Report

By
George O. G. Lof
Mark A. Westhoff
Susumu Karaki

February 1984

Work Performed Under Contract No. AC03-81CS30569

Colorado State University
Solar Energy Applications Laboratory
Fort Collins, Colorado

Technical Information Center
Office of Scientific and Technical Information
United States Department of Energy

DISCLAIMER

DOE/CS/30569-30
(DE84010813)
Distribution Category UC-59a

PERFORMANCE EVALUATION OF AN ACTIVE SOLAR COOLING SYSTEM UTILIZING LOW COST PLASTIC COLLECTORS AND AN EVAPORATIVELY-COOLED ABSORPTION CHILLER

FINAL REPORT

PREPARED FOR THE

U.S. DEPARTMENT OF ENERGY

CONSERVATION AND SOLAR APPLICATIONS

PREPARED BY

GEORGE O.G. LOF
MARK A. WESTHOFF
SUSUMU KARAKI

SOLAR ENERGY APPLICATIONS LABORATORY

COLORADO STATE UNIVERSITY

FORT COLLINS, COLORADO 80523

FEBRUARY 1984

TABLE OF CONTENTS

LIST OF FIGURES

LIST OF TABLES

EXECUTIVE SUMMARY

INTRODUCTION

During the summer of 1982, air conditioning in Solar House III at Colorado State University was provided by an evaporatively-cooled absorption chiller. The single-effect lithium bromide chiller provided by Arkla Industries is an experimental three-ton unit from which heat is rejected by direct evaporative cooling of the condenser and absorber walls, thereby eliminating the need for a separate cooling tower. Domestic hot water was also provided by use of a double-walled heat exchanger and 300-ℓ (80-gal) hot water tank. A schematic of the system appears in Figure 1.

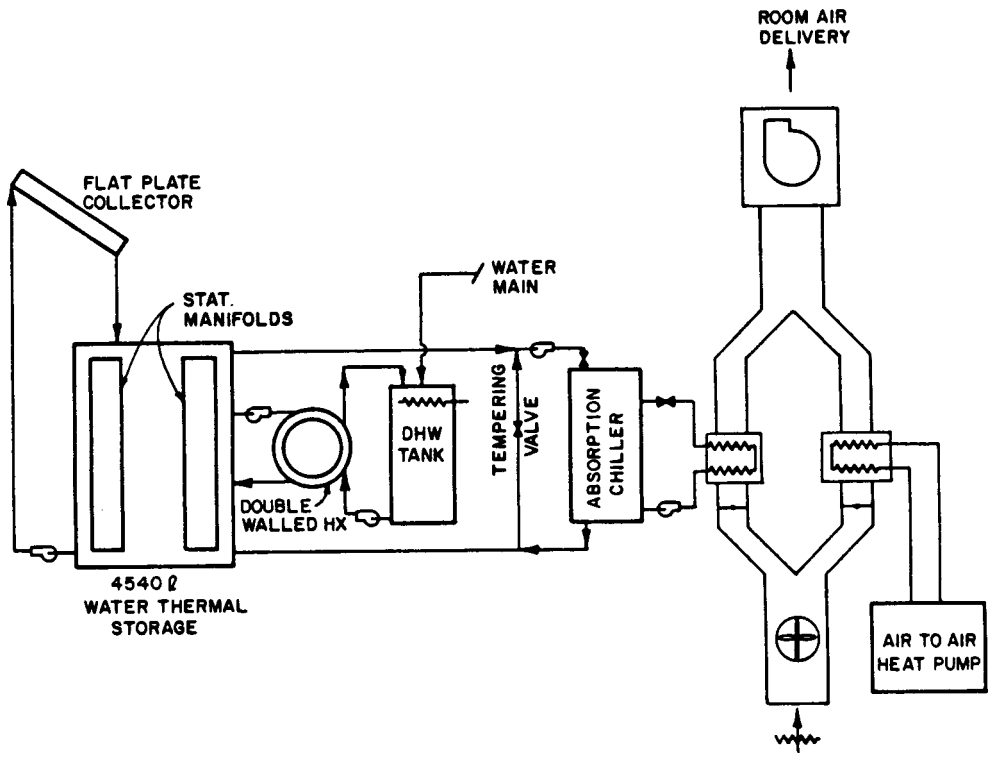

Figure 1. System schematic.

For solar heat supply to the cooling system, plastic thin film collectors developed by Brookhaven National Laboratory were installed on the roof of Solar House III. Failure to withstand stagnation temperatures forced replacement of solar energy with an electric heat source.

Objectives of the project were: (1) evaluation of system performance over the course of one cooling season in Fort Collins, Colorado; (2) optimization of system operation and control; (3) development of a TRNSYS compatible model of the chiller; and (4) determination of cooling system performance in several U.S. climates by use of the model.

RESULTS

Collector

The laminated thin film collector contains a selectively coated aluminum foil absorber, the back of which is adhesively bonded to a "Teflon" FEP film which forms passages down through which water flows. The collector is covered with a "Tedlar" PVF film window stressed across a roll-formed aluminum frame. Foil-backed rigid isocyanurate foam and a glass fiber batt provide thermal insulation.

Although the collectors were easily and rapidly erected on the roof, delamination of the absorber assembly occurred after being subjected to stagnation temperatures for two days. Since replacement collectors could not be obtained for the 1982 cooling season, the system was modified as shown in Figure 2. In place of solar collectors, an electric resistance boiler provided hot water to a thermal storage tank. Hot water from storage was supplied to the chiller.

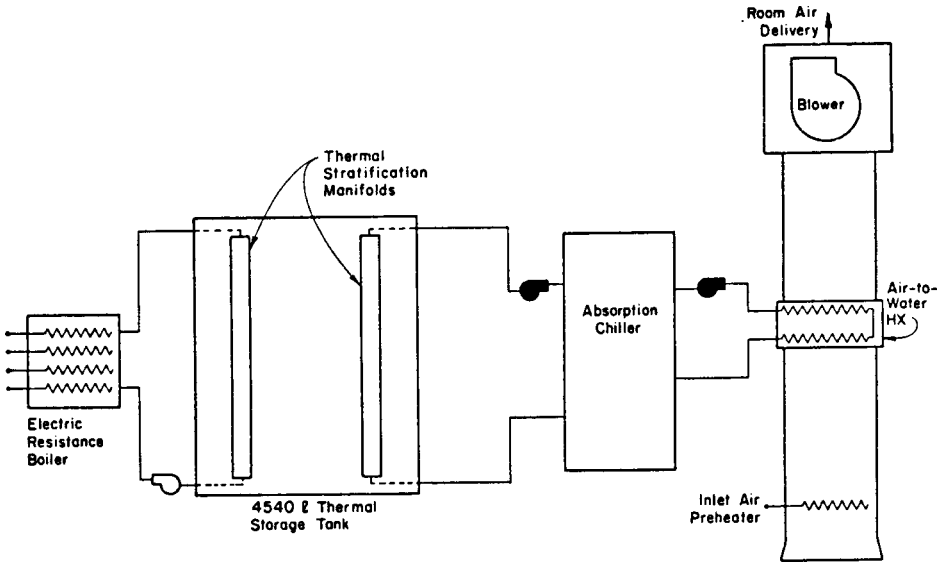

Figure 2. Schematic of modified system.

Chiller

The chiller was operated for 475 hours under a variety of operating conditions. By use of data obtained under quasi-steady-state operating conditions, chiller performance was correlated with hot water supply temperature, flow rate, and ambient outdoor wet bulb temperature. These performance maps are shown in Figures 3, 4, and 5.

Transient performance of the chiller was investigated only to a limited extent. Steady-state capacities are reached in approximately 24 minutes as shown in Figure 6. By allowing the chiller to operate for four minutes after the thermostat is satisfied and hot water supply is discontinued, refrigerant in transit between condenser and evaporator is utilized. The coefficient of performance during the start-up and shut-down periods is approximately 90 percent of steady-state levels.

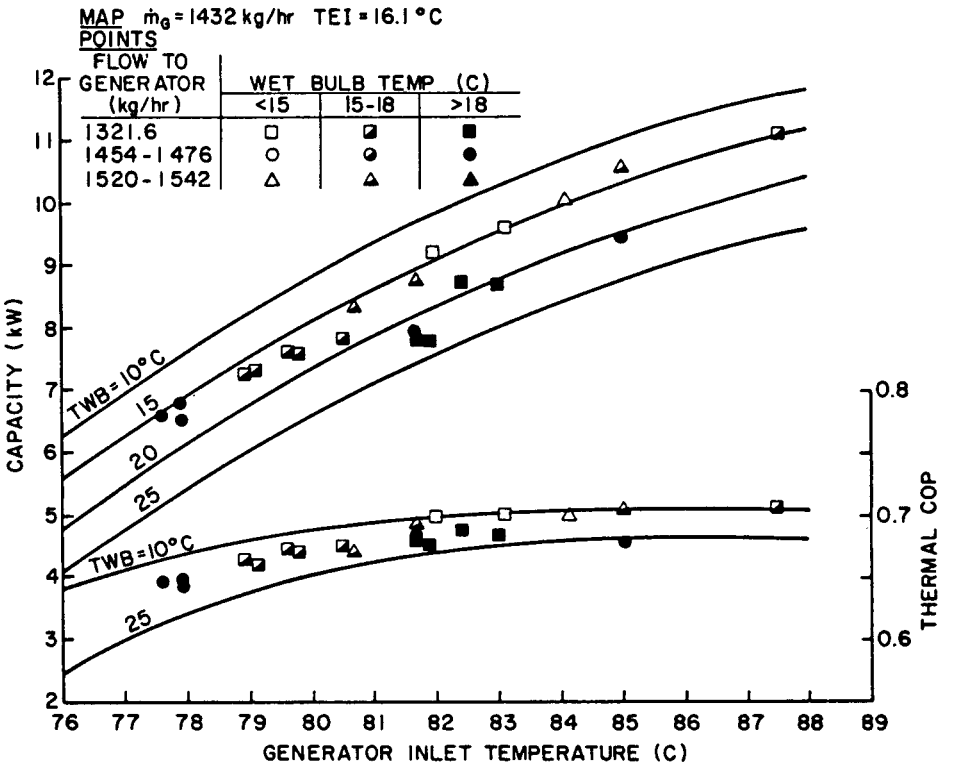

Figure 3. Performance map of Arkla XWF-3600 #7-2 evaporatively-cooled absorption chiller ($\dot{m}_g$ = 1432 kg/hr = 6.5 gpm).

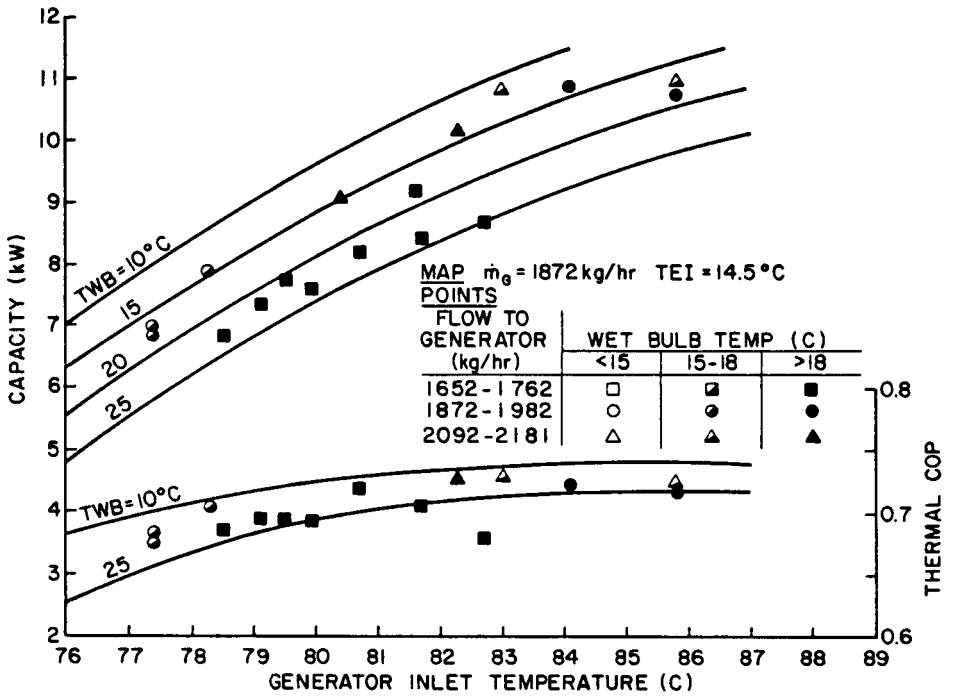

Figure 4. Performance map of Arkla XWF-3600 #7-2 evaporatively-cooled absorption chiller ($\dot{m}_g$ = 1872 kg/hr = 8.5 gpm).

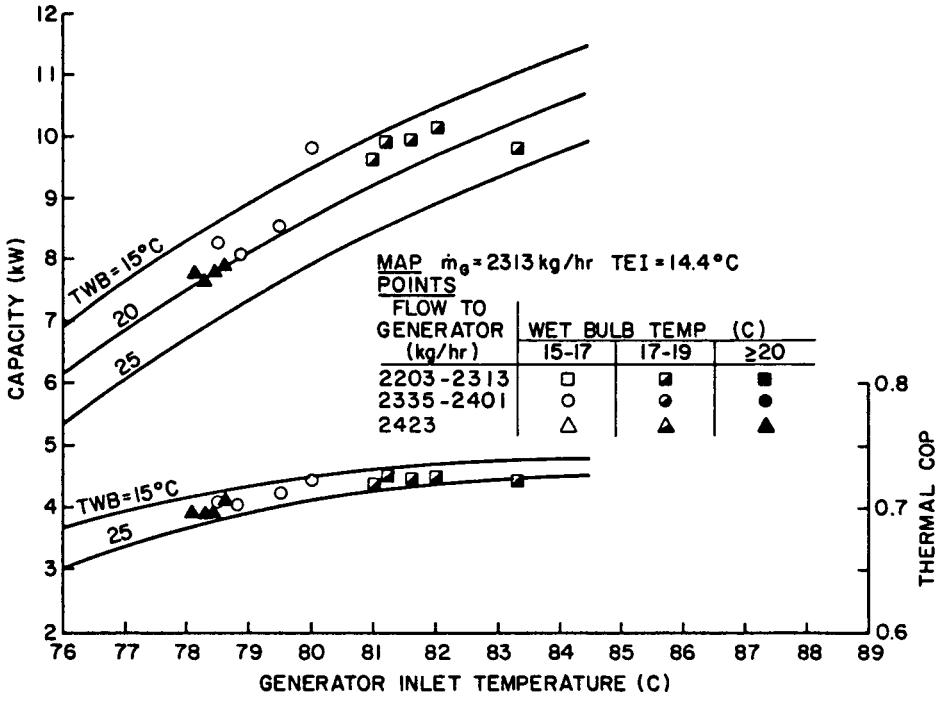

Figure 5. Performance map of Arkla XWF-3600 #7-2 evaporatively-cooled absorption chiller ($\dot{m}_g$ = 2313 kg/hr = 10.5 gpm).

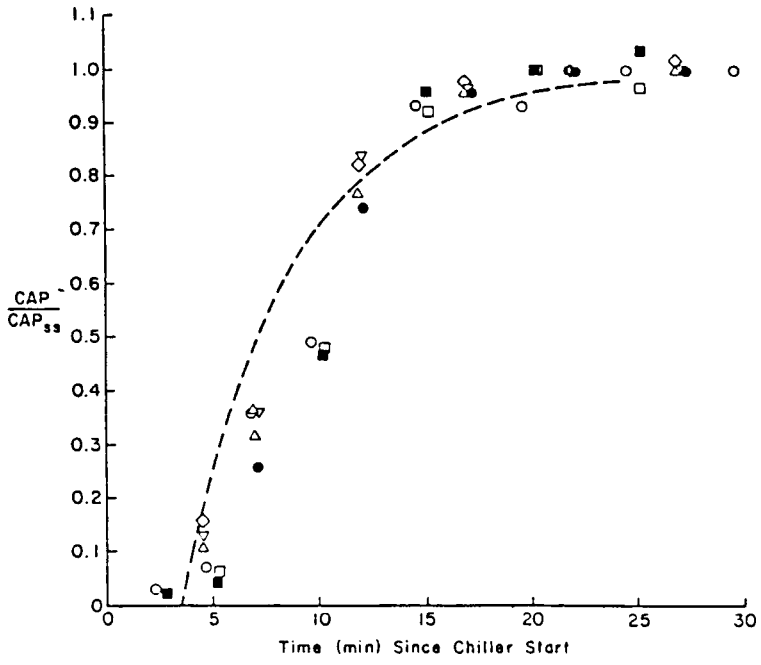

Figure 6. Transient performance of chiller at start-up.

Computer Model

A TRNSYS compatible computer model of the chiller was developed from relationships for both quasi-steady-state and transient operation. The simulated results compared favorably with steady-state measurements. Insufficient data prevented verification of transient performance modeling. Simulations of a system in which the evaporatively-cooled chiller was supplied with solar-heated water were run for Phoenix, AZ, Denver, CO, Washington, DC, and Miami, FL.

CONCLUSIONS

Collector

The BNL thin film plastic collectors could not withstand the high temperatures reached under stagnation conditions. Additional research in materials and fabrication methods is required to develop further the type of collector designed by BNL.

Chiller

With respect to the Arkla XWF-3600 #7-2 absorption chiller, it can be concluded that:

1. Capacities in excess of 10.55 kW (3-ton) can be achieved at hot water supply temperatures of 75 to 90 C, compatible with flat plate collectors of good performance characteristics ($F_R\tau\alpha \geq 0.7$ and $F_RU_L \leq 4.0$ W/m^{2}C).

2. The capacity of the chiller is affected by, in order of importance, hot water temperature, hot water flow rate, and ambient outdoor wet bulb temperature. Performance maps of capacity and energy into the

generator have been developed for the following ranges of operating conditions:

hot water supply temperature : 76-90 C [169-194 F]

hot water flow rate : 880-2420 kg/hr [4-11gpm]

ambient outdoor wet bulb temperature: 12-22 C [54-72 F]

3. The coefficient of performance (COP) was generally above 0.7 (but rarely over 0.75) at hot water temperatures above 80 C. The major effect of increasing hot water temperatures is an increase in capacity.

4. The degrading effect of start-up transients on the overall thermal COP have largely been mitigated by spin-down operation (allowing the unit to continue running for four minutes after hot water flow to the generator has stopped). Average COP during spin-up and spin-down periods is approximately 90 percent of the steady-state value.

5. A TRNSYS-compatible chiller model has been shown to agree well with measured data. The model incorporates steady-state performance relations as well as start-up, shut-down, and heat-rejection fan cycling transients.

6. Simulation results show that on hot sunny days in four types of summer climates (including Phoenix), a good quality 56 m^2 plate collector and the XWF-3600 chiller can provide 2 to 3 tons of cooling for 6 to 9 hours and maintain room temperature below 25 C (27 in Phoenix) in the typical house used in the analysis.

7. Simulation computations show a maximum daily cooling delivery of 412 MJ (32 ton-hours), in Phoenix, representing 27 percent of incident solar radiation (overall conversion of solar energy to cooling), at ambient temperatures reaching 41.5 C (107 F) in mid-afternoon.

PERFORMANCE EVALUATION OF AN ACTIVE SOLAR COOLING SYSTEM UTILIZING LOW COST PLASTIC COLLECTORS AND AN EVAPORATIVELY-COOLED ABSORPTION CHILLER

1.0 INTRODUCTION

1.1 Objectives of the Project

1. Obtain operational data for an array of low-cost plastic collectors developed at the Brookhaven National Laboratory (BNL).

2. Determine the seasonal performance of the three-ton Arkla XWF-3600 evaporatively-cooled lithium bromide absorption chiller in a solar cooling system.

3. Develop a TRNSYS compatible model of the chiller.

4. Evaluate overall system performance.

1.2 Description of the Environment

1.2.1 Location

The Solar Energy Applications Laboratory (SEAL) at Colorado State University is located 6.4 km west of the center of Fort Collins, Colorado at latitude 40.6 N, longitude 105.1, and elevation 1585 m above sea level. Five solar heated and cooled structures are situated on the south slope of a hill approximately 60 m above the city of Fort Collins. The terrain to the east is generally flat, and the foothills of the Rocky Mountains begin approximately 1 km to the west.

1.2.2 Climate

Moderate temperatures, generally clear air, low humidity, light precipitation, and light winds interrupted occasionally by strong north

westerly winds characterize the climate. The cooling season extends from June through September. Average monthly maximum temperature during this period varies from 24 C in September to 30 C in July. Afternoon thunderstorms occur frequently in the summer but precipitation is generally light.

The average daily solar radiation on a horizontal surface ranges from 24.6 MJ/m^2-day in June to 17.4 MJ/m^2-day in September. Monthly average daily solar radiation on a horizontal surface and on a south-facing surface tilted at 45 degrees is shown in Figure 1-1. Cooling requirements are moderate, as shown in Figure 1-2, averaging a total of 240 C-days in four summer months [1].

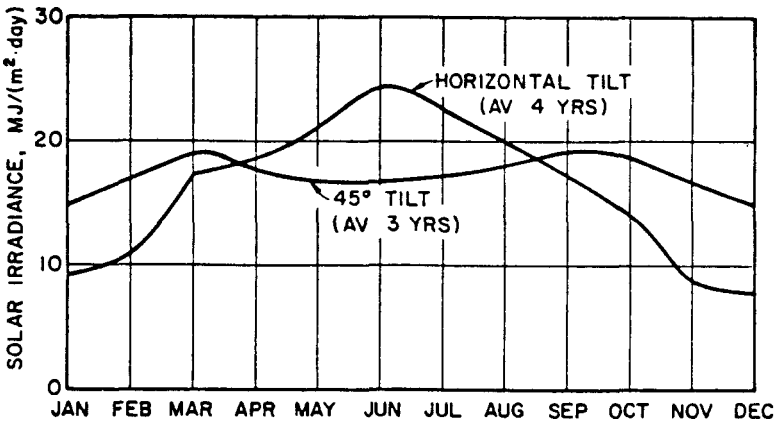

Figure 1-1. Monthly average daily solar radiation on horizontal and 45 degree tilted surfaces in Fort Collins, Colorado.

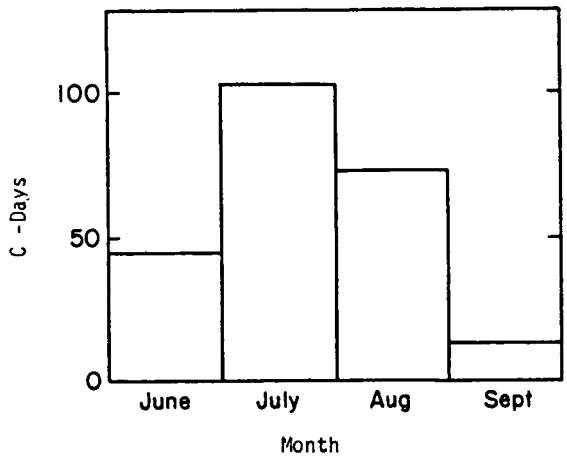

Figure 1-2. Average monthly C-days of cooling in Fort Collins, Colorado.

Average daily maximum wet bulb temperatures range from 21 C in August to 12.7 C in September, and the seasonal average minimum wet bulb temperature is 11 C. Relatively low humidities result in a latent cooling load about 20 percent of the total.

2.0 DESCRIPTION OF THE BUILDING AND SYSTEM

2.1 The Building

2.1.1 General Description

Solar House III is a residential-size building located in the Solar Village at the Foothills Research Campus of Colorado State University, Fort Collins, Colorado. The building size is appropriate for a three-bedroom house, although the rooms are used as offices for the staff of the Atmospheric Science Department. There are two levels in the building, each with about 128.5 m^2 (gross) floor area. The mechanical equipment for the solar system, other than the collectors, is located in the basement, which has a walk-out arrangement as shown in the photograph of Figure 2-1.

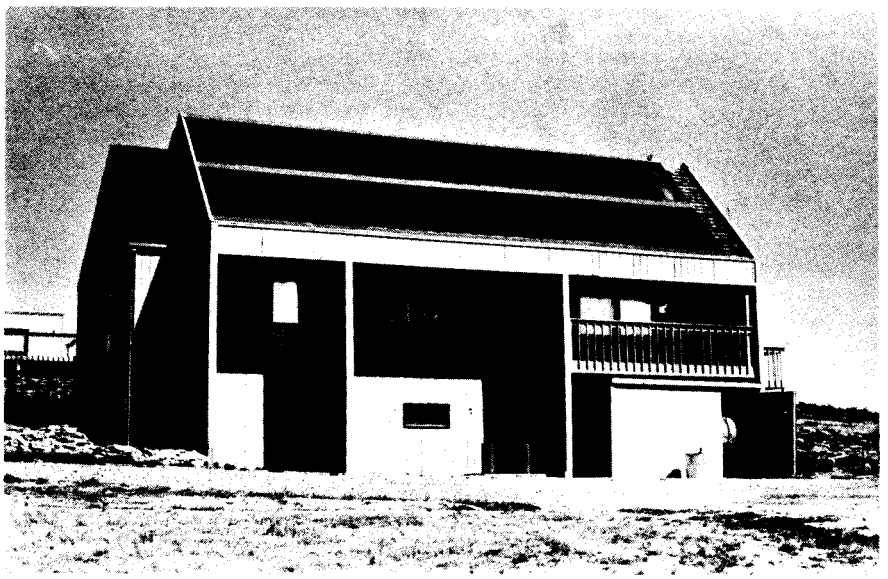

Figure 2-1. Solar House III.

2.1.2 Plans, Elevations and Cross-Sections

The first floor and basement floor plans are shown in Figures 2-2 and 2-3; elevation views, as well as a cross-section of the building, are shown in Figures 2-4 through 2-6. The attached room on the northeast corner of the building was originally designed to be an unheated garage, but it has been converted to graduate student offices. The room is not heated or cooled with the solar system.

The collectors are placed on the roof and face due south. As seen in Figure 2-6, there is a second, weather-proof roof underlying the collector mounting surface, which is a special feature of this experimental building to permit periodic replacement of collectors with no risk of roof leakage. There is an overhang of 1.83 m at the eave, and the roof is supported by vertical walls which serve both as structural members and shading for the windows on the south wall.

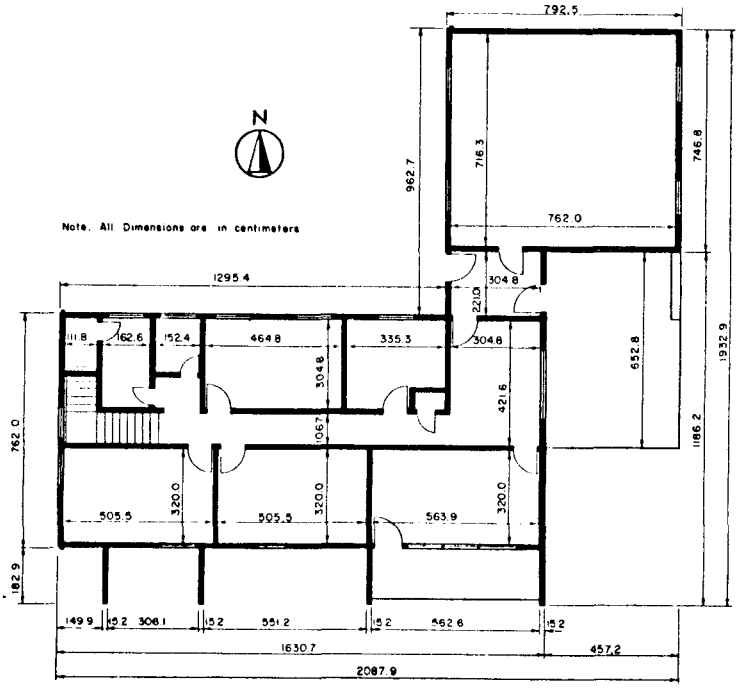

Figure 2-2. First floor plan of Solar House III.

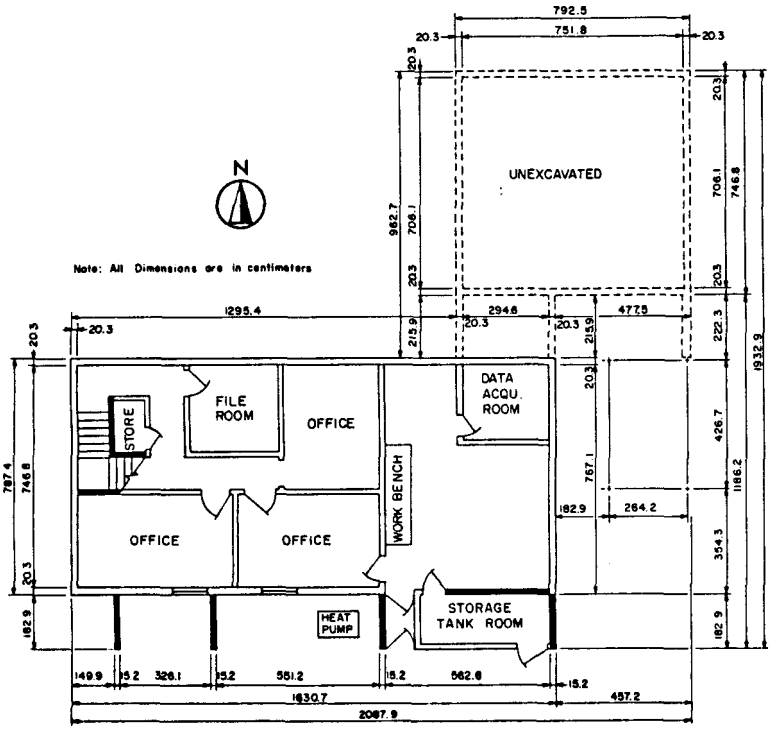

Figure 2-3. Basement floor plan of Solar House III.

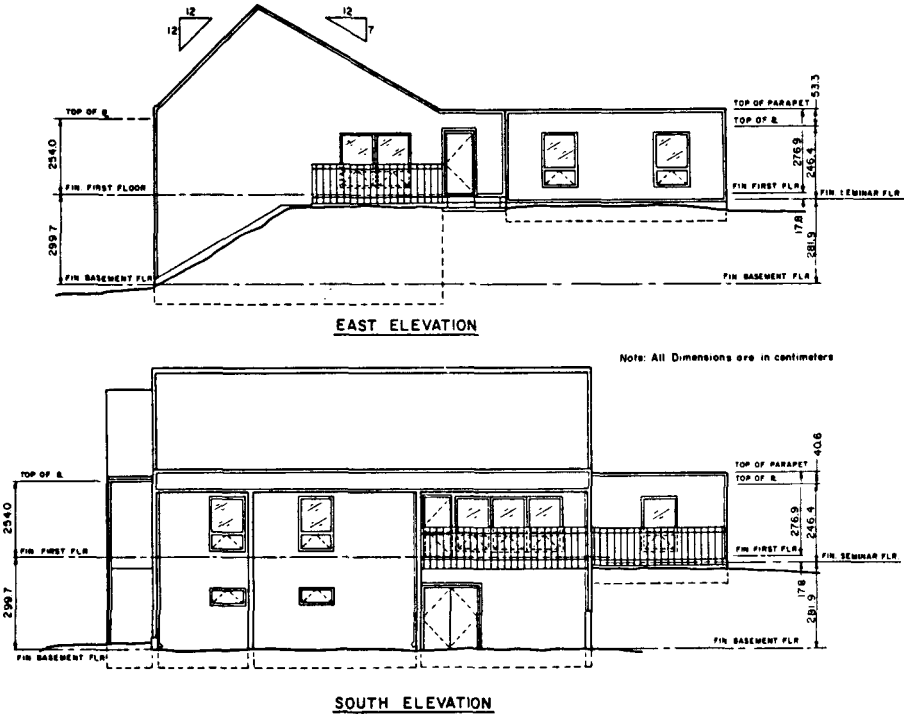

Figure 2-4. East and south elevations of Solar House III.

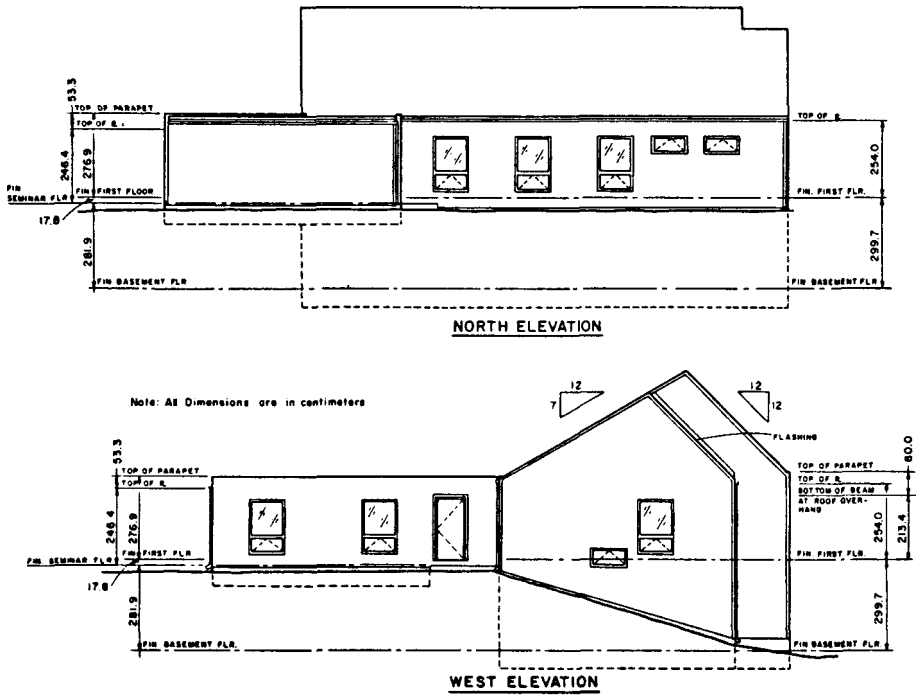

Figure 2-5. North and west elevations of Solar House III.

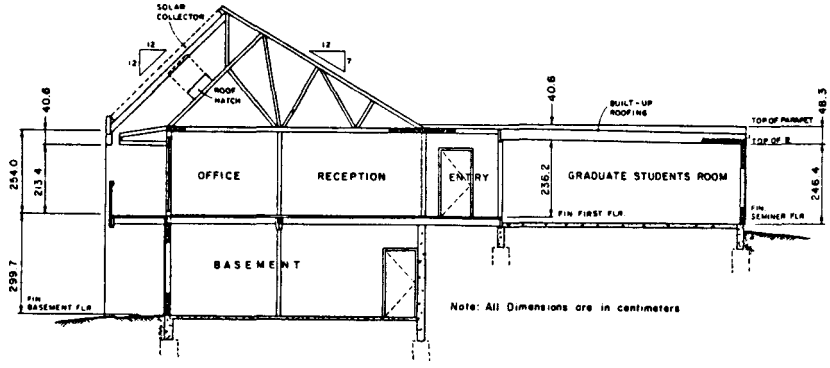

Figure 2-6. Cross section of Solar House III.

2.1.3 Building Materials and Cooling Load

The building walls are constructed of 50x100 mm (2x4-in.) studs on 406-mm (16-in.) centers. The sheathing on the exterior is 12-mm (1/2-in.) plywood with a 10-mm (3/8-in.) thick plywood siding over it. The interior surface is 16-mm (5/8-in) gypsum board and the space between studs is filled with glass fiber batt insulation. Ceiling joists are 50x150 mm (2x6-in.) beams on 610-mm (24-in.) centers, and covered with 165 mm (6.5 in.) of batt insulation.

The exposed wall area of the building totals about 110 m^2 (1180 ft^2) and the underground wall area is about 73 m^2 (785 ft^2). There are 28.25 m^2 (304 ft^2) of double-glazed windows in wood frame with 80 percent glass area, and about 3.9 m^2 (40 ft^2) of door area, half of which is a solid core door and the other door has 0.56 m^2 (6 ft^2) of single pane glass. The calculated heat conductance rate of the building is about 420 W/C (796 Btu/F.hr), including an estimate of one air change per hour of infiltrating air.

2.2 The Solar System

The solar cooling system evaluated in Solar House III during the summer of 1982 is shown schematically in Figure 2-7 and consisted of 54.7 m^2 (588 $ft^2$of thin film, flat-plate solar collectors developed at Brookhaven National Laboratory (BNL), 4540 ℓ (1200 gals) of water thermal storage, a 10.55-kW (3-ton) Arkla XWF-3600 evaporatively-cooled absorption chiller, and an Arkla water-to-air heat exchanger nominally rated at 14 kW (4-tons). Auxiliary cooling is accomplished with a 10.55-kW (3-ton) air-to-air heat pump.

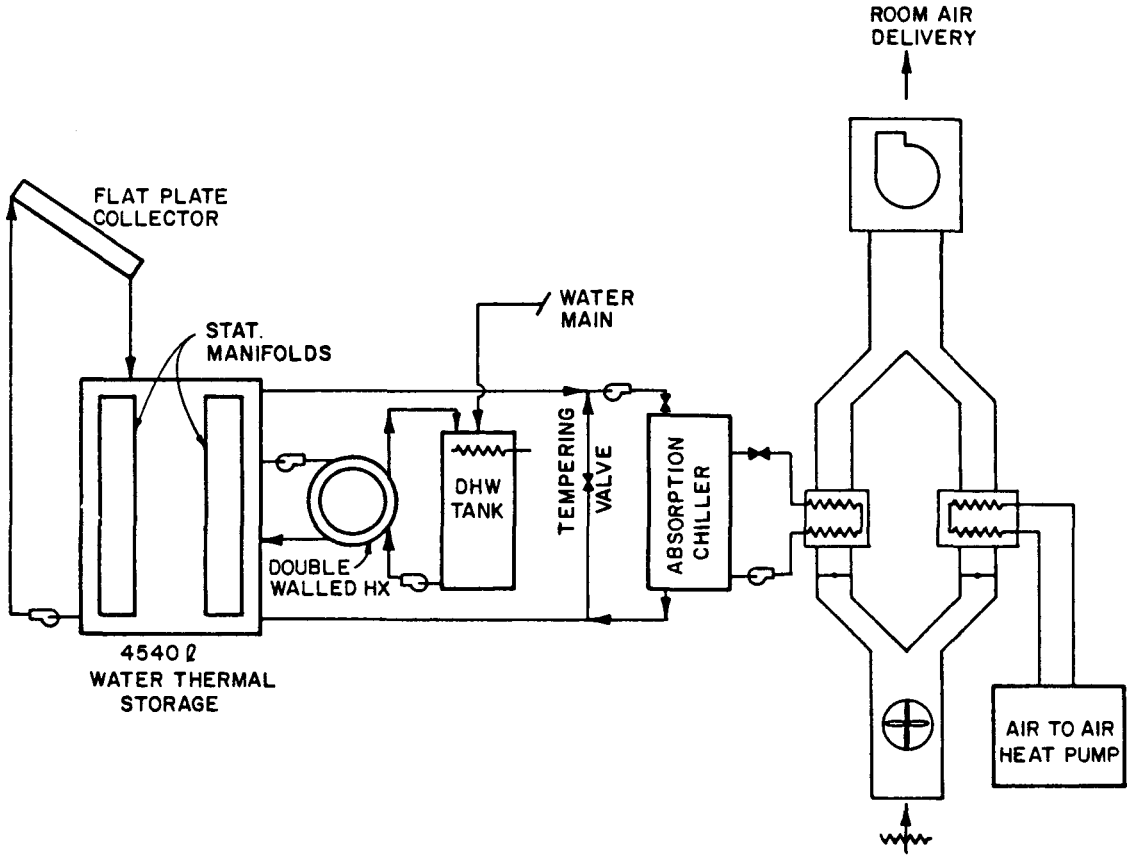

Figure 2-7. Solar House III system schematic summer 1982.

The solar domestic water heating system consisted of a double-walled heat exchanger and a 300-ℓ (80-gal) hot water tank. Hot water is circulated from storage through the heat exchanger where energy is transferred by another circulating loop to the domestic hot water (DHW) tank. A 2.5-kW electric resistance heating element located in the upper portion of the DHW tank provides auxiliary heating.

Solar Collectors. An exploded view of the BNL thin-film solar flat plate collector is shown in Figure 2-8. The absorber is made with thin polymer film and aluminum foil. The aluminum foil is 0.51 mm thick with a selective surface coating on one side and a polymer film (0.25 mm "Teflon" FEP) laminated to the other. With the exception

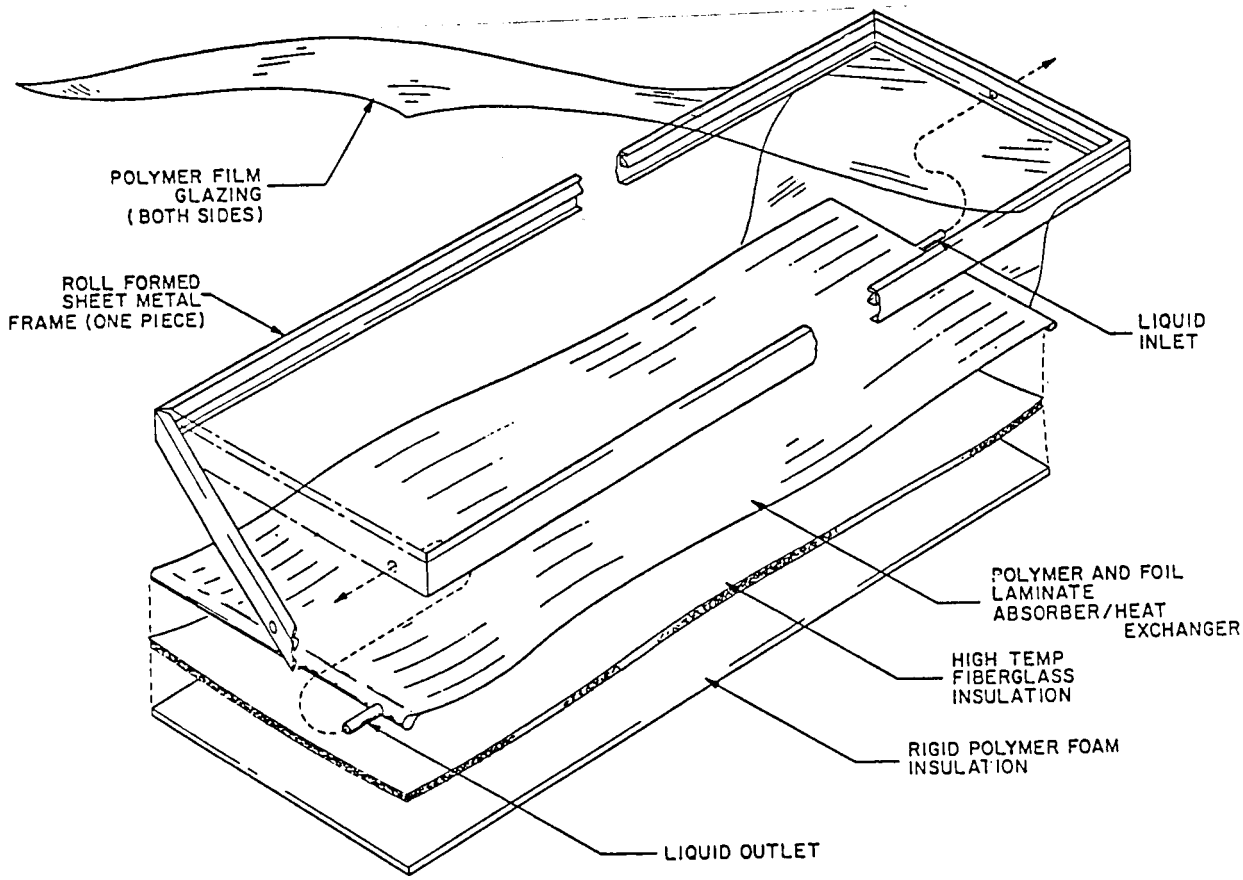

Figure 2-8. BNL thin film solar flat plate collector (provided by Brookhaven National Laboratory).

of the selective surface coating, the lower half of the absorber has the same polymer film lamination and the two halves are glued together in such a way as to form vertical flow channels between the two polymer films. Immediately behind the absorber is a high temperature fiberglass insulation and below that is rigid polymer foam insulation. The absorber and insulation are encased in a roll-formed sheet metal frame and the assembly is sealed within a "TEDLAR PVF" polymer film of 1 mm thickness. The entire collector assembly weighs about 2.4 kg/m^2. Performance tests by Grumman Energy Systems indicated $F_R\tau\alpha = 0.74$ and $F_RU_L = 4.63$ W/m^2-C. More detailed discussions of the BNL collector can be found in References [2] and [3].

The light-weight collectors were installed on the roof of Solar House III and were allowed to stagnate for two days to "condition" the materials before use. During this conditioning period most of the collectors failed due to partial delamination of the absorber.

The time required to replace the BNL collectors with another collector was incompatible with the progression of summer and the chiller testing schedule. Therefore, electric heat supply was used in order to obtain operational performance data for the absorption chiller. Procurement of sufficient cooling performance data to permit assessment of chiller characteristics became the principal objective of the project. Since electrical energy was used to heat water in storage, preheating of domestic water under such circumstances was not of interest and the space cooling system was modified as shown in Figure 2-9.

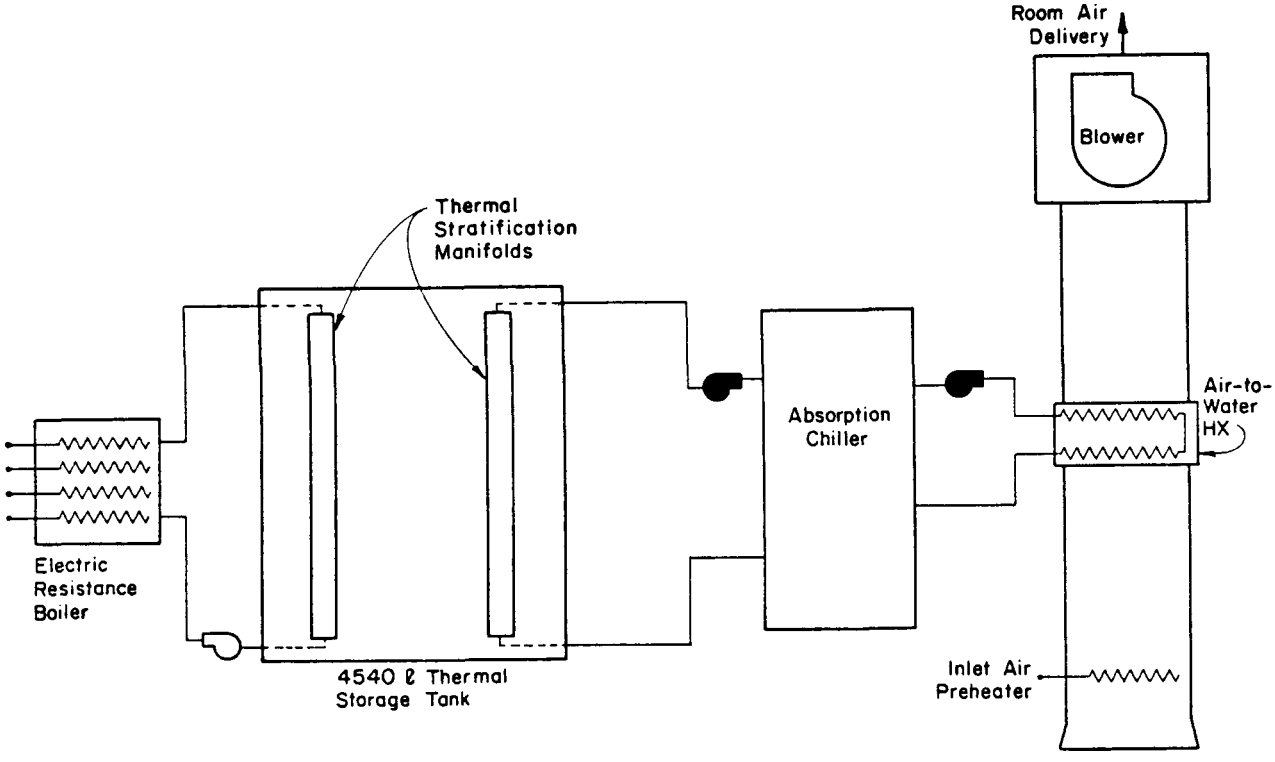

Figure 2-9. Schematic of modified system in CSU Solar House III summer 1982.

2.3 Components

2.3.1 Electric Resistance Boiler

Failure of the new collectors prompted the need for an alternate energy source for the system. Therefore, an electric resistance boiler, nominally rated at 20 kW (with a 220 V source), was used. The unit has four heating elements, each rated at 5 kW, but at a supply voltage of 208 V, the capacity is 17.9 kW and is just adequate for the chiller. Since experimental flexibility for chiller operation would be severely restricted if the boiler is fixed in the hot water supply loop to the generator, it was decided to use the boiler to heat water in the thermal storage unit. Then the flow rate from storage to the generator could be varied without immediate interaction with supply temperature.

2.3.2 Thermal Energy Storage

Thermal energy was stored as sensible heat in 4540 liters of water contained in a horizontal cylindrical tank, 1.353 m in diameter and 2.819 m long. Polyurethane foam is applied to the tank exterior to an average thickness of 100 mm and the saddle supports are insulated with polyurethane foam within a styrofoam jacket. Although the tank can be pressurized to 689 kN/m^2 (100 psi), it was vented to the atmosphere during most of the 1982 cooling season. Stratification manifolds and baffles were provided within the tank on the return pipes from collector and chiller. These devices, developed and used at CSU for the past 4 years, consist of two concentric CPVC pipes with a series of staggered holes drilled along their entire length. After dissipating

kinetic energy at the entrance to the tanks, the hot or cold return water reaches an appropriate level in the tank and diffuses outward with little disturbance to water within the tank. Principles of operation and details of design are described in Reference [4].

2.3.3 Absorption Chiller

The Arkla XWF-3600 is a single-effect evaporatively-cooled lithium bromide-water absorption chiller. Thermal energy is provided to the generator from storage and heat is removed by circulating chilled water through a cooling coil in the central air distribution duct. Heat is rejected from the chiller by direct evaporative cooling of condenser and absorber walls. Electrical energy is required to run the solution pump, cooling water pump, and heat rejection fan.

2.3.4 Air-to-Water Heat Exchanger

A 14-kW Arkla duct coil, model DCH 48-109, is used as the cooling coil. Air flow rate in the central air distribution system was maximized by careful sizing and orientation of the duct work in the equipment room. The coil is rated at 14 kW with air flow rate of 40.8 m^3/min (1440 SCFM), inlet air temperature of 26.7 C, chilled water flow rate of 36.3 ℓ/min at inlet temperature of 7.2 C, and 30 percent latent cooling load. Typical operating conditions were air flow rate of 45.3 m^3/min (1560 SCFM) at approximately 24 C, chilled water flow rate of 27 ℓ/min at 7.2 C, and less than a 10 percent latent load.

2.3.5 Pumps

Most of the pumps in the system were oversized, because criteria for selection were immediate availability and the ability to meet maximum flow requirements. The primary objective of the experiment being to evaluate the thermal performance of the chiller, pumps were not selected to minimize electrical energy requirements for operation. Besides, a significant portion of the head loss in the piping loops of this system was due to instrumentation, particularly flow meters. Hence detailed measurements of actual electrical energy use in this system would be of limited value, and there are reliable design methods for sizing pumps and determining head losses so that electrical energy requirements for specific installations can be calculated.

2.3.6 Inlet Air Preheater

As mentioned in Section 2.3.4, the design conditions used to rate the air cooling coil were significantly different from those encountered in Solar House III. It was not evident that at normal interior temperature and humidity, the coil could remove 10.55 kW of heat (3 tons of refrigeration) for which the chiller was designed. An inlet air preheater, capable of 4.1 kW of heating, was therefore installed upstream of the air-to-water heat exchanger. Heat supplied to the air stream increased the temperature difference between chilled water and air thereby raising the heat removal rate in the cooling coil to a desired level.

3.0 THE EVAPORATIVELY-COOLED ARKLA XWF-3600 ABSORPTION CHILLER

3.1 Chiller Description

The Arkla XWF-3600 is a 1055-kW (3-ton) absorption air conditioner designed for residential cooling applications. A diagram of the unit appears in Figure 3-1. It is a stand-alone unit located outside the conditioned space. The chiller is equipped with its internal controls and can be activated with a thermostat. The generator and chilled water circulating pumps can also be controlled by the chiller controls. Integration with the balance of the system involves pipe connections to a hot water source and to a cooling coil. A cooling tower is not

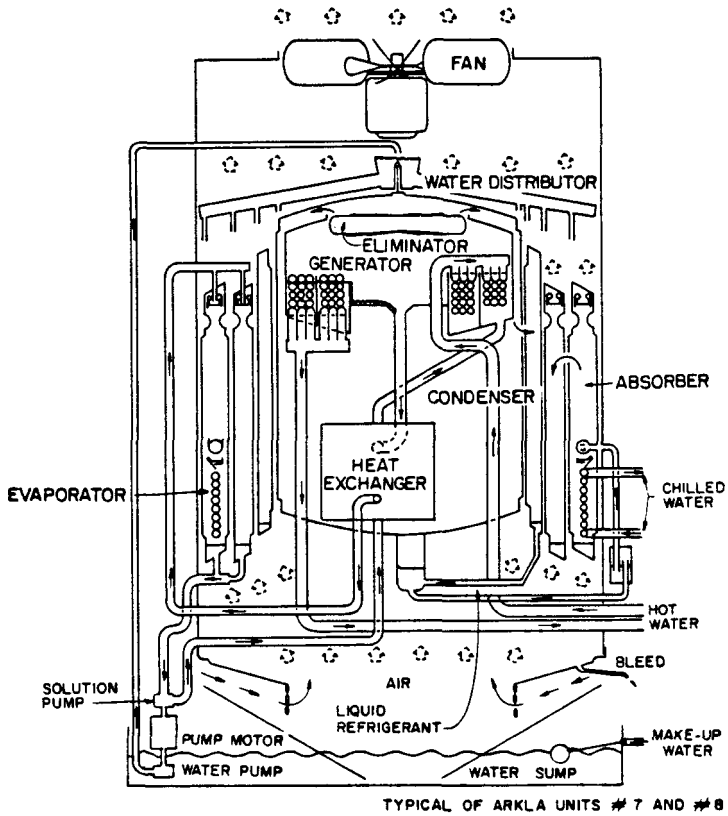

Figure 3-1. Diagram of evaporativelyccooled solar chiller (provided by Arkla Industries, Inc.).

required because heat rejection is accomplished by direct evaporative cooling of the condenser and absorber walls.

3.1.1 Components of the XWF-3600

The basic components of the XWF-3600 are the same as those of a conventional absorption chiller. These include the generator, condenser, expansion valve (flash chamber), evaporator, absorber, heat recovery unit, and solution pump. In addition, the XWF-3600 has a cooling water pump, water distributor, and evaporative cooling fan. The added components are the result of incorporating the functions of the cooling tower with the chiller.

As shown in Figure 3-1, the generator is located in the upper portion of the innermost chamber of the unit and is separated from the condenser by an eliminator. Baffles in the eliminator prevent absorbent droplets from being carried over to the condenser.

The condenser consists of the innermost chamber of the unit and the adjacent annular chamber surrounding the inner cylinder. These two chambers are connected as shown by an arrow. The two-chamber configuration provides sufficient surface area over which evaporative cooling takes place. A liquid refrigerant sump at the bottom of the condenser serves as a liquid trap separating the higher pressure in the generator-condenser compartments from the lower pressure in the evaporator-absorber compartments.

The flash chamber (expansion valve) is a tube which circles the outermost chamber of the unit. In this tube, liquid refrigerant from the condenser encounters the low pressure in the evaporator. Vaporization on the surface of the tubes in the outermost chamber of the

chiller immediately below the flash chamber chills the water circulating through the evaporator tubes.

Vapor absorption occurs in the outermost annular chamber of the unit and the adjacent chamber inside it. The process in the absorber, like that in the condenser, is exothermic. Heat is rejected by the direct evaporative cooling of the walls of the two-chambered absorber.

Absorbent solution is returned to the generator by a pump located near the bottom of the unit. A magnetically-coupled impeller moves solution with an increased concentration of refrigerant from the absorber through a heat exchanger into the generator. Another pump on the same motor shaft circulates cooling water from a sump at the bottom of the unit to a distributor near the top. Cooling water trickles down the walls of the condenser and absorber. A fan located on top of the unit draws air from the intakes at the base of the machine upward over the walls of the condenser and absorber to a discharge opening on top of the unit.

3.1.2 Absorption Cycle

The absorption cooling cycle is depicted in the mass and energy flow diagram of Figure 3-2 and the equilibrium diagram of Figure 3-3. The refrigerant-absorbent pair used in the XWF-3600 is an aqueous lithium bromide (LiBr) solution. At a concentration of about 53 percent, the solution enters the generator in which the absolute pressure is about 50 mm Hg. Water is evaporated from the solution by means of heat transferred through a tubing coil through which hot water is supplied from solar-heated storage or an auxiliary water heater. The

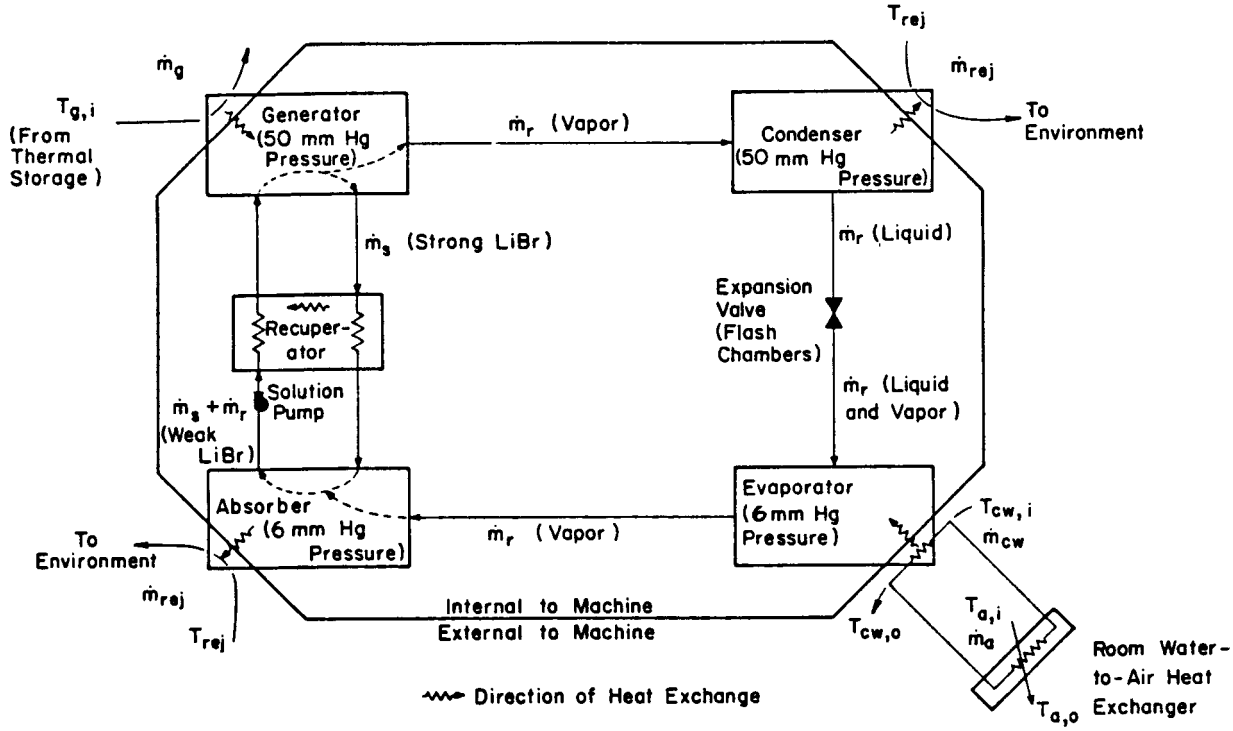

Figure 3-2. Absorption cooling cycle (steady-state) energy and mass flow diagram.

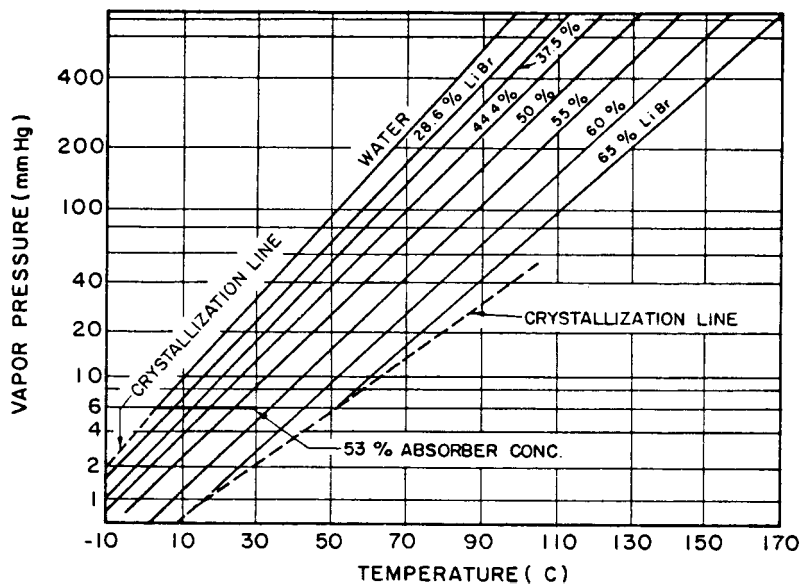

Figure 3-3. Equilibrium diagram for lithium bromide-water absorption cycle.

solution leaves the generator with a LiBr concentration of about 57 percent while refrigerant vapor passes through an eliminator into a condenser. A set of baffles in the eliminator prevents droplets of lithium bromide solution being carried over into the condenser.

Evaporative cooling of the external walls of the condenser causes water vapor to condense on the inner walls and liquid water refrigerant collects in a small condenser sump located at the bottom of the chamber. The sump acts as a trap between the pressure in the condenser (approximately 50 mm Hg) and the low pressure in the evaporator (approximately 6 mm Hg). Refrigerant temperature in the condenser is approximately 38 C. Liquid refrigerant is forced from the condenser sump to the flash chamber by the pressure difference between the two units.

In the flash chamber, located immediately above the evaporator tubes, the liquid refrigerant encounters the 6 mm Hg pressure of the evaporator-absorber chamber. A portion of the refrigerant flashes into vapor, the energy required to change phase being drawn from the remaining liquid refrigerant, thereby reducing its temperature to about 5 C. The cold refrigerant then drips into a circular distribution tray between the flash chamber and the evaporator tubes. Capillary action draws the refrigerant from the tray and distributes it over the evaporator tubes. Water flowing through the tubes is chilled by the refrigerant evaporating at about 5 C, the energy required to vaporize the refrigerant being drawn from the water which has extracted heat from the building in an air-to-water fan-coil exchanger. The refrigerant vapor is now ready to be recombined with the solution, strong in LiBr, that has been concentrated in the generator.

While the refrigerant follows the path just described, the absorbent solution flows out of the generator and is forced to the absorber by the pressure difference between those components. On its way, the solution passes through a heat exchanger in which it is cooled by heat transfer to the dilute solution returning to the generator. At the top of the absorber chambers, the concentrated solution drips into a tray where it is distributed to the absorber walls by capillary action. The liquid flows down the walls as a film. Refrigerant vapor produced at the evaporator tubes is absorbed into the solution that has a high concentration of LiBr and a high affinity for water. The absorption process is exothermic, so the exterior walls of the absorber are evaporatively cooled in the same manner as the condenser. The solution, now with a higher water content, collects in the bottom of the absorber where the solution pump lifts it through the elevation head and pressure difference through the heat exchanger back to the generator.

3.2 Effect of Ambient Wet Bulb Temperature on Chiller Performance

An important parameter in terms of its effect on chiller performance is atmospheric wet bulb temperature. Since condenser and absorber are evaporatively cooled, their temperatures are limited by the wet bulb temperature of the atmosphere. Condenser pressure is therefore fixed by that limit, so temperature in the generator, which operates at the same pressure as the condenser, is also established. The rate of heat transfer to the generator (a measure of capacity) is proportional to the temperature difference between hot water supply and solution, and thus depends on all the above factors which are limited by the wet bulb temperature.

4.0 CONTROLS

Internal controls of the XWF-3600 chiller provide protection, performance improvement, and activation of pumps and blower motors. The protection controls prevent crystallization of the absorbent and freezing of the refrigerant. Controls for performance improvement govern normal spin-up and spin-down as well as prevent spilling of excess liquid refrigerant from the evaporator into the absorbent which would otherwise adversely affect the thermal COP of the unit.

The system was controlled by a microprocessor in two basic modes: (1) supplying energy to thermal storage and (2) space cooling with the absorption chiller. The only interaction between the system controller and the internal chiller controls occurred when the house thermostat called for cooling through the microprocessors.

4.1 Chiller Controls

When the house thermostat calls for cooling, internal control elements in the chiller start the generator pump, and if operating conditions are satisfied, the chilled water pump and house blower are actuated. A schematic of the control wiring is shown in Figure 4-1.

4.1.1 Normal Operation Controls: Spin-up and Spin-down

The entire chiller is typically at ambient temperature when cooling is called for by the thermostat. As stated above, heat is immediately supplied to the generator when the thermostat calls for cooling, but the chiller does not begin full operation until the generator temperature is sufficient to produce refrigerant vapor. The period of

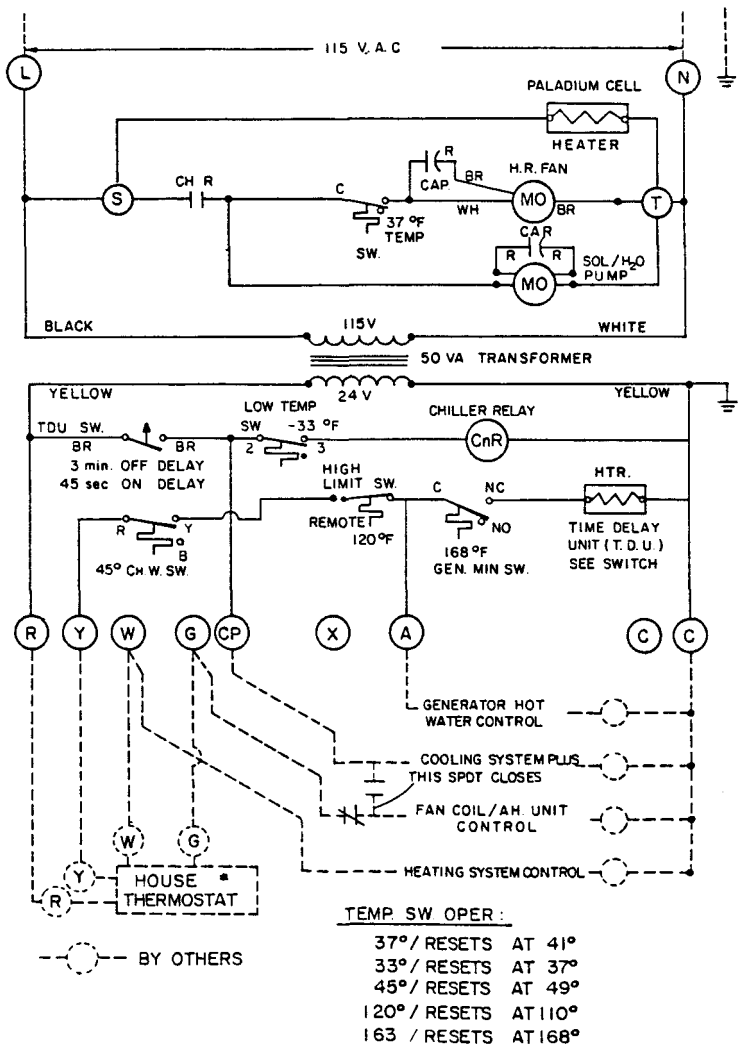

Figure 4-1. Arkla XWF-3600 chiller electric schematic.

time between the initial call for cooling and full chiller operation is generally referred to as spin-up. Spin-up is regulated entirely by the chiller controls. The following discussion refers to Figure 4-1.

The chilled water minimum temperature switch, low temperature limit switch, and the high temperature limit switch are typically closed when the unit is first called on for cooling. When the thermostat closes and provides electricity to the "Y" terminal, the generator

pump is activated immediately. Water in the generator loop is typically at ambient temperature. A sensor in the water at the generator inlet is connected to the generator minimum temperature switch. This switch remains open until hot water from the thermal storage tank displaces the cold water in the loop and the inlet temperature to the generator exceeds 76 C. At this temperature, the switch closes and the time delay unit (TDU) heater is activated. Approximately 45 seconds later, the TDU switch closes and the chiller relay is energized. The solution pump, chilled water pump and house blower are then activated. The condenser fan switch is typically open until the condenser temperature reaches 27 C, at which point the evaporative cooling fan on top of the unit begins operating.

When the room thermostat is satisfied and cooling is no longer needed, hot water supply to the generator is discontinued. The chiller has some remaining refrigeration capability by virtue of the refrigerant just produced and in transit to the evaporator. The period during which this remaining increment of cooling is extracted from the unit is commonly called spin-down.

When the thermostat is satisfied, electricity is no longer supplied to the "Y" terminal and the generator pump is turned off. The time delay unit heater is activated, and for approximately three minutes the solution pump, evaporative cooling fan, chilled water pump, and house blower continue to operate until the TDU switch opens. The opening of the TDU switch interrupts power to the chiller relay and the unit then shuts down.

4.1.2 Controls for Performance Improvement

This set of controls is inside the XWF-3600 and is designed to maximize the thermal performance of the chiller. Included are the controls involved with spin-up and spin-down under normal operating conditions as well as under other conditions. There is also a switch that prevents the spilling of unevaporated liquid refrigerant from the evaporator into the absorber.

Spilling is a condition under which part of the liquid refrigerant that is dripped over the evaporator tubes does not vaporize but instead drips off the tubes and runs into the absorber section where it mixes with the absorbent solution. The heat of vaporization of that portion of the refrigerant is not extracted from the chilled water and the loss of refrigeration capability lowers the thermal COP of the unit. This condition can occur when the chilled water entering the evaporator coil is too cold to provide sufficient energy to boil off all the refrigerant being supplied from the generator and condenser.

The chilled water minimum temperature switch is designed to prevent this refrigerant spilling. When the temperature of the chilled water leaving the evaporator coil falls below 7.2 C, a switch opens, the generator pump is turned off, and the unit enters the normal spin-down mode. Refrigerant production is thus reduced so that the temperature of the exiting chilled water rises. When this temperature rises above 9.2 C, the switch closes and the unit resumes normal operation. But if the temperature has not risen to 9.2 C in about three minutes, spin-down has finished and the unit shuts down. After some additional minutes, heat from the room will warm the water and increase

its temperature above 9.2 C, whereupon the switch will close. If cooling is still required, the unit will go into spin-up and return to normal operation. This type of cycling operation occurred frequently during the summer of 1981 in Solar House I [5]. The condition was the result of an undersized cooling coil in the house air circulation system. Its capacity was not sufficient for the full 10.55 kW of cooling that the XWF-3600 chiller was designed to supply.

4.1.3 Controls for Chiller Protection

Controls designed to protect the chiller are for prevention of crystallization of the absorbent and freezing of the refrigerant. Crystallization of absorbent in the generator due to excessive concentration of solute is prevented by a high temperature limit switch that is actuated by a sensor on the exterior wall of the innermost chamber directly above the generator. The temperature at this point lies somewhere between that of the air-water coolant and that of the vapor passing to the condenser. If refrigerant vapor is produced in the generator faster than it can be reabsorbed in the absorber, pressure and temperature in the generator increase and the concentration of lithium bromide rises. But before crystallization becomes likely, the sensor temperature would reach 49 C at which point a switch opens and the unit enters the normal spin-down mode. The generator pump is turned off and refrigerant vapor production declines. When the sensor temperature falls below 43 C, the switch closes and normal operation resumes. If normal operation is not resumed within three minutes, the chiller shuts down.

Crystallization in the generator due to low temperature heat supply from thermal storage is prevented by a minimum temperature control switch. Temperatures in the generator must be sufficient to produce enough refrigerant vapor to create a pressure difference between the generator-condenser and the evaporator-absorber adequate for driving the absorption cycle. If generator temperature is too low, the refrigerant is slowly boiled off and accumulates in the condenser sump. The solution in the generator may thus increase in strength until it crystallizes. Prevention is accomplished by the opening of the generator minimum temperature switch which is activated by a sensor located at the inlet to the generator. The switch opens when the temperature drops below 73 C and closes when the temperature rises above 76 C. An open switch sends the unit into normal spin down with the exception that the generator pump continues to operate. If the temperature has not recovered in three minutes the unit shuts down.

Further protection against crystallization is provided by the condenser fan switch located on the exterior wall of the condenser near the condenser sump. The driving force for moving liquid refrigerant from the condenser to the evaporator is the pressure difference that exists between the two components. An indication that this pressure difference is too low is a low condenser temperature. This situation can occur when the wet bulb temperature is relatively low. The unit rejects heat from the condenser at a greater rate than the condensation of vapor refrigerant requires, resulting in a decline in condenser temperature. The amount of refrigerant vapor produced in the generator and subsequently condensed in the condenser may require less heat

rejection than that provided by the evaporative cooling cycle. The result is a drop in the condenser temperature with an associated drop in the pressure of the generator and condenser. If either condition persists there is a slow accumulation of liquid refrigerant at the bottom of the condenser. The concentration of lithium bromide in the generator solution may thus increase to the point that crystallization occurs. To prevent this series of events, the condenser fan switch opens if the temperature decreases to 27 C, thereby turning off the evaporative cooling fan. The fan remains off until the condenser temperature rises to 30 C. While the fan is off, heat rejection from the condenser is greatly reduced. Temperature and pressure in the condenser therefore rise and refrigerant flow into the evaporator increases. Increased rate of refrigerant return flow to the generator then alleviates crystallization risk.

Freezing of the refrigerant in the flash chamber is prevented by the operation of a low temperature limit switch actuated by a sensor on the external wall of the flash chamber. If the temperature in the flash chamber falls below 1 C, the switch opens and the entire unit shuts down immediately. There is no spin down when this switch opens. When the temperature rises above 3 C, the switch closes and normal chiller operation can resume.

A flowchart of the chiller control logic is shown in Figure 4-2.

4.2 System Controls

The basic modes of system operation are: (1) supplying energy to storage and (2) space cooling with the XWF-3600 chiller. The call for

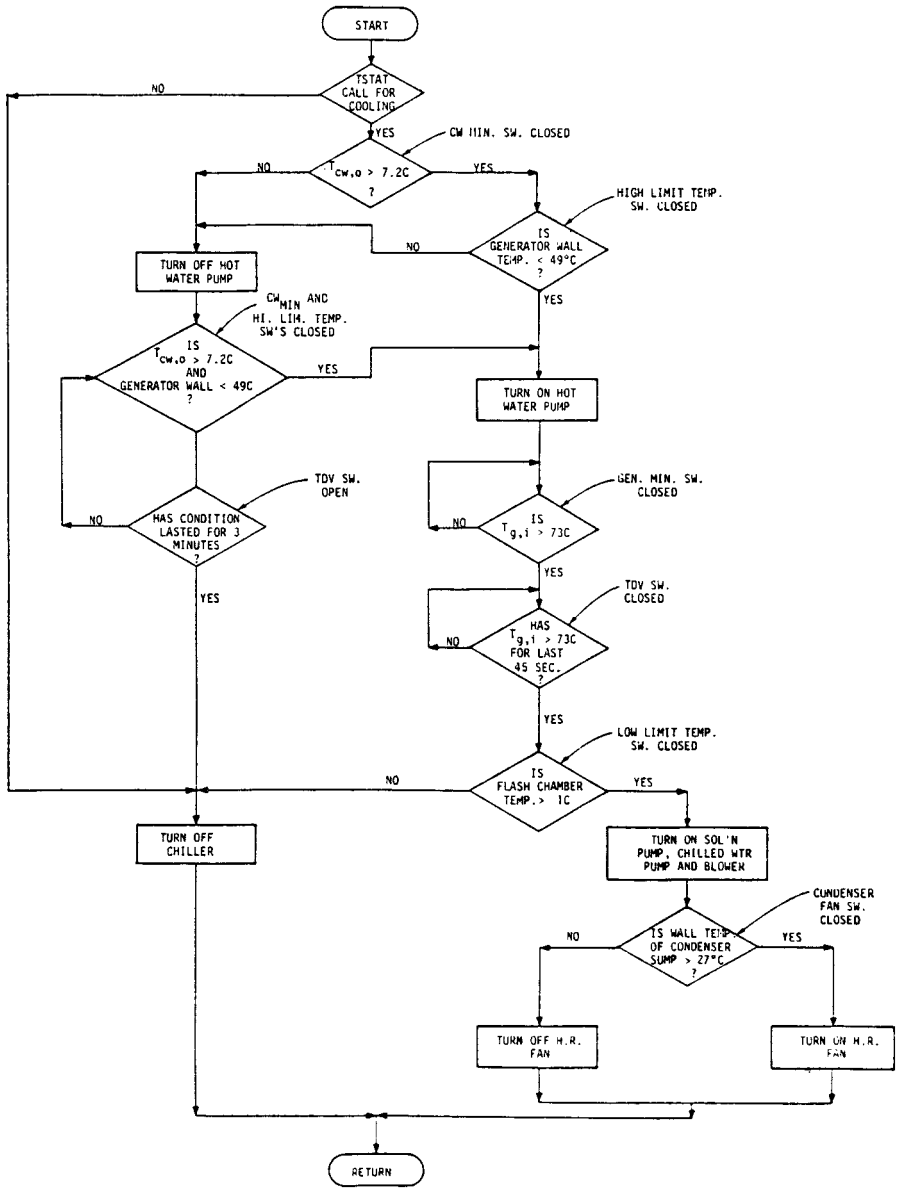

Figure 4-2. Internal controls of Arkla XWF-3600 #7-2 chiller.

cooling is the only interaction between controller and chiller. The chiller controls are solely responsible for operating chiller, generator pump, chilled water pump, and house blower.

4.2.1 Control Hardware

The controller used in Solar House III is the Modular Electronic Control Assembly, MECA II, developed by GTE Products, Incorporated. It comprises a microcomputer (MC-4A), computer base (CB-1), motherboard (MB-1), and the input/output devices. The microcomputer operates with 4K bytes of non-volatile memory stored on plug-in chips or PROMS (programmable read only memory). Chips are programmed in modified BASIC with the MECA programming system. The microcomputer rests on the computer base which is the communications interface with the motherboard. Linkage between the computer base and the input/output device is provided by the motherboard.

Four types of input/output devices were used. An AI-4 input module converts an analog signal from a temperature sensor (RTD) from a voltage to a count which is proportional to temperature. An SC-1 input module monitors switch closures such as a thermostat contact. The LD-1 output module sends a 0 or 5V signal to a system component to start or stop operation. An encoded signal is sent to the data acquisition system from the DO-1 output module so that the system mode can be recorded. This one-way linkage is the only communication between the system controller and data acquisition system.

4.2.2 Sensor Location and Resolution

RTD temperature sensors are located in the conditioned space and in the bottom and top of storage. A voltage signal that is inversely

proportional to temperature is sent to a card containing a resistance-capacitance network which inverts, amplifies, and scales the signal to a 0-5V scale that is directly proportional to temperature. This voltage is converted to a digital signal between 0 and 127 counts by the AI-4 module. Scaling at the card determines the resolution with which the temperature sensor can be read. The room temperature sensor is scaled to zero voltage at 15 C and 5V at 40 C. This translates to a resolution in the MECA of 5 counts per degree (127 cts ÷ [40 - 15 C]). The sensor at the top of the storage tank is scaled from 0-100 C which translates to 1.27 counts/C resolution in the MECA.

4.2.3 System Control Software

The experiments described in this report were controlled by a relatively small portion of the program developed to control the entire solar space cooling system. Among twelve modes of system operation originally programmed, four were used with the system discussed here. These modes were: (1) do nothing; (2) supply energy to storage; (3) cool with the absorption chiller; (4) supply energy to storage and cool with the chiller.

Energy was provided to the storage tank from the boiler when the temperature at the top of storage was below 74 C. The boiler remained on until the tank reached 81 C. These set points were subject to change as the thermal energy requirements of the chiller were evaluated.

The controller acted as a thermostat, calling for space cooling when the room temperature reached 24 C, provided, however, that storage

tank temperature was adequate. Cooling continued until the room temperature dropped below 22 C. The call for cooling was made only when the temperature at the top of the storage tank was greater than 78 C; if storage temperature fell below 74 C, the call for cooling ended. This operating range was also subject to change. Although internal controls in the chiller are designed to shut down operation if generator heat supply decreases past a limit, the MECA controller and storage sensors provided added assurance that operation would not be impaired by inadequate heat supply.

5.0 DATA ACQUISITION SYSTEM

5.1 General Description

The data acquisition system (DAS) consists of (1) instrumentation to sense temperatures, temperature differences, air and water flow rates, barometric pressure and relative humidity; (2) an analog-to-digital (A/D) converter and data logger; (3) an on-line microcomputer with peripheral cassette drive, typewriter and CRT, for real-time data reduction; (4) a magnetic tape recorder to store data in digital form; and (5) an uninterruptible power supply. The components of the DAS are depicted in Figure 5-1. Complete scans were made every 5 minutes throughout the day, every day through the season. Unavoidably, gaps occur in the data sequence.

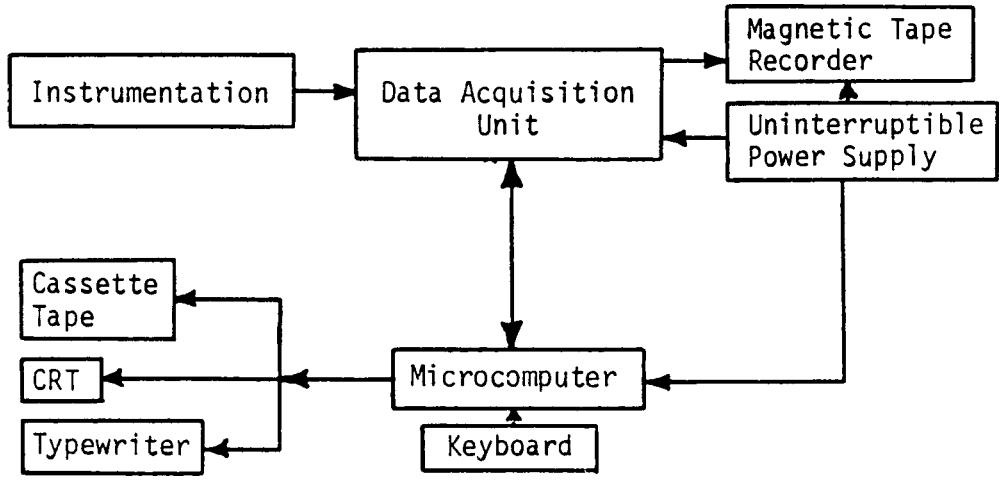

Figure 5-1. Block diagram of the data acquisition system.

5.2 Instruments

The instruments used for measurement of temperatures, temperature differences, water and air flow rates, barometric pressure, relative humidity, solar flux and auxiliary energy quantities are listed in Table 5-1. Listed also in the table are instrument types, manufacturers and models, range of each instrument, accuracies, and comments which reflect the experience in Solar House III. All conditions monitored by the data acquisition unit are listed in Table 5-2.

5.2.1 Solar Flux

Solar radiation measurements are made with Epply PSP pyranometers placed on the roof of Solar House III. Total and diffuse radiation are measured on a horizontal plane and total radiation is also measured in a plane parallel to the collectors which are tilted at 45 degrees with respect to the horizontal. Both instantaneous and integrated values of solar radiation are included in the data set.

5.2.2 Temperature and Temperature Differences

Copper-constantan (Type T) thermocouples are used to measure temperatures of both air and water. Sheathed thermocouples are used to measure water temperatures. Reference junction compensation and linearization are provided by the data logging unit.

Temperature differences are measured with multiple-junction thermopiles, and electrical output is converted to temperature differences according to standard procedures [6, 7, 8]. Five-junction thermopiles are used for water temperature differences. Temperature differences in

Table 5-1. Transducers and Specifications

FUNCTION	INSTRUMENT TYPE	MANUFACTURER, DESCRIPTION	QUANTITY	INSTRUMENT/ DATA RANGE	(1) ACCURACY	COMMENTS
Temperature measurement (2)	Thermocouple Type T	Leeds and Northrup, Omega, Thermo-Electric: 22 and 26 gage ThermoElectric, sheathed:	67	-184 to +390 C -40 to +150 C	±0.4 C	Consider: Temperature gradients, heat transfer to and from the measuring junctions, thermoelectric homogeneity of wire, reference junction calibration, linearization errors, use of extension wire and connections, mechanical integrity, grounding, common mode voltage sources (including lightning).
		Grounded (3)	2			
		Ungrounded (3)	2			
Differential temperature measurement (2), (4)	Thermopile, Type T	Leeds and Northrup, Omega 26 gage	7	-184 to 370 C ±100 C diff.	±(1 % R + 0.05 C)	
Water flow	Turbine Flowmeter	Cox, Series 21	3	0.19-1.9 µs	0.5 % F	Pressure drop at maximum flow, 5.5 psi.
Air flow	Vane-type Anemometer	Assembled by Nat'l. Research Council of Canada	1	0.15-15.2 µs	not specified	
Solar flux measurement on 45° tilt	Pyranometer	Eppley precision pyranometer Model PSP	3	0 to 2800 w/m^2 0 to 1200 w/m^2	±(1.5 % R + 0.5 % F)	Both instantaneous and and integrated values of pyranometer output are logged. A "double-glazed" pyranometer with axially symmetric black and white sensing surfaces is required to maintain accuracy when measuring global radiation on a tilt.
Electric power transducers	Current coil and hall effect transducer	F. W. Bell, Inc., PX-2202B	6	±1 KW or ±2 KW	±(0.25 % R + 0.25 % F)	Models offered by Ohio Semitronics are available with offset, scale factor adjustments and in a greater range of capacities.
		Ohio Semitronics, PC5	5	0 to 800 W		
Integrators Pulse counters		AGM Electronics EA-4011-5	12	Unipolar input/ output range specified per individual module	±(0.25 % R + 0.25 % F)	Pick range carefully. Large accumulated errors due to effect avoiding by settling offsets slightly negative and rejecting negative values during data processing.
		AGM Electronics EA-4050-2	4			
Barometric pressure	Variable capacitance diaphragm; vacuum reference	Rosemont 1332A	1	0 to 15 psia 0.73 to 0.83 atm	±0.2 % R	
		Mercury Weathertronics	1	508-790 mmkg	±0.1 mm	
Relative humidity	Hair Hygrometer		1	-18-38 C db 0-100 % R.H.	1 % 1 %	Not monitored by DAU. Data manually reduced using high altitude psychrometric chart.
A/D data logging	µP controlled analog multiplexing; dual slope digitizer	Doric 220-160-05-34 -61-K5-TK1-KK1-31 -53-4K-43-73	1	±11.0 VDC; -165 to +435 C ±1.0 VDC; -40 to 150 C	±(0.03 % R + 0.005 % F + 1.5 µv) Thermocouple conversion ±0.3 C	Integraion of computer and D/A functions should be considered now that such equipment is increasingly available. Provision for digital inputs would be helpful.

Table 5-2. Doric Channels and Data Array Indices.

CHANNEL NO. I1	WANG DATA ARRAY D1	PRINT FORMAT NO. I3	LABEL	UNITS	DESCRIPTION
1	1	2	T700	C	Temperature at "thermostat"
2	2	2	T701	C	Room temperature at west end of building
3	3	2	T702	C	Temperature in equipment room
4	4	2	T703	C	Storage tank room
5	5	2	T210	C	Storage - Top level (1)
6	6	2	T220	C	Storage - Level 2
7	7	2	T230	C	Storage - Level 3
8	8	2	T240	C	Storage - Level 4
9	9	2	T250	C	Storage - Bottom level (5)
10	10	2	T001	C	Dry bulb temperature, atmospheric air
23	23	2	T450	C	Outlet from storage, to generator
24	24	2	T451	C	Inlet to generator
25	25	2	T452	C	Outlet from generator, to storage
26	26	2	T453	C	Return to storage from generator
27	27	2	T550	C	Outlet from evaporator
28	28	2	T551	C	Inlet to duct HX
29	29	2	T552	C	Outlet from duct HX
30	30	2	T553	C	Inlet to evaporator
31	31	2	T650	C	Air temperature u/s of coils
32	32	2	T651	C	Air temperature d/s of coils
33	33	2	T652	C	Air temperature after blower
38	38	2	T211	C	Storage top
51	51	2	TD400	mv	Storage to generator
52	52	2	TD401	mv	Across generator
53	53	2	TD402	mv	Generator to storage
54	54	2	TD403	mv	Across storage generator side
55	55	2	TD500	mv	Evaporator to room HX
56	56	2	TD501	mv	Across room HX
57	57	2	TD502	mv	HX to evaporator
58	58	2	TD503	mv	Across evaporator
59	59	2	TD600	mv	Across cooling coils
60	60	2	TD601	mv	Across blower
61	61	2	TD602	mv	Room delivery to room return
63	63	2	T212	C	Storage level 1
64	64	2	T222	C	Storage level 2
65	65	2	T232	C	Storage level 3
66	66	2	T242	C	Storage level 4
67	67	2	T252	C	Storage level 5
68	68	1	T002	C	Wet bulb sensor
69	69	2	T231	C	Storage level 3
70	70	2	T241	C	Storage level 4
71	71	2	T251	C	Storage level 5
72	72	1	B001	V	Barometric pressure
73	73	1	I001	mv	Instantaneous total horizontal
74	74	1	I002	mv	Instantaneous diffuse horizontal
75	75	1	I003	mv	Instantaneous total 45
76	76	1	M001	V	Mode indicator
77	77	1	M002	V	Mode change flag
78	78	1	C001	V	Condensate
80	80	1	EP600	V	Blower
83	83	1	EP400	V	Arkla chiller unit (fans, pumps)
84	84	1	EP401	V	Generator supply pump
85	85	1	EP500	V	Chilled water circulating pump
86	86	1	EP700	V	Electric to heat air stream
87	87	1	W600	V	Air flow
92	92	1	W400	V	Flow out of storage to generator
93	93	1	W401	V	Flow into generator
94	94	1	W500	V	Chilled water circulation
95	95	1	M003	V	Mode change integrator
96	96	1	I004	V	Total solar, horizontal
97	97	1	I005	V	Diffuse solar, horizontal
98	98	1	I006	V	Total solar on 45
99	99	1	I007	V	Total solar on 45 while operating

air are measured with nine- or twelve-junction thermopiles with each junction located in the center of equal area grids.

5.2.3 Water Flow Rates

Water flow rates through the chiller generator and evaporator are measured with turbine flow meters, the output signals from which are integrated to obtain the total volume of liquid flow during the period between scans. The meters are calibrated in situ with standard verturi meters placed in the recirculating loop during the calibration.

5.2.4 Air Flow Rate

Air flow rate in the central air distribution duct is measured with a vane-type anemometer. The output pulses from the device are summed with a pulse accumulator to obtain the volumetric flow of air in the five minutes between scans. Calibration of the anemometer is accomplished by means of a pitot tube traverse in the duct section immediately upstream of the device.

5.2.5 Ambient Outdoor Wet Bulb Temperature

A continuous record of ambient outdoor dry bulb temperature and relative humidity is made by use of a thermo-hygrograph, employing a horse-hair hygrometer. Temperature and relative humidity are recorded on a strip chart which is replaced weekly. Wet bulb temperature is obtained by use of a high altitude psychrometric chart. The results are compared periodically to measurements taken with a sling psychrometer.

5.2.6 Barometric Pressure

Barometric pressure is measured with a Rosemont Series 1332 pressure transducer. The output of this device was periodically checked against a standard barometer.

5.2.7 Electric Power Meters

Watt transducers are used to record electrical energy consumption of various components in the system. Total energy consumed by a component during the time between scans is obtained by integration of each watt transducer output.

5.2.8 Mode and Mode Change

The state of the system devices is referred to as the mode. The mode signal originates at the MECA II controller where the mode is determined with the control software. This signal is in the form of a discrete voltage associated with a unique mode. Information about a mode change during the five minutes between scans also originates in the MECA controller. The output signal is 0 or 5V. If the current signal is different from the previous signal (e.g. 0V then and 5V now) a mode change has occurred. Mode change signals are integrated as well as read instantaneously at the scan. Integrated values show when the mode change occurred.

5.2.9 Integrators

Analog signals from selected transducers are integrated during the interval between scans. Solar flux, flow rates, electrical energy consumption, and the mode change indicator are integrated. The integrators are reset at the end of each scan.

5.3 Data Acquisition Unit

The Data Acquisition Unit (DAU) is a Doric Scientific Model Digitrend 220. It consists of a scanner, analog-to-digital converter and printer with a capability to interface with several peripheral units. A Kennedy magnetic tape recorder and a Wang microcomputer communicate with the DAU.

The scan interval was selected to be every 5 minutes. Sampling is done in order from Channel 0 to Channel 99. The data are multiplexed and digitized before being transmitted to both the magnetic tape recorder and the microcomputer.

6.0 DATA PROCESSING

6.1 General Procedure

Data sampled by the data acquisition unit (DAU) are accumulated in a read buffer and transmitted to the Kennedy Incremental 1600 tape recorder and the on-line Wang 2200 microcomputer. Preprocessed data are recorded on 7-track magnetic tapes which are used as a back-up data record. Data are reduced in real-time using the on-line microcomputer.

The flow chart for on-line data processing is shown in Figure 6-1. Selected channels of reduced data are printed every five minutes. All

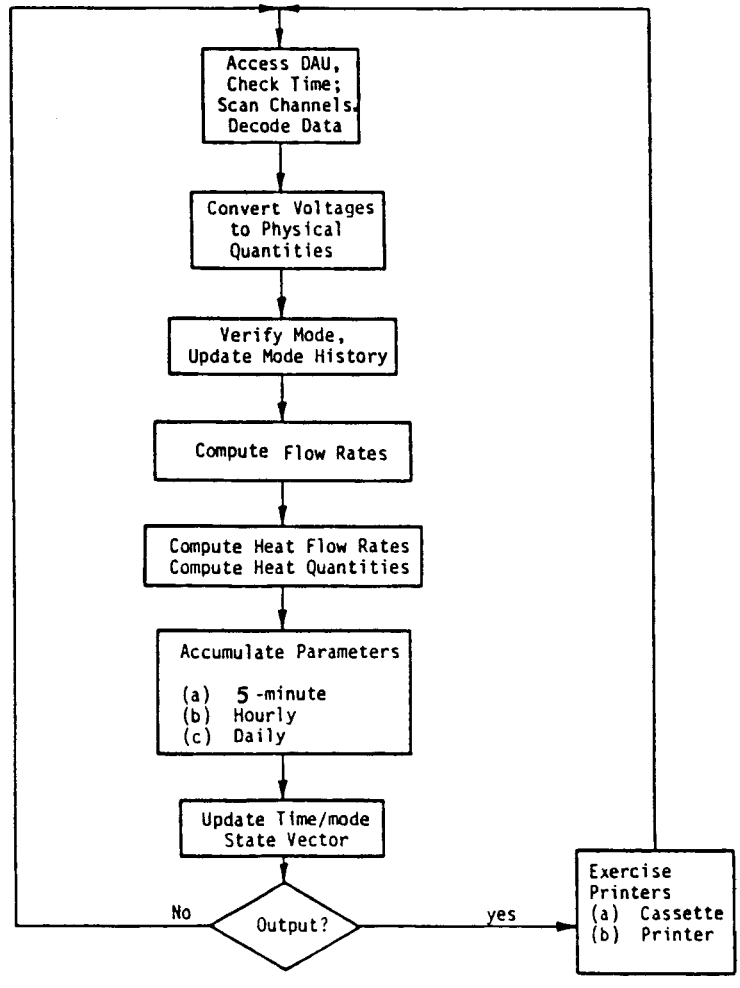

Figure 6-1. Flow chart for on-line data processing.

of the processed data are averaged or summed for the hour and stored in computer memory. Once each day, the hourly data are written on a cassette tape and printed out with the averaged and summed quantities for the day.

6.2 Conversions

The data which require conversion from voltages to physical quantities are:

1) solar flux
2) integrated air and liquid flow rates
3) temperature differences from thermopiles
4) electrical energy consumption
5) barometric pressure.

The operating mode signal from the MECA controller must also be converted.

6.2.1 Calibration

Conversion constants and functions were first determined by calibration. With the exception of thermopiles and thermocouples, each instrument was calibrated through its associated signal processing module (integrator or pulse accumulator) and the DAU. The voltage received by the microcomputer was compared with a measurement of the output of a secondary or tertiary standard instrument, and conversion constants or curves were determined. The outputs of randomly selected thermocouples of precision copper-constantan wire were spot checked in

a constant temperature bath and found to coincide with values in standard Type-T thermocouple conversion tables provided by the manufacturer. The DAU is calibrated with precision input voltages and adjusted so that the output voltages are identical to the input voltages.

6.2.2 Temperature Differences

Thermopile outputs (Δe) in microvolts were converted to temperature differences (ΔT) by a polynomial representation of the Type-T thermocouple curve. Because the curve of temperature vs. emf is nonlinear, temperature difference determination is dependent on Δe and a reference temperature on the curve. The reference temperature can be at either end of the thermopile. With the reference temperature (T_1) known, the procedure for calculation of ΔT is as follows:

1. Calculate e_1 corresponding to reference temperature T_1 by use of Equation (6-1).
2. Determine e_2 by adding Δe to e_1 ($e_2 = e_1 + \Delta e$).
3. Convert e_2 to T_2 by use of Equation (6-2).
4. Calculate ΔT ($\Delta T = T_1 - T_2$).

The equations for converting e to T and T to e are (6-1) and (6-2).

$$e = \sum_{i=1}^{3} a_i T^i \qquad (6\text{-}1)$$

and

$$T = \sum_{i=1}^{3} b_i \, e^i \qquad (6\text{-}2)$$

Coefficients a_i and b_i are listed in Table 6-1.

Table 6-1. Polynomial Coefficients.

Temperature Range	i	a_i		b_i	
		Value	Exponent	Value	Exponent
-50 C to 0 C	1	3.87408	1	2.58126	-2
	2	3.84373	-2	-7.39074	-7
	3	2.06663	-5	1.02788	-10
0 C to 120 C	1	3.85972	1	2.58126	-2
	2	4.28044	-2	-6.53650	-7
	3	-9.96760	-6	1.94253	-11

6.2.3 Volumetric Liquid Flow Rate

A turbine flow meter produces a frequency proportional to velocity, which, for a fixed cross-sectional area becomes volumetric flow rate. A pulse accumulator receives the signal and generates a voltage proportional to the total volume passing through the meter between scans. The volumetric flow during the time interval is calculated from:

$$\int_{0}^{\Delta t} \dot{V} dt = K(mV) \qquad (6\text{-}3)$$

where $\dot{V}$ is the flow rate (ℓ/s)

Δt is the time interval between resets of the pulse accumulator (5 min)

K is the conversion constant determined by calibration (ℓ/mV)

mV is the output voltage from the pulse accumulator.

6.2.4 Volumetric Air Flow Rate

A vane-type anemometer is calibrated so that output frequency is proportional to volumetric air flow rate through a duct. Frequency is converted to voltage and voltage is integrated over time. The volume of air flow during a time interval is calculated by Equation (6-3), where K differs from water turbine meters.

6.3 Thermal Energy Calculations

The method for calculating enthalpy flux in a fluid system is an approximation to the equation:

$$Q = \iiint \rho \dot{V} C_p dT dt \qquad (6\text{-}4)$$

ρ is density of the fluid (kg/ℓ)

C_p is the specific heat of the fluid (kJ/kg-C)

T is temperature (C)

t is time

Density and specific heat are temperature-dependent properties and the temperature and flow rate may vary with time. The product of density and specific heat is calculated as a function of fluid temperature nearest the flow meter and is assumed constant over the time interval between scans. A reference temperature is measured during the current scan and Equation (6-5) is used to calculate $\rho C_p(T)$ for water.

$$\rho C_p(T)[kJ/\ell C] = 4.22-0.001686*T[C] \qquad (6\text{-}5)$$

Temperature difference across a component is calculated as the simple average of the temperature difference at the previous scan and the current scan. Volumetric flow is determined by methods discussed in Sections 6.2.3 and 6.2.4. Equation (6-4) reduces to:

$$Q = \rho C_p(T) \int_{5=0}^{5min} \dot{V} dt \left[\frac{\Delta T_i + \Delta T_{i-1}}{2}\right] \qquad (6\text{-}6)$$

Heat flux calculations are made using Equation 6-6 for all scans, whether or not flow is in steady state. If flow rates and temperatures vary rapidly, errors will be introduced, but for long-term performance assessment, heat flux calculations using 5-minute scans have proven satisfactory. For transient conditions or energy flux meters ("Btu meters") with sensitive temperature sensors must be used.

7.0 CHILLER PERFORMANCE

The XWF-3600 chiller operated for 475 hours between July 15 and September 10, 1982. Chronological events during the summer are summarized in Table 7-1. Typical chiller performance can be seen in the time traces of several key parameters provided in Appendix A. Cooling capacities typically ranged from five to eleven kilowatts (1.4 to 3.1 tons) at thermal coefficients of performance between 0.65 and 0.75. Electrical power to operate the chiller solution pump and heat rejection fan averaged 0.43 kW during normal operation.

7.1 Quasi-Steady-State Performance

Quasi-steady-state conditions are characterized by (1) nominal settings of the internal control switches of the unit (see Chapter 4), (2) constant hot water supply and chilled water flow rates, and (3) little or no variation in the temperatures of hot water, chilled water, and ambient outdoor wet bulb.

7.1.1 Performance Map

Chiller performance can be described by steady-state performance graphs given in Figures 7-1, 7-2 and 7-3. These graphs (called maps) show capacity and coefficient of performance as functions of hot water supply temperature and ambient outdoor wet bulb temperature at three constant hot water flow rates. Curves were fitted to the data points by the least-squares method and satisfactory correlations were obtained for cooling capacity, CAP, and energy into the generator, Q_g. Thermal coefficients of performance were obtained by dividing capacity by Q_g determined by Equations (7-1) and (7-2).

Table 7-1. Summary of Experimentation -- ARKLA/BNL Project, Summer 1982.

WEEK OF	HOURS OF CHILLER OPERATION	CAPACITY FOR WEEK KWH	OPERATING RANGES						COMMENTS
			$T_{g,i}$ (C)	$T_{cw,i}$ (C)	T_{wb} (C)	$\dot{m}_g$ (kg/hr)	CAPACITY (kW)	COP	
June 1	0								BNL Arrive with Collectors
June 7	0								Failure of BNL Collectors Noted
June 13-19	0								System Reconfigured Boiler Modifications Made
June 20-26	0								Reconfiguration Continues Instrumentation Installed
June 27-July 3	0								System Modifications Completed Instrument Calibration
July 4-10	0								Instrument Calibrations System Shake-down
July 11-17	6.8	41.9	79.4-77.0	---	---	---	---	---	First Operation of Chiller DAS/Software Shake-down
July 18-24	90.3	657.4	83.3-76.4	19.0-12.0	20.0-9.7	2423	7.97-2.4	.770-.452	Small Heat Rejection Fan Blades Installed July 22
July 25-31	98.4	571.3	81.1-75.2	19.6-12.5	19.4-13.6	2423-1542	7.92-3.19	.759-.519	Lower Hot Water Flow Rates Tried for First Time July 30. Informed No BNL Collectors
August 1-7	90.4	586.2	88.3-76.0	19.0-12.2	20.6-15.6	2423-881	9.61-2.89	.734-.510	Large Heat Rejection Fan Blades Reinstalled Aug. 3. Three Ton Capacity Achieved Aug. 4
August 8-14	87.3	690.47	89.1-75.4	19.5-12.3	20.3-12.8	2357-881	11.14-3.44	.736-.447	Highest Capacities and COP Reached Aug. 10
August 15-21	78.3	520.66	85.8-77.1	22.3-11.0	22.2-9.4	2114-1322	9.44-5.72	.761-.579	Minimum Hot Water Temperature to Start. Raised to 82 C
August 22-28	3.4	20.26	83.3-78.1	14.2-12.3	18.3-17.2	1465	6.97-6.17	.689-.654	System Shut Down Aug. 23 To Prepare for Chamberlain Collector Installation
August 29-Sept. 4	0								Collector Installation Problems Persist. Chiller Piped Directly to Boiler
Sept. 5-11	23.5	155.4	79.5-75.5	17.5-12.7	15.7-11.7	2423-1101	7.89-5.67	.765-.604	Crystallization Problem Encountered Sept. 11
Total/Range	478.4	3244.0	89.1-75.2	22.3-11.0	22.2-9.4	2423-881	11.14-2.4	0.77-0.45	

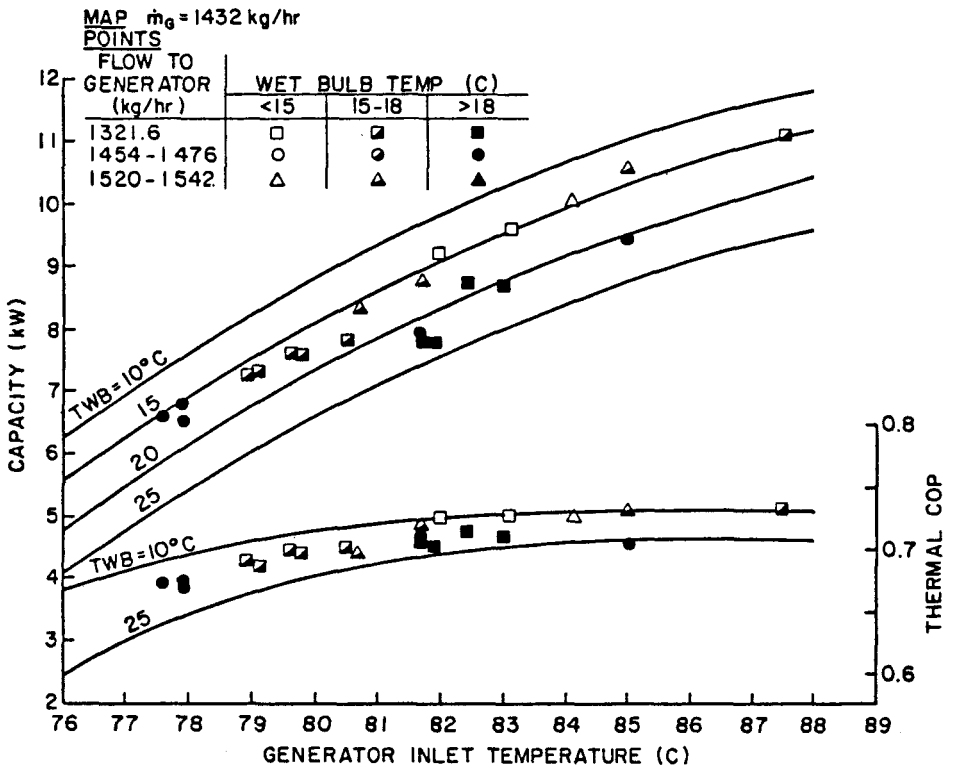

Figure 7-1. Performance map of Arkla XWF-3600 #7-2 evaporatively-cooled absorption chiller ($\dot{m}_g$ = 1432 kg/hr = 6.5 gpm).

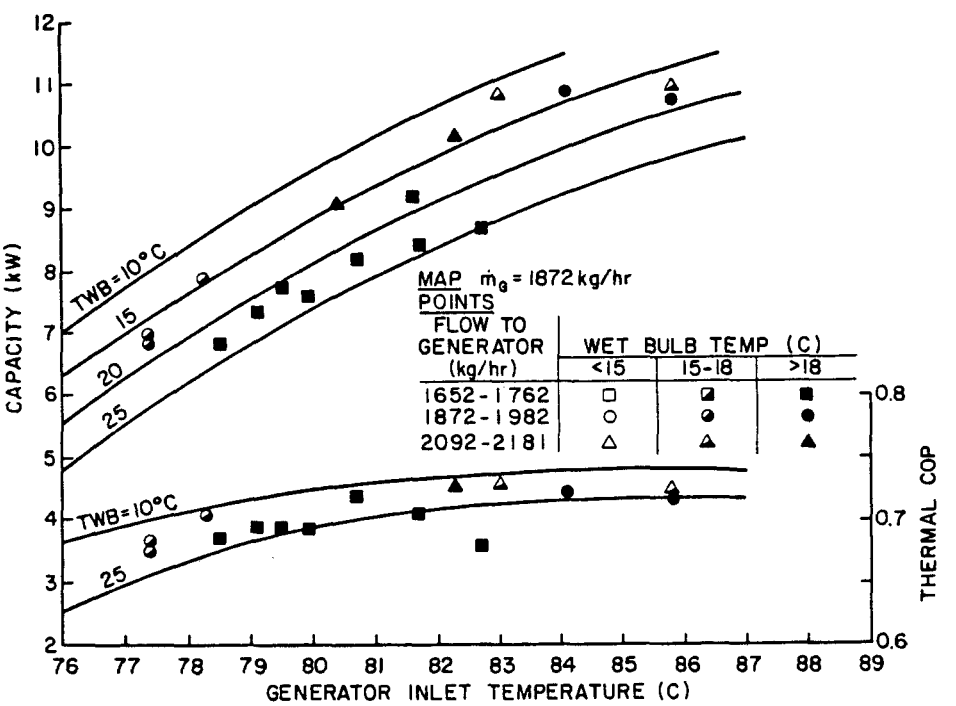

Figure 7-2. Performance map of Arkla XWF-3600 #7-2 evaporatively-cooled absorption chiller ($\dot{m}_g$ = 1872 kg/hr = 8.5 gpm).

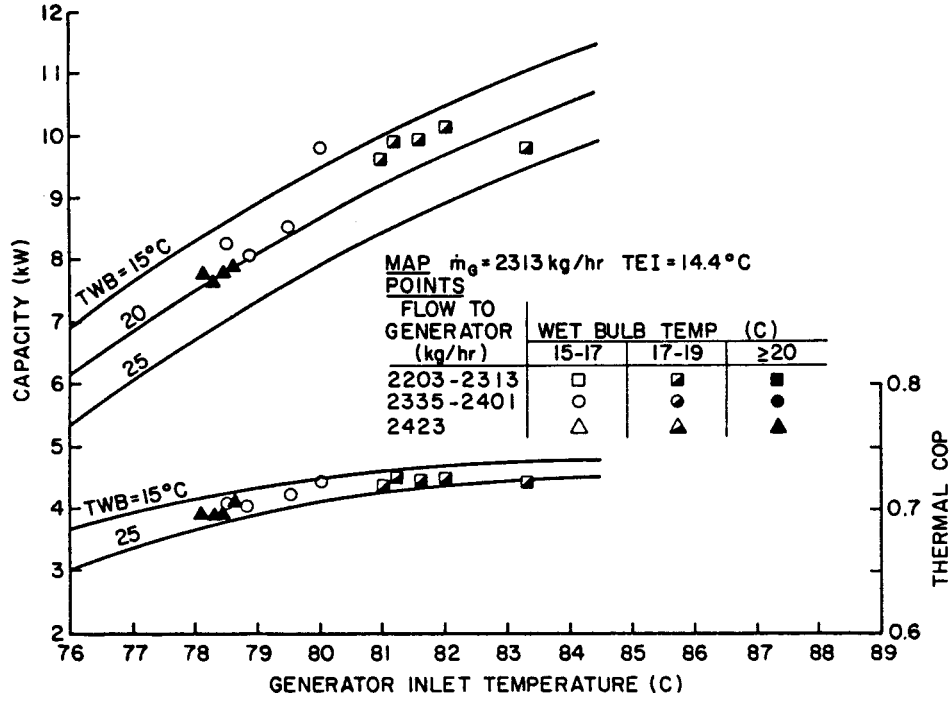

Figure 7-3. Performance map of Arkla XWF-3600 #7-2 evaporatively-cooled absorption chiller ($\dot{m}_g$ = 2313 kg/hr = 10.5 gpm).

$$CAP = 6.13 - 0.0218(T_{g,i}-78.)^2 + 0.639*(T_{g,i}-78.) - 0.149*(T_{wb}-16.) + 0.0013*(\dot{m}_g-881.) \quad (7\text{-}1)$$

$$Q_g = 9.30 - 0.0217(T_{g,i}-78.)^2 + 0.740*(T_{g,i}-78.) - 0.177*(T_{wb}-16.) + 0.0014*(\dot{m}_g-881.) \quad (7\text{-}2)$$

where

CAP = capacity (kW)

$T_{g,i}$ = generator hot water supply temperature (C)

T_{wb} = ambient outdoor wet bulb temperature (C)

$\dot{m}_g$ = mass flow rate of hot water (kg/hr)

Q_g = energy input to the generator (kW)*

*Complete nomenclature is listed in Section 11.

The data and derived equations show that cooling capacity increases about 0.5 kW for each 1 C rise in hot water supply temperature. Wet bulb temperature change has a smaller effect in that capacity decreases a little more than 0.1 kW for each 1 C rise. Increase in hot water flow rate of 220 kg/hr (1 gpm) improves cooling capacity about 0.3 kW.

Coefficient of performance (COP) is typically between 0.65 and 0.75 over a broad range of operating conditions. This factor is not very sensitive to the wet bulb temperature nor to temperature and flow rate of the hot water supply. For the conditions encountered in the summer of 1982, COP was generally above 0.7 but rarely exceeded 0.75 at hot water temperatures above 80 C.

For a complete performance map, an attempt was made to correlate chiller performance with all operating conditions, namely $T_{g,i}$, $\dot{m}_g$, T_{wb}, and chilled water inlet temperature, $T_{cw,i}$. The mass flow rates of air for heat rejection and of chilled water were essentially constant and could therefore be removed from consideration. The resulting correlations between chiller performance and operating conditions involve only three variables, $T_{g,i}$, $\dot{m}_g$, and T_{wb}. A meaningful relationship between chiller performance and $T_{cw,i}$ could not be established, mainly because there was insufficient range in the variation of this parameter at constant values of $T_{g,i}$, T_{wb} and $\dot{m}_g$. The inability to incorporate $T_{cw,i}$ into the correlations limits the usefulness of the performance map.

7.1.2 Influence of the Room Heat Exchanger (Cooling Coil)

The space cooling subsystem consists of the chiller and the water-to-air heat exchanger (cooling coil) that is located in the central air distribution duct. A schematic of the cooling subsystem appears in Figure 7-4. As described in Chapter 3, the absorption chiller can be thought of as five heat exchangers, which are generator, condenser, evaporator, absorber, and recuperator. When the chiller is integrated with a space cooling system, the cooling coil is the sixth heat exchanger that completes the system.

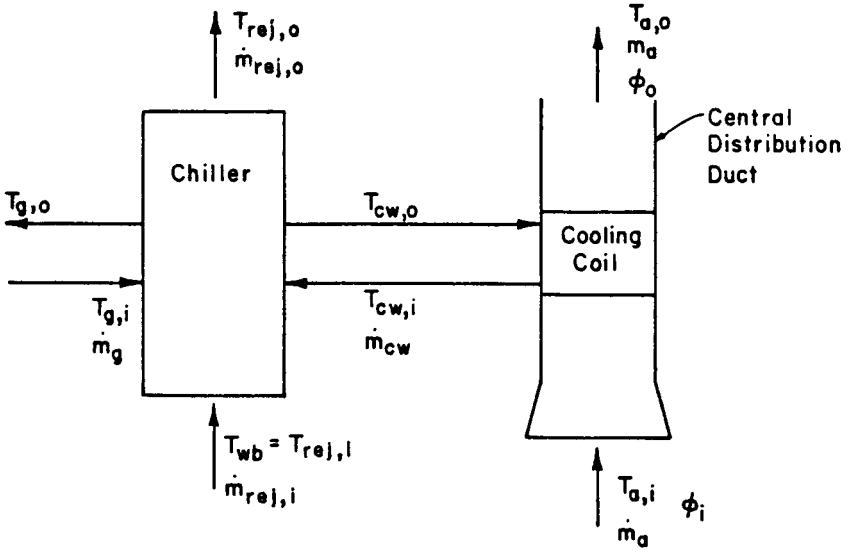

Figure 7-4. Schematic of space cooling subsystem.

The chiller was evaluated in a complete space cooling system, the performance of which depended on the operation of the cooling coil as well as the chiller. To evaluate the chiller-coil system performance, the operating conditions of interest are $T_{g,i}$, $\dot{m}_g$, T_{wb}, and return air

temperature, $T_{a,i}$, mass flow rate, $\dot{m}_a$, and relative humidity, ϕ. Since ϕ and $\dot{m}_a$, were essentially constant at 45 percent and 3190 kg/hr (1560 SCFM), they were not considered factors in appraising cooling system performance. Ordinarily $T_{a,i}$ would be reasonably constant as well, but the use of electric resistance air preheaters upstream of the cooling coil provided significant variation in this parameter. A correlation between cooling system capacity and $T_{g,i}$, $\dot{m}_g$, T_{wb}, and $T_{a,i}$ was obtained but is of little use in a general sense because it is specific to the system that operated in Solar House III. A model of the chiller, independent of the cooling system, would be of more general value. Such a model must include chilled water temperature as an operating variable.

The amount of energy transferred from air into chilled water, Q_T, can be expressed as:

$$Q_T = (\dot{m}C_p)_{air} \; \varepsilon(T_{a,i} - T_{cw,o}) \tag{7-3}$$

where

$(\dot{m}C_p)_{air}$ = the minimum capacitance flow rate to the cooling coil

ε = effectiveness of the cooling coil

$T_{a,i}$ = air temperature upstream of the coil

$T_{cw,o}$ = chilled water temperature out of the chiller.

It is assumed that piping heat gains between the chiller and cooling coil are negligible. The temperature difference in Equation (7-3) can be written to include $T_{cw,i}$, the temperature of chilled water entering the chiller, by considering the mass flow rate of chilled water.

$$Q_T = \frac{\varepsilon(\dot{m}C_p)_{air}\,(T_{a,i} - T_{cw,i})}{1 - \frac{\varepsilon(\dot{m}C_p)_{air}}{(\dot{m}C_p)_{cw}}} \qquad (7\text{-}4)$$

It was observed that the cooling coil operated at a nearly constant $\varepsilon(\dot{m}C_p)_{air}$ of 1775 $\frac{kJ}{hr\text{-}C}$. The capacitance flow rate of chilled water averaged 7845 $\frac{kJ}{hr\text{-}C}$. If the capacitance flow rates are held constant then Equation (7-4) reduces to:

$$Q_T = 2294.*(T_{a,i} - T_{cw,i})\ kJ/hr \qquad (7\text{-}5)$$

The coil capacity, Q_T, is shown in Figure 7-5 as a function of $T_{cw,i}$ for constant values of $T_{a,i}$.

The results of the cooling coil and chiller-coil system analyses can be combined so that the cooling capacity of the chiller can be described as a function of $T_{cw,i}$. Under steady-state conditions, the chiller cooling capacity is equal to the coil capacity. With $T_{g,i}$, T_{wb} and $\dot{m}_g$ constant, chiller capacity can be plotted against $T_{cw,i}$ as points on the lines of constant $T_{a,i}$ as shown in Figure 7-6. The result is a plot of the chiller capacity slowly rising with increasing $T_{cw,i}$, energy transferred at the coil falling with increasing $T_{cw,i}$, and the points of intersection representing the operating points of the chiller-coil cooling system.

As shown by the slowly rising curve in Figure 7-6, chiller capacity was not strongly affected by chilled water temperatures between 12 and 21 C, but this relationship must be viewed as a result derived from

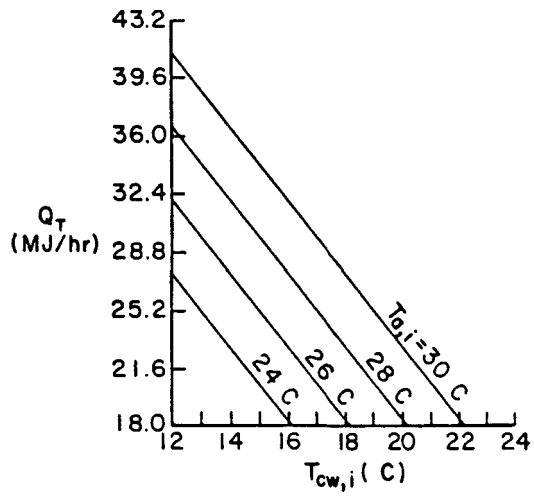

Figure 7-5. Cooling coil performance as a function of $T_{cw,i}$ and $T_{a,i}$.

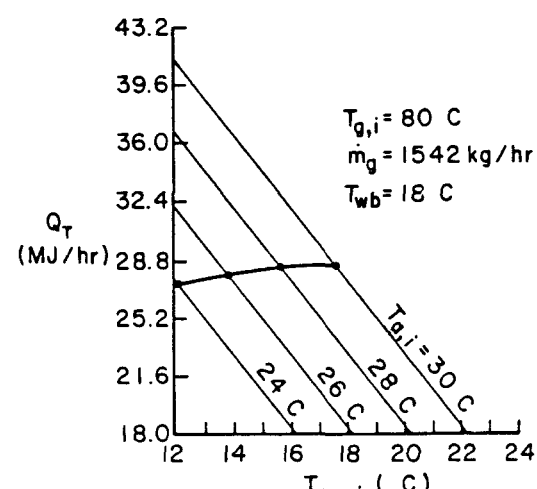

Figure 7-6. Cooling coil, chiller and cooling system performance as functions of $T_{cw,i}$ and $T_{a,i}$.

manipulation of data obtained with simultaneous variation in all of the operating conditions. The accuracy of the results is therefore limited and not of known levels. The results generally agree with data for the Yazaki absorption chiller described by Ward, et al [9].

For a given set of operating conditions, there is a minimum temperature at which cold water returning to the chiller has sufficient enthalpy to boil all of the refrigerant produced in the generator. Below this minimum temperature, a portion of the refrigerant does not evaporate and runs from the evaporator into the absorber with consequent reduction in capacity and COP. In view of the results, the 12.8 C temperature setting of the Arkla chilled water minimum temperature switch (see Chapter 4) is appropriate.

7.2 Transient Performance

The original objectives of the experiment included an evaluation of the overall seasonal performance of a solar cooling system. Measurement of system conditions every five minutes is adequate for this purpose. This schedule is not well suited, however, for examination of the transient performance of an absorption chiller in which time constants can be on the order of 5 minutes or less. With this limitation duly noted, examination of the transient performance of the XWF-3600 chiller is attempted.

The start-up or spin-up of the chiller is of primary interest, but the shut-down (spin-down) operation must also be examined because the unit does not stop immediately after the thermostat is satisfied. Both spin-up and spin-down were described in Chapter 4. Transient performance can also be encountered when the internal controls of the unit

respond to changes in various operating conditions. Of these cases, only the cycling of the heat rejection fan and its effects will be discussed.

7.2.1 Start-up Performance

Start-up transients that are examined involve cold start-ups, i.e. after the unit has been off for several hours and has approached ambient temperatures. Typical start-up data are shown in Figures 7-7, 7-8 and 7-9. The rise of capacity and energy transfer in the generator, Q_g, are normalized to steady-state values and shown as function of time.

The energy transferred in the generator begins to rise as soon as the thermostat calls for cooling and the hot water pump is started. As observed in Figure 7-7, it rises to a point slightly higher than its steady-state level before falling back to that level. The time constant for the start-up curve is approximately 3 minutes with Q_g reaching 98 percent of steady-state levels in about 12 minutes.

Figure 7-8 shows that no cooling is actually supplied during the first 3.5 minutes of operation. This delay is the combined result of not operating the chilled water pump during the first minute and the time required for generating sufficient refrigerant to begin the absorption cycle. The time constant for the start-up capacity curve, once cooling is produced, is approximately 5 minutes. Capacity rises to 98 percent of steady-state levels after about 24 minutes. The

	□	◇	△	▽	○	■	●
Date	8-10	8-15	8-15	8-16	8-19	8-20	8-20
Time	11:20	09:45	21:10	11:30	11:59	10:38	19:00
Off Time (hrs)	1.75	3.75	4	4	1.25	19	4.5
$T_{g,i}$(C)	90.3	84	84	83.9	84.3	84.0	81.0
T_{amb}	24.0	29.1	24.2	31.0	32.5	25.2	20.4
$\dot{m}_g$(kg/hr)	881	1322	1322	1322	2092	1476	1454
$\dot{m}_{cw}$	2115	1652	1652	1652	1652	1652	1674
∿Δt*(min)	1.2	0.8	1.4	0.85	0.85	0.97	1.28

*Δt - time between chiller start and start of chilled water pump (approx.)

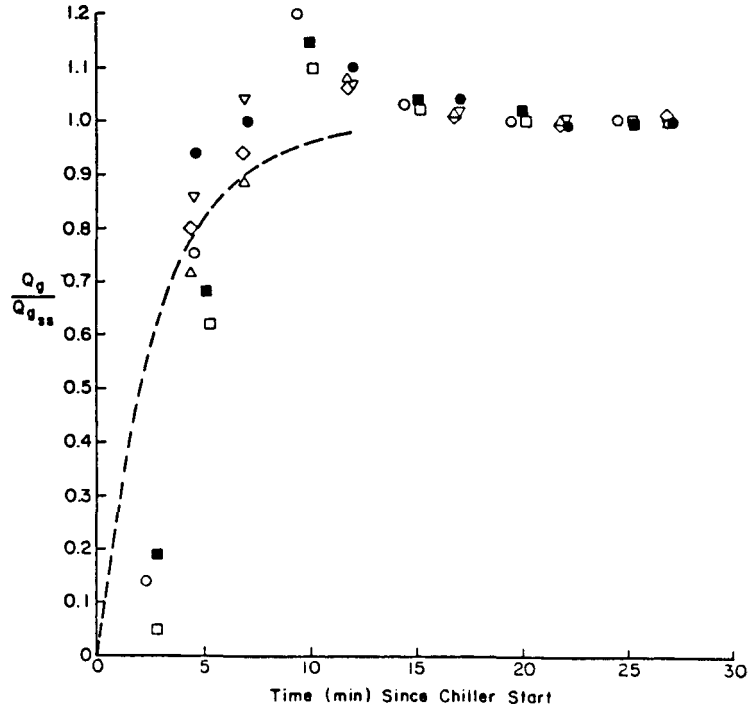

Figure 7-7. Energy input to generator, Q_g, at start-up.

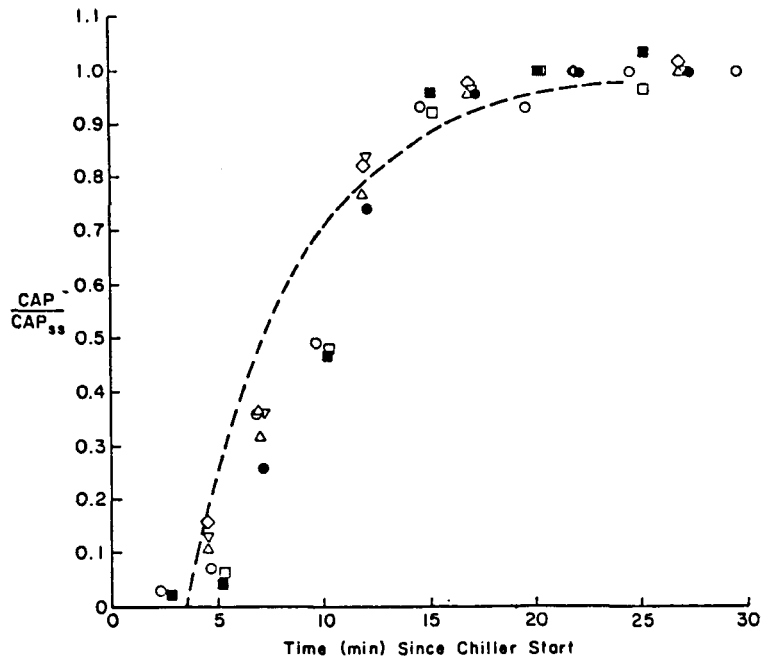

Figure 7-8. Capacity at start-up.

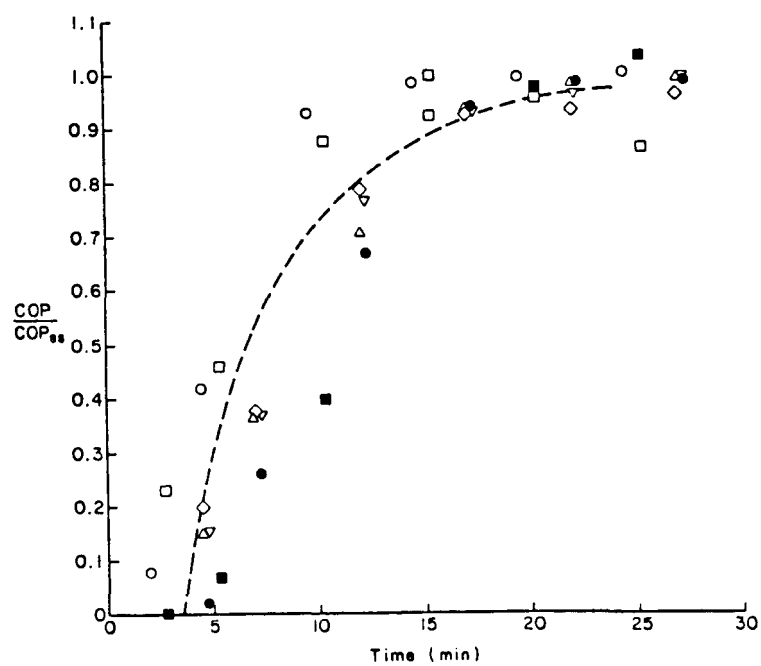

Figure 7-9. COP at start-up.

average thermal coefficient of performance (Figure 7-9) over the first 24 minutes of operation is approximately 70 percent of the steady-state COP.

7.2.2 Shut-down Performance

When the thermostat is satisfied, the generator pump stops immediately, but the chiller continues to operate for approximately 4 minutes with no energy input. During this spin-down period, refrigerant already in transit from the generator to the evaporator is used. The result is approximately 4 minutes of quasi-steady-state performance. This operation is illustrated in Figure 7-10. Energy is no longer being supplied to the generator so the condenser fan typically cycles off and on once during this period as the condenser cools. In most cases this cycling does not affect capacity, but if the fan cycles more than once, output declines rapidly as shown in Figure 7-11. The drop in capacity can probably be attributed to a rise in evaporator temperature and pressure due to interruption in the flow of air for heat rejection. Higher evaporator pressure causes an increase in the boiling point of the refrigerant and lessens the pressure difference between the condenser and evaporator. It is this pressure difference that forces refrigerant from condenser to evaporator.

7.2.3 The Effect of Heat Rejection Fan Cycling

The effect of cycling of the heat rejection fan has been described in the preceding section and in Chapter 4. Fan cycling typically

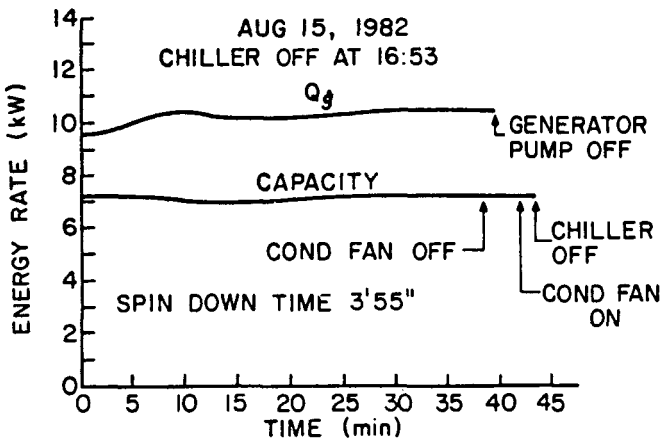

Figure 7-10. Typical chiller spin-down performance (spin-down time is time between generator pump shut off and chiller shut off).

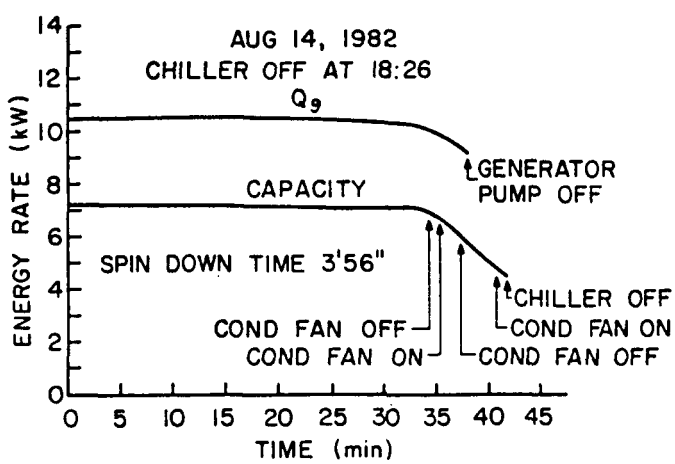

Figure 7-11. Spin-down performance with excessive fan cycling (spin-down is time between generator pump shut off and chiller shut off).

occurs in morning and evening when wet bulb temperatures are low or when hot water supply temperatures are low. The resulting reduction in chiller output is related to the amount of time the heat rejection fan is off. Capacity is temporarily reduced about 30 percent if the fan is off for 30 percent of the time.

Generator temperature rises when the heat rejection fan operates intermittently. Energy transfer rate in the generator is thus reduced. Heat transfer rate temporarily decreases approximately 20 percent if the fan is off for 30 percent of the time. The coefficient of performance during this period is unstable and typically drops by 10 percent.

7.3 Crystallization

Late in the cooling season the evaporatively-cooled chiller ceased to produce chilled water, and what was thought to be a failure of the unit turned out to be crystallization caused by refrigerant freeze up in the feed tube to the evaporator. In efforts to obtain operating data, with the chiller, experiments were being performed through periods of abnormally low ambient dry and wet bulb temperatures resulting in sub-freezing refrigerant temperatures. To prevent reoccurrence of the freezing condition, Arkla has added an air temperature sensor to the controls to prevent unit operation when the ambient dry bulb temperature is less than 15.5 C (60 F). Details of the problem and remedy are provided in Reference [10].

8.0 SOLAR COOLING SYSTEM SIMULATION

The Arkla chiller could not be operated with solar energy in 1982 because of the failure of the experimental collectors. It is of interest to know how the chiller would perform with energy supplied by a solar water heating system. Knowledge of the performance of an active solar cooling system using the Arkla XWF-3600 in different climates was also desired. Since it was not possible to obtain this information experimentally, a TRNSYS program was used to simulate the cooling system performance in four climates in the continental United States.

There are limitations on investigations of this kind. First, a solar system designed for a cooling load in Denver, Colorado, is not necessarily well-designed for Phoenix, Arizona. Second, the chiller model has been derived (see Appendix B) by comparing simulated performance with limited data obtained only in Fort Collins, Colorado, during the summer of 1982. For operating conditions outside the range of measured data, the performance map must be extrapolated. Finally, the results of the simulation are no better than the assumptions on which it is based. Chiller performance as a function of chilled water temperatures could not be reliably established. Either chiller performance must be assumed to be independent of chilled water temperatures, or, in different locations, cooling coil capacity must be assumed independent of return air temperature and relative humidity but dependent on chilled water temperatures exactly as in the experimental system. Neither of these assumptions is strictly valid, but the latter was used in the analysis.

8.1 The TRNSYS Model

In the TRNSYS model, a typical solar cooling system, comprising conventional flat-plate collectors, 4500 ℓ of water storage, and the Arkla chiller, is represented. The system supplies space cooling to a typical dwelling. Parameters applicable to commercially available systems were chosen. These parameters and the assumptions made in the modeling of each component are presented.

Cooling performance during a full day of operation in each of four locations was determined. The sites, each with a different type of summer climate, are: Denver, Colorado; Phoenix, Arizona; Washington, D.C.; and Miami, Florida.

8.1.1 Input Data

The meteorological data used to drive the system model are the Typical Meteorological Year (TMY) data prepared by the National Oceanic and Atmospheric Administration of the U.S. Department of Commerce. A full description of this data base is given in Reference [11]. The data (Appendix B) for one day at the beginning of July were selected in each location. These days are characterized by high insolation and ambient temperatures.

The radiation data used in the simulations are the "Standard Year" corrected data for total radiation on a horizontal surface (kJ/m^2). Total radiation on the fixed slope of a collector was computed by use of correlations by Liu and Jordan [12]. These correlations are incorporated in the TRNSYS Type 16 radiation processor. Collector slope was set equal to the latitude at each location.

Outdoor ambient dry bulb and dew point temperatures were also obtained from TMY data. Wet bulb temperature was calculated by use of psychrometric curve fits from ASHRAE which are available in the TRNSYS Type 33 Wet Bulb Calculation routine.

8.1.2 Collector-Storage Subsystem

A TRNSYS Type 21 Liquid Collector-Storage Subroutine was used in the simulation. The collector, heat exchanger (assumed to have an effectiveness of 1.), storage tank, pumps and controller are contained in this subsystem model. Flat plate collector performance was modeled with the Hottel-Whillier-Bliss equation.

$$\frac{Q_u}{A_c} = F_R\tau\alpha H_T - F_R U_L (T_i - T_a) = \frac{\dot{m} C_p}{A_c}(T_o - T_i) \qquad (8\text{-}1)$$

where (values used in the simulation appear in parentheses)

Q_u = useful energy collected

A_c = area of the collector ($56.34 m^2$)

F_R = heat removal factor

τ = transmissivity of the cover glass

α = absorptivity of the absorber surface ($F_R \tau\alpha = 0.8$)

H_T = incident radiation per unit area

U_L = collector loss coefficient ($F_R U_L = 17.58$ kJ/hr·m^2 - C)

T_i = fluid inlet temperature

T_a = ambient temperature

$\dot{m}$ = fluid mass flow rate (3000 kg/hr)

C_p = fluid specific heat (4.19 kJ/kg-C)

T_o = fluid outlet temperature

Heat storage is modeled as a single node tank containing 4.5 m^3 of water. The height to diameter ratio of the right cylindrical tank was taken to be 1. and the loss coefficient 3 kJ/C-m^2. Initial tank temperature was set at 75 C, two degrees below the minimum useful temperature for operating the chiller. The tank is assumed to be unpressurized so energy from the collectors is "dumped" when tank temperature would exceed 100 C.

8.1.3 Cooling Demand and Room Temperature Calculations

The energy/degree day concept has been shown by ASHRAE to be useful in estimating the monthly heating and cooling load of a residence. In this model, the concept is extended to estimate the hour-by-hour load with one-node capacitance and a floating room temperature. Space cooling determined in this manner may depart considerably from actual use, but the model offers an estimation of the load with a minimum of computational effort. For the purposes of modeling a typical residence and for comparing performance in different climates, it is considered adequate.

Thermal losses from the tank are assumed to be to the environment and not to the conditioned space. It is also assumed that the heat input to the house from people and other energy sources is equivalent to a constant heat generation of 3250 kJ/hr. Direct solar gain through windows is neglected. Net heat input into the building from sources other than HVAC system or ambient air temperature is therefore

$$\dot{Q}_{GAIN} = 3250 \text{ kJ/hr} \tag{8-2}$$

The rate at which sensible heat is gained by the building by transfer from the exterior and by internal generation is $-\dot{Q}_L$, whence, the cooling load,

$$\dot{Q}_L = UA\ (T_R - T_a) - \dot{Q}_{GAIN} \tag{8-3}$$

The effective heat loss coefficient, UA, for an energy efficient building is assumed to be 835 kJ/hr-C. Initial room temperature, T_R, is set at 23.5 C and initial ambient temperature, T_{amb}, is taken from TMY data.

The rate of heat removal by the chiller, $-\dot{Q}_{COOL}$, is divided into two parts, sensible and latent. The latent portion is taken as a constant fraction, ℓ_f, of the total. The latent fraction for Denver and Phoenix is taken to be 0.2, and for Washington, DC and Miami 0.3 is used. The net rate of sensible energy decrease in the house is

$$\dot{Q}_S = \dot{Q}_L - \dot{Q}_{COOL}\ (1 - \ell_f) \tag{8-4}$$

Room temperature is found by solving

$$\text{CAPHSE}\ \frac{dT_R}{dt} = \dot{Q}_S \tag{8-5}$$

where CAPHSE is the thermal capacitance of the building and t is time. The capacitance was chosen to be 20,000 kJ/C.

A summary of the nomenclature and definitions of heat flow quantities is as follows:

$\dot{Q}_{GAIN}$ = rate of internal heat generation in building

$\dot{Q}_L$ = the negative value of sensible heat flow rate into the building from conduction infiltration, and internal heat generation

$\dot{Q}_{COOL}$ = the negative value of the rate at which heat is removed from the building by the chiller (equal to chiller capacity for prevailing operating conditions)

$\dot{Q}_S$ = net rate of sensible energy decrease in the building

8.1.4 Room Thermostat

House temperature is controlled by a one-stage cooling thermostat. Cooling is indicated when the room air temperature is above 24 C. A temperature deadband of 2 C provides that once space cooling is initiated it continues until room temperature decreases to 22 C. If the temperature of water in storage is less than 77 C, solar cooling will not be used. The system model does not include use of auxiliary energy for cooling.

8.1.5 The Chiller

The chiller modeled is the Arkla XWF-3600 evaporatively-cooled absorption chiller with a nominal capacity of 37,980 kJ/hr. The unit has been described in preceding chapters and the TRNSYS model of this component is described in Appendix B. Parameters used in the simulation are listed below:

1. MODE 1 = steady-state operation
2. τ_{Q_g} = 0.05 hr = time constant for generator inflow start-up curve (not used in MODE 1)
3. τ_{CAP} = 0.0888 hr = time constant for capacity start-up curve (not used in MODE 1)

4. t_d = 0.0583 hr = time delay for start-up capacity curve (not used in MODE 1)

Start-up and shut-down transients are not considered, and steady-state performance is assumed whenever the unit is operating. This assumption is valid for "well-designed" systems in which the unit cycles only once or twice during the day. Start-up and shut-down transients, in this case, have a negligible effect on chiller performance.

8.1.6 Mixing Valve and Tee

When storage temperature exceeds 87 C and cooling is required, hot water returning from the chiller is mixed with hot water supply from the tank so that the maximum temperature to the chiller is 87 C. If the storage temperature is below 87 C, no mixing is done. The maximum supply temperature was set to ensure that the chiller performance model was not extrapolated beyond the range of operations at CSU.

8.1.7 Hot Water Supply Pump

The hot water supply pump for the chiller generator was modeled to provide 2423 kg/hr (11 gpm) whenever the thermostat called for cooling and when storage temperature was at least 77 C.

8.2 Results of the Simulation

Simulations were run with one-hour time steps. The results are summarized on an hourly and daily basis for each location in Tables 8-1 through 8-4. A more detailed simulation summary for each location appears in Appendix B.

Table 8-1. TRNSYS Simulation for Denver, Colorado.

MNEMONICS

HT	-INSOLATION ON A TILTED SURFACE	(MJ/M2)
QU	-USEFUL ENERGY COLLECTED	(MJ)
QLD	-ENERGY SUPPLIED TO LOAD FROM STORAGE	(MJ)
QTL	-ENERGY LOSSES FROM STORAGE	(MJ)
QDUMP	-ENERGY DUMPED WHEN STO. IS AT 100 C	(MJ)
QCOOL	-CHILLER CAPACITY	(MJ)
QG	-ENERGY SUPPLIED TO CHILLER GENERATOR	(MJ)
QSENS	-SENSIBLE HEAT REMOVED FROM AIR	(MJ)
QLAT	-LATENT HEAD REMOVED FROM AIR	(MJ)
TAMB	-AMBIENT DRY BULB TEMPERATURE	(C)
TWB	-AMBIENT WET BULB TEMPERATURE	(C)
TSTO	-STORAGE TANK TEMPERATURE	(C)
TGI	-INLET TEMP. TO CHILLER GENERATOR	(C)
TGO	-OUTLET TEMP. FROM CHILLER GENERATOR	(C)
TSR	-RETURN TEMPERATURE CHILLER TO STORAGE	(C)
TBP	-TEMP. OF WATER BYPASSED TO MIX VALVE	(C)
TRM	-ROOM TEMPERATURE	(C)
DE	-CUMULATIVE CHANGE IN STORED ENERGY	(MJ)
MG	-MASS FLOW TO CHILLER GENERATOR	(KG/HR)
MSR	-MASS FLOW OF RETURN TO STORAGE	(KG/HR)
MB	-MASS FLOW BYPASSED TO MIXING VALVE	(KG/HR)
GAM	-ON/OFF CONTROL FUNCTION TO CHILLER	
CEFF	-COLLECTOR EFFICIENCY	
COP	-THERMAL COEF. OF PERFORMANCE OF CHILLER	

TRNSYS SIMULATION FOR DENVER, COLORADO
ACTIVE SOLAR COOLING SYSTEM
---CONVENTIONAL FLAT-PLATE COLLECTORS
---ARKLA WF-3600#7-2 ABSORPTION CHILLER

SIMULATION SUMMARY

HOUR	TAMB	TWB	TSTO	TGI	TRM	HT	QU	CEFF	QCOOL	QG	COP
0.	23.0	13.3	75.0	0.0	23.5	0.00	0.00	0.000	0.00	0.00	0.000
1.	21.4	12.9	74.9	0.0	23.5	0.00	0.00	0.000	0.00	0.00	0.000
2.	20.6	12.6	74.8	0.0	23.6	0.00	0.00	0.000	0.00	0.00	0.000
3.	20.0	12.1	74.7	0.0	23.6	0.00	0.00	0.000	0.00	0.00	0.000
4.	18.9	11.8	74.5	0.0	23.6	0.00	0.00	0.000	0.00	0.00	0.000
5.	19.2	12.1	74.4	0.0	23.6	.05	0.00	0.000	0.00	0.00	0.000
6.	21.1	13.2	74.3	0.0	23.6	.18	0.00	0.000	0.00	0.00	0.000
7.	23.6	14.5	74.2	0.0	23.7	.78	0.00	0.000	0.00	0.00	0.000
8.	26.1	15.7	74.9	0.0	23.9	1.77	31.60	.316	0.00	0.00	0.000
9.	28.6	15.9	76.5	76.3	23.7	2.56	47.79	.471	-25.09	36.44	.689
10.	30.9	15.6	78.4	78.1	23.1	3.04	89.82	.525	-29.65	41.68	.711
11.	32.5	15.9	80.7	80.4	22.3	3.27	99.69	.541	-34.31	47.14	.728
12.	33.6	16.1	84.3	0.0	22.2	3.16	92.31	.518	0.00	0.00	0.000
13.	32.3	16.1	87.8	0.0	22.8	2.25	46.29	.365	0.00	0.00	0.000
14.	30.9	16.1	89.7	0.0	23.4	1.98	31.02	.278	0.00	0.00	0.000
15.	30.9	15.8	90.4	0.0	23.8	1.27	0.00	0.000	0.00	0.00	0.000
16.	28.7	15.4	88.5	87.1	23.4	.61	0.00	0.000	-44.03	59.39	.741
17.	26.2	15.0	86.8	0.0	22.8	.35	0.00	0.000	0.00	0.00	0.000
18.	25.6	14.9	86.7	0.0	23.1	.16	0.00	0.000	0.00	0.00	0.000
19.	25.3	14.8	86.5	0.0	23.4	.00	0.00	0.000	0.00	0.00	0.000
20.	24.5	14.7	86.4	0.0	23.6	0.00	0.00	0.000	0.00	0.00	0.000
21.	23.1	14.8	86.2	0.0	23.7	0.00	0.00	0.000	0.00	0.00	0.000
22.	21.7	14.7	86.1	0.0	23.8	0.00	0.00	0.000	0.00	0.00	0.000
23.	21.1	14.7	85.9	0.0	23.9	0.00	0.00	0.000	0.00	0.00	0.000
24.	21.1	14.7	85.8	0.0	24.0	0.00	0.00	0.000	0.00	0.00	0.000
DAY	25.2	14.5	81.5	80.4	23.4	21.42	458.52	.380	-133.08	184.65	.721

Table 8-2. TRNSYS Simulation for Phoenix, Arizona.

TRNSYS SIMULATION FOR PHOENIX, ARIZONA
ACTIVE SOLAR COOLING SYSTEM
---CONVENTIONAL FLAT-PLATE COLLECTORS
---ARKLA XWF-3600#7-2 ABSORPTION CHILLER

SIMULATION SUMMARY

HOUR	TAMB	TWB	TSTO	TGI	TRM	HT	QU	CEFF	QCOOL	QG	COP
0.	31.3	18.9	75.0	0.0	23.5	0.00	0.00	0.000	0.00	0.00	0.000
1.	31.2	18.7	75.0	0.0	23.7	0.00	0.00	0.000	0.00	0.00	0.000
2.	31.1	18.5	74.8	0.0	24.2	0.00	0.00	0.000	0.00	0.00	0.000
3.	31.1	18.4	74.7	0.0	24.6	0.00	0.00	0.000	0.00	0.00	0.000
4.	31.2	18.4	74.6	0.0	25.1	0.00	0.00	0.000	0.00	0.00	0.000
5.	31.3	18.5	74.5	0.0	25.5	0.00	0.00	0.000	0.00	0.00	0.000
6.	31.6	18.8	74.4	0.0	25.9	.11	0.00	0.000	0.00	0.00	0.000
7.	32.0	19.2	74.3	0.0	26.3	.80	0.00	0.000	0.00	0.00	0.000
8.	33.0	19.7	75.4	0.0	26.7	1.89	43.10	.405	0.00	0.00	0.000
9.	34.5	20.1	77.5	77.2	26.6	2.69	78.41	.518	-25.14	36.40	.691
10.	36.0	20.5	79.9	79.5	26.1	3.21	101.10	.559	-30.20	42.27	.714
11.	37.4	21.0	82.9	82.4	25.4	3.48	111.90	.570	-35.14	48.19	.729
12.	38.7	21.4	85.7	85.2	24.6	3.54	112.80	.566	-38.87	52.93	.734
13.	40.0	21.9	88.4	87.7	23.8	3.37	104.00	.548	-41.07	56.01	.733
14.	40.8	21.9	90.4	87.4	23.0	2.97	84.68	.506	-40.81	55.64	.733
15.	41.2	21.5	91.3	87.4	22.3	2.34	55.86	.424	-41.00	55.86	.734
16.	41.5	21.2	91.8	0.0	22.5	1.57	20.87	.236	0.00	0.00	0.000
17.	41.1	20.6	92.2	0.0	23.4	.56	0.00	0.000	0.00	0.00	0.000
18.	39.8	19.6	90.6	86.3	23.4	.07	0.00	0.000	-41.65	56.54	.737
19.	38.5	18.7	87.2	86.3	22.6	0.00	0.00	0.000	-41.58	56.34	.738
20.	36.8	17.8	85.6	0.0	22.6	0.00	0.00	0.000	0.00	0.00	0.000
21.	34.8	17.0	85.4	0.0	23.3	0.00	0.00	0.000	0.00	0.00	0.000
22.	32.7	16.2	85.3	0.0	23.8	0.00	0.00	0.000	0.00	0.00	0.000
23.	31.3	15.8	83.7	83.7	23.5	0.00	0.00	0.000	-40.50	54.72	.740
24.	31.3	15.8	81.1	81.5	22.5	0.00	0.00	0.000	-36.56	49.84	.734
DAY	35.2	19.2	82.1	84.1	24.2	26.59	712.72	.476	-412.52	564.74	.730

Table 8-3. TRNSYS Simulation for Washington, DC.

TRNSYS SIMULATION FOR WASHINGTON, D.C.
ACTIVE SOLAR COOLING SYSTEM
---CONVENTIONAL FLAT-PLATE COLLECTORS
---ARKLA XWF-3600#7-2 ABSORPTION CHILLER

SIMULATION SUMMARY

HOUR	TAMB	TWB	TSTO	TGI	TRM	HT	QU	CEFF	QCOOL	QG	COP
0.	22.3	21.4	75.0	0.0	23.5	0.00	0.00	0.000	0.00	0.00	0.000
1.	22.1	21.2	74.9	0.0	23.6	0.00	0.00	0.000	0.00	0.00	0.000
2.	22.0	21.0	74.8	0.0	23.7	0.00	0.00	0.000	0.00	0.00	0.000
3.	21.8	20.9	74.7	0.0	23.7	0.00	0.00	0.000	0.00	0.00	0.000
4.	22.0	21.0	74.6	0.0	23.8	0.00	0.00	0.000	0.00	0.00	0.000
5.	22.5	21.6	74.4	0.0	23.9	.02	0.00	0.000	0.00	0.00	0.000
6.	23.1	22.1	74.3	0.0	24.0	.15	0.00	0.000	0.00	0.00	0.000
7.	23.9	22.6	74.2	0.0	24.2	.45	0.00	0.000	0.00	0.00	0.000
8.	25.0	23.2	74.1	0.0	24.3	.87	0.00	0.000	0.00	0.00	0.000
9.	26.2	23.8	74.2	0.0	24.5	1.29	10.64	.146	0.00	0.00	0.000
10.	27.6	24.3	75.4	0.0	24.8	1.85	36.11	.346	0.00	0.00	0.000
11.	29.2	24.7	76.9	76.7	24.7	2.37	59.72	.447	-21.41	32.02	.669
12.	30.9	25.1	78.6	78.3	24.3	2.81	79.36	.501	-25.12	36.28	.692
13.	31.7	25.2	80.3	80.0	23.8	2.66	71.97	.480	-28.63	40.40	.709
14.	31.7	24.9	81.0	80.0	23.3	2.34	56.55	.429	-28.76	40.55	.709
15.	31.7	24.7	80.7	80.0	22.8	1.85	34.25	.334	-28.88	40.70	.710
16.	30.7	24.4	79.5	80.0	22.4	1.25	8.23	.116	-29.05	40.90	.710
17.	28.7	24.0	78.2	0.0	22.3	.67	0.00	0.000	0.00	0.00	0.000
18.	26.6	23.6	78.6	0.0	22.7	.18	0.00	0.000	0.00	0.00	0.000
19.	25.0	23.0	78.5	0.0	23.0	0.00	0.00	0.000	0.00	0.00	0.000
20.	23.7	22.1	78.3	0.0	23.2	0.00	0.00	0.000	0.00	0.00	0.000
21.	22.4	21.2	78.2	0.0	23.3	0.00	0.00	0.000	0.00	0.00	0.000
22.	21.6	20.7	78.1	0.0	23.4	0.00	0.00	0.000	0.00	0.00	0.000
23.	21.4	20.6	77.9	0.0	23.5	0.00	0.00	0.000	0.00	0.00	0.000
24.	21.4	20.5	77.8	0.0	23.6	0.00	0.00	0.000	0.00	0.00	0.000
DAY	25.4	22.7	76.9	79.2	23.6	18.76	357.33	.338	-161.85	230.85	.701

Table 8-4. TRNSYS Simulation for Miami, Florida.

TRNSYS SIMULATION FOR MIAMI, FLORIDA
ACTIVE SOLAR COOLING SYSTEM
---CONVENTIONAL FLAT-PLATE COLLECTORS
---ARKLA XWF-3600#7-2 ABSORPTION CHILLER

SIMULATION SUMMARY

HOUR	TAMB	TWB	TSTO	TGI	TRM	HT	QU	CEFF	QCOOL	QG	COP
0.	24.2	23.0	75.0	0.0	23.5	0.00	0.00	0.000	0.00	0.00	0.000
1.	23.6	22.9	74.9	0.0	23.6	0.00	0.00	0.000	0.00	0.00	0.000
2.	23.3	22.8	74.8	0.0	23.7	0.00	0.00	0.000	0.00	0.00	0.000
3.	23.3	22.8	74.7	0.0	23.9	0.00	0.00	0.000	0.00	0.00	0.000
4.	23.1	22.5	74.6	0.0	24.0	0.00	0.00	0.000	0.00	0.00	0.000
5.	23.1	22.5	74.4	0.0	24.1	0.00	0.00	0.000	0.00	0.00	0.000
6.	24.5	23.3	74.3	0.0	24.3	.09	0.00	0.000	0.00	0.00	0.000
7.	26.7	23.9	74.2	0.0	24.5	.67	0.00	0.000	0.00	0.00	0.000
8.	28.1	24.0	74.7	0.0	24.8	1.51	21.94	.258	0.00	0.00	0.000
9.	28.9	24.2	76.6	0.0	25.1	2.25	54.14	.427	0.00	0.00	0.000
10.	29.7	24.5	78.9	78.3	25.0	2.74	74.77	.485	-25.47	36.70	.694
11.	30.0	24.7	80.7	80.3	24.4	3.00	85.15	.503	-29.56	41.50	.712
12.	30.9	24.2	82.6	82.3	23.7	3.04	85.77	.501	-33.26	45.96	.724
13.	31.7	23.5	84.0	83.7	23.0	2.77	73.03	.468	-35.81	49.10	.729
14.	31.7	23.7	84.7	83.7	22.3	2.38	55.26	.412	-35.72	49.00	.729
15.	31.7	24.0	84.9	0.0	22.2	1.77	26.93	.271	0.00	0.00	0.000
16.	31.4	24.3	85.5	0.0	22.8	1.15	0.00	0.000	0.00	0.00	0.000
17.	31.1	23.9	85.4	0.0	23.3	.56	0.00	0.000	0.00	0.00	0.000
18.	30.3	23.9	85.3	0.0	23.7	.00	0.00	0.000	0.00	0.00	0.000
19.	28.6	24.0	83.8	83.8	23.5	0.00	0.00	0.000	-35.93	49.27	.729
20.	27.3	23.4	81.3	81.7	22.7	0.00	0.00	0.000	-32.78	45.36	.723
21.	26.4	23.2	80.2	0.0	22.4	0.00	0.00	0.000	0.00	0.00	0.000
22.	25.6	23.2	80.1	0.0	22.7	0.00	0.00	0.000	0.00	0.00	0.000
23.	25.0	23.2	79.9	0.0	23.0	0.00	0.00	0.000	0.00	0.00	0.000
24.	25.0	23.2	79.8	0.0	23.2	0.00	0.00	0.000	0.00	0.00	0.000
DAY	27.4	23.5	79.4	82.0	23.6	21.93	476.99	.386	-228.53	316.89	.721

8.2.1 Collector Efficiency

The simulation results for collection are also presented in Figures 8-1 through 8-4. As shown in the tables, the highest daily collector efficiency was obtained in Phoenix, η_c = 0.476, and the lowest in Washington, DC, η_c = 0.338. Useful daily energy collected ranged from 713 MJ in Phoenix to 357 MJ in Washington, D.C.

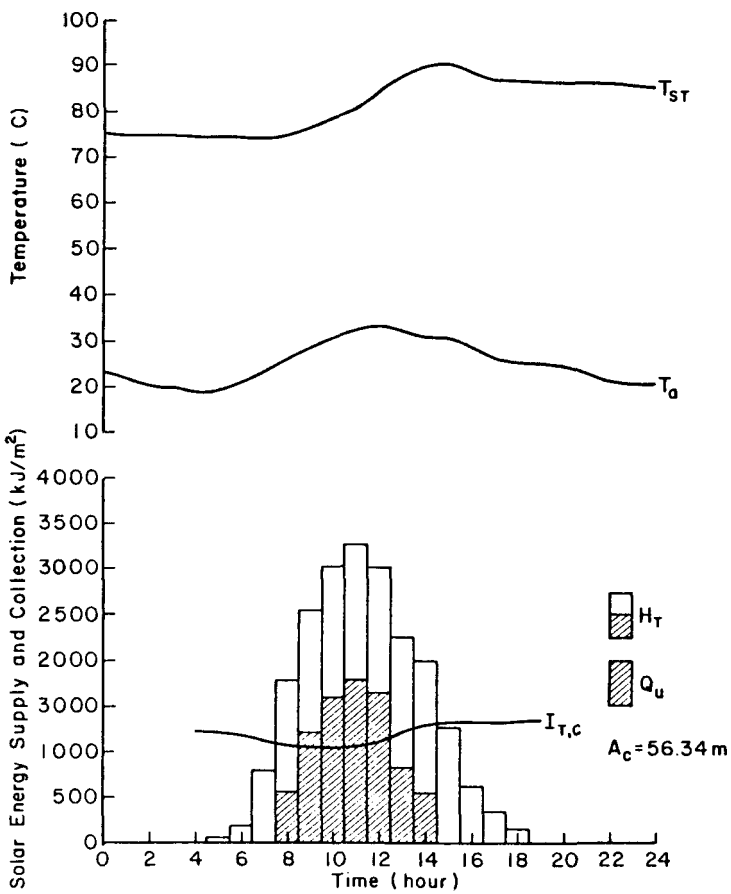

Figure 8-1. Simulated collection results for Denver, CO.

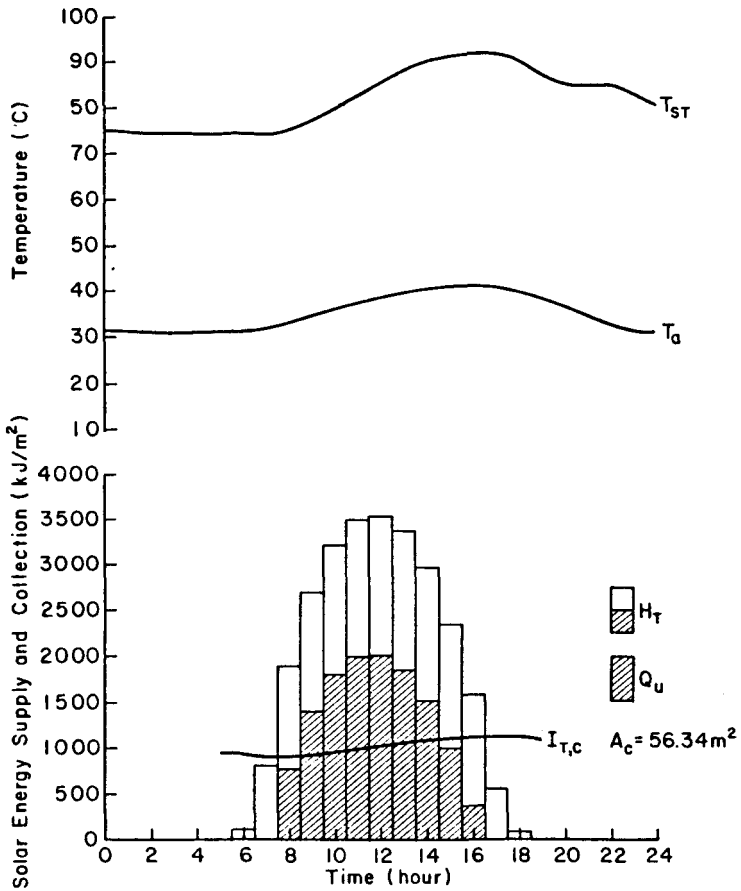

Figure 8-2. Simulated collection results for Phoenix, AZ.

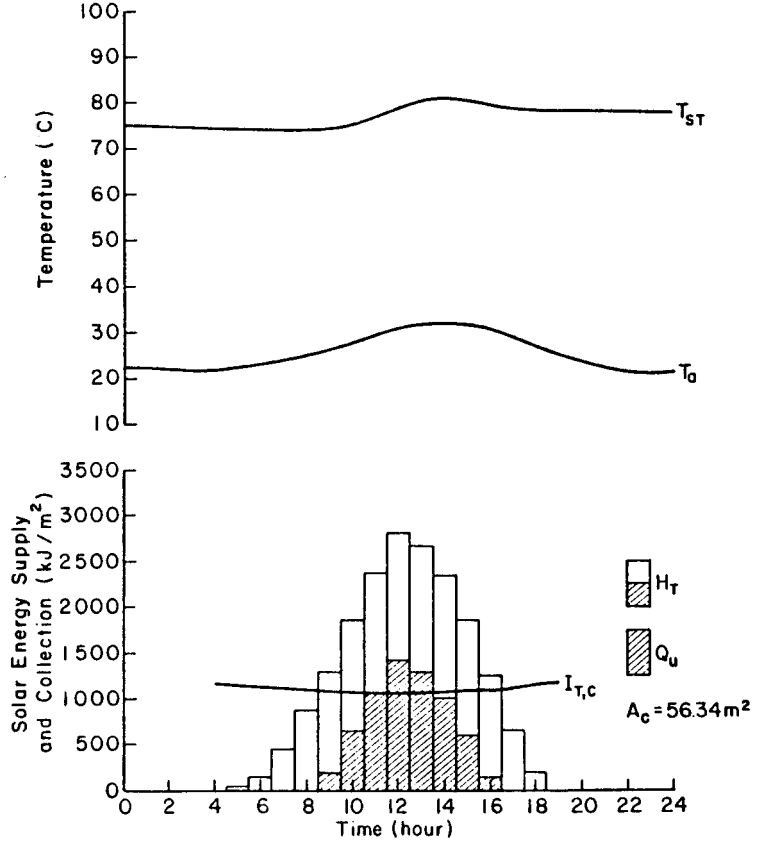

Figure 8-3. Simulated collection results for Washington, DC.

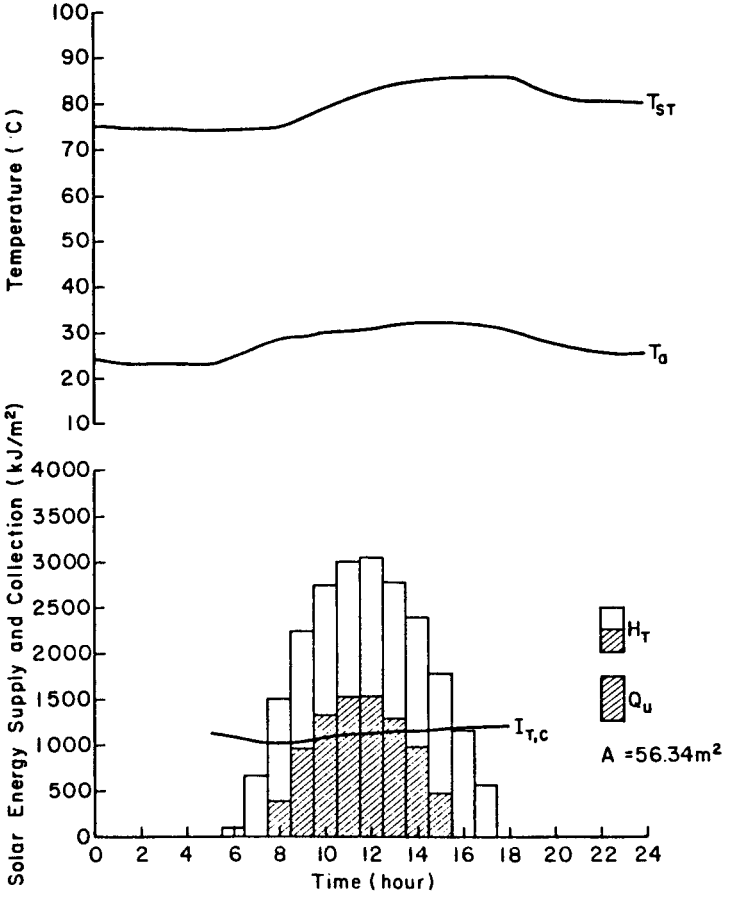

Figure 8-4. Simulated collection results for Miami, FL.

8.2.2 Cooling System Performance

The simulation results for the space cooling system are also shown in Figures 8-5 through 8-8. The initial temperatures in storage and conditioned space were set at 75 C and 23.5 C, respectively. These values are just below the minimum chiller operating temperature (77 C) and the temperature at which the thermostat calls for cooling (24 C). At each location, cooling could not be provided until enough solar energy was collected to raise the storage temperature to 77 C.

The results for Denver indicate that the entire cooling demand was met by the solar cooling system, room temperature not exceeding 24 C. The chiller provided 133 MJ of cooling capacity at a COP of 0.72. Average temperatures of hot water supply and ambient outdoor wet bulb during chiller operation were 80.4 and 15.7 C, respectively.

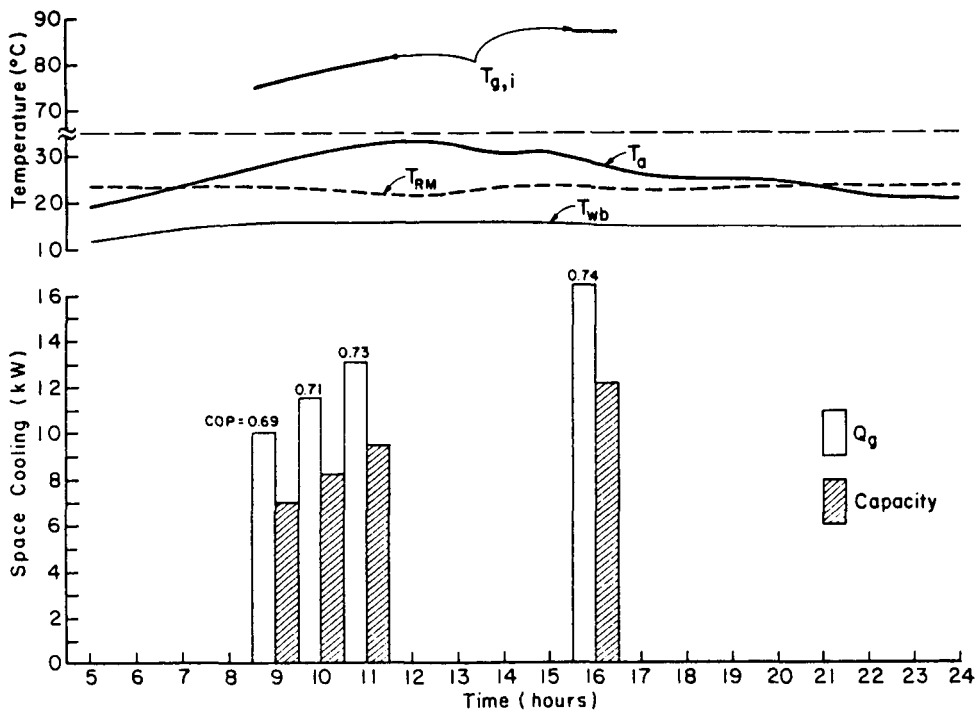

Figure 8-5. Simulated space cooling results for Denver, CO.

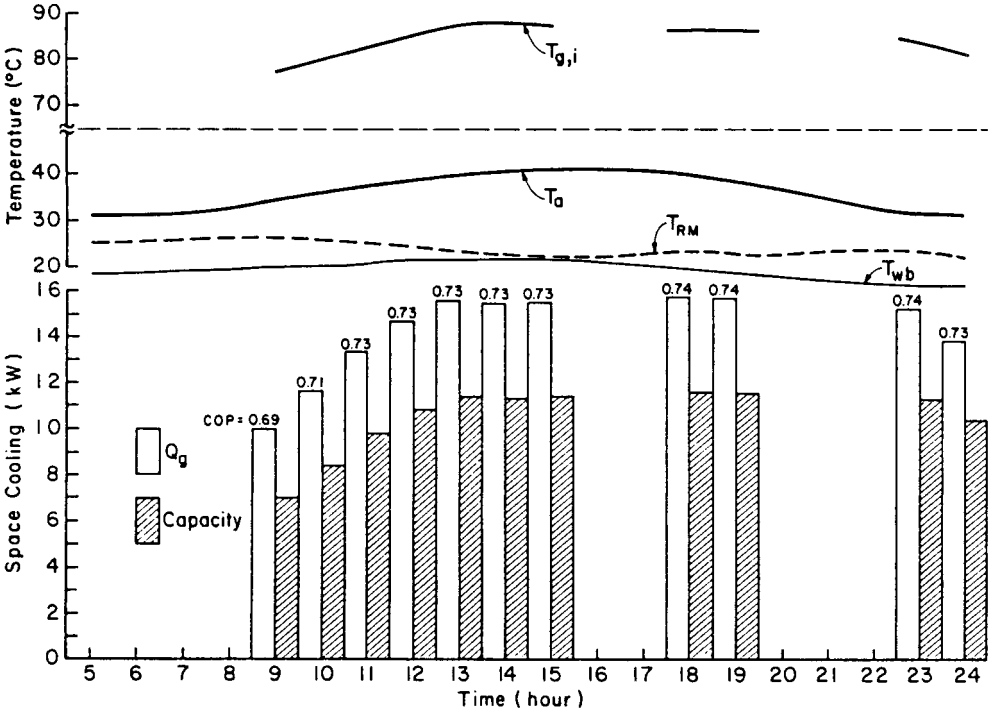

Figure 8-6. Simulated space cooling results for Phoenix, AZ.

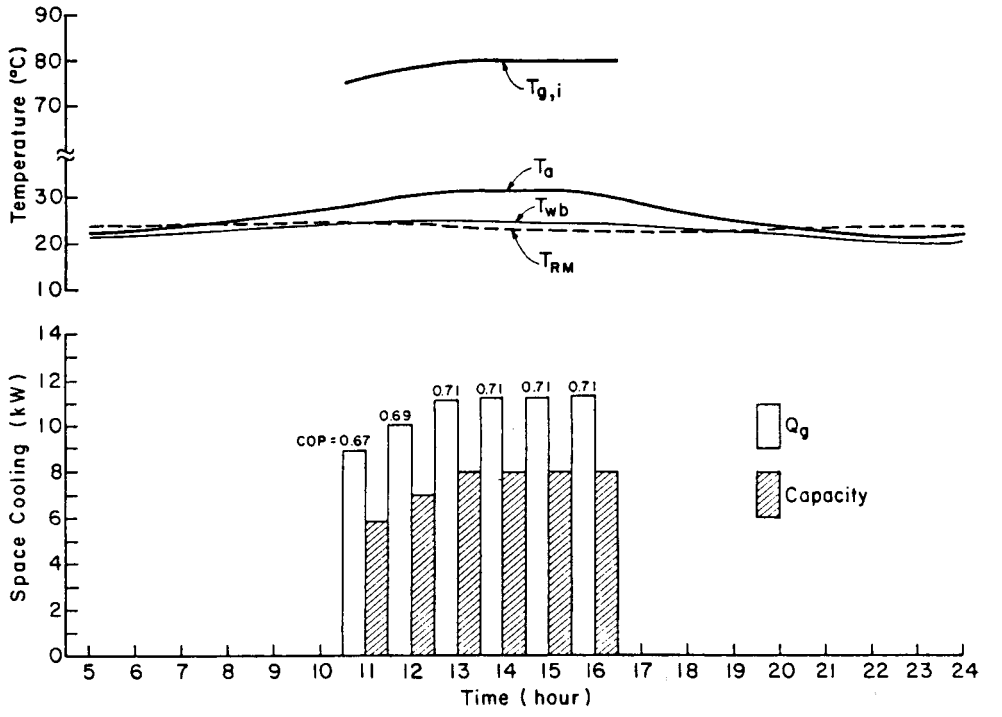

Figure 8-7. Simulated space cooling results for Washington, DC.

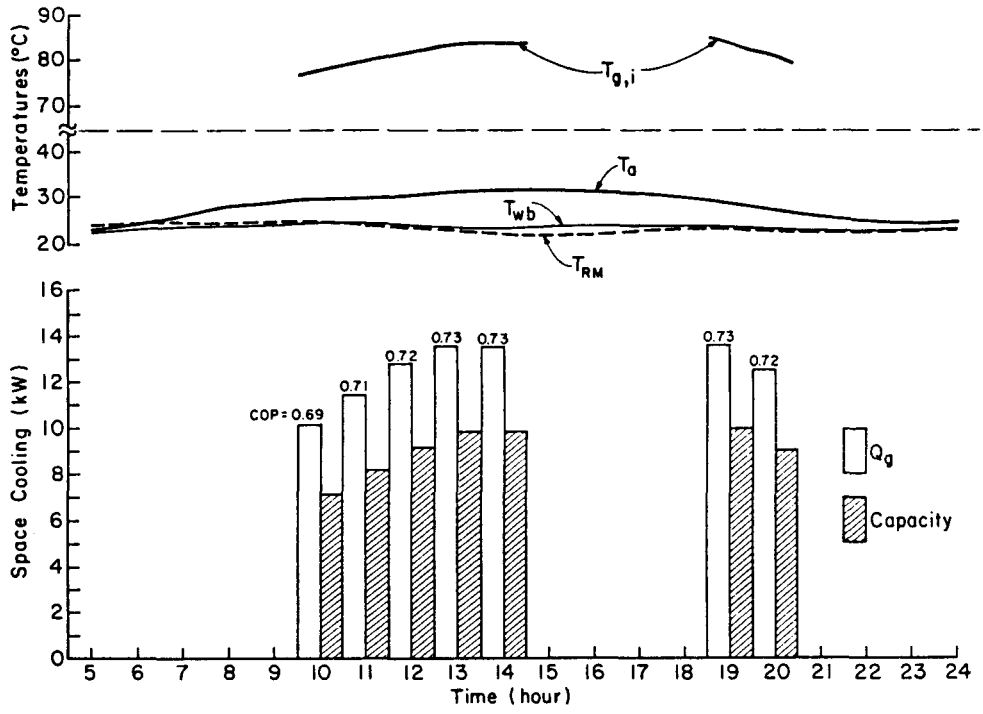

Figure 8-8. Simulated space cooling results for Miami, FL.

In Phoenix, room temperature reached 26.7 C before enough solar energy was collected to raise the storage temperature above 77 C. The solar cooling system then operated for eleven hours in three duty cycles providing 412 MJ of cooling at a COP of 0.73. Average temperatures of hot water supply and ambient outdoor wet bulb were 84.1 C and 19.8 C, respectively.

The Washington, D.C. results indicated a maximum room temperature of 24.8 C before space cooling could begin. The space cooling system provided 162 MJ of cooling in six hours of continuous operation at a COP of 0.70. Operating conditions included average hot water temperatures of 79 C and average wet bulb temperature of 25 C.

In Miami, room temperature reached 25 C before cooling could begin. The chiller operated for seven hours in two duty cycles providing 230 MJ of cooling at a COP of 0.72. Hot water supply temperatures averaged 82 C and wet bulb temperatures averaged 24 C while the chiller operated.

9.0 DISCUSSION AND RECOMMENDATIONS

The Arkla XWF-3600#7-2 evaporatively-cooled absorption chiller was tested over a broad range of operating conditions. Cooling capacities typically ranged from 6 kW to 11.5 kW at thermal coefficients of performance between 0.65 and 0.75. Capacity increases with hot water temperature and flow rate and decreases as outdoor wet bulb temperature rises. The thermal coefficient of performance was found to be relatively constant at hot water temperatures between 80 C and 90 C and at wet bulb temperatures between 15 C and 22 C.

Cooling capacity is primarily a function of the rate of heat transfer in the generator. Heat transfer rate in the generator, hence cooling capacity, can be modulated by varying hot water supply temperature and/or flow rate. Because solar heat supply is normally characterized by wide temperature variations, an absorption chiller operated with a solar system will often be subjected to "off-design" conditions, i.e., temperatures significantly different from that at which it operates at the design capacity. If supplied with solar-heated water at temperatures and flow rates appreciably higher than the design conditions, the chiller-cooling coil COP may decrease and, in the extreme case, crystallization may occur in the generator. The reasons for the decline in chiller-coil COP are described below in more detail. By providing suitable control of hot water supply temperature (by means of automatic by-pass and mixing of hot water) or by controlling hot water flow rate, these adverse operating conditions can be avoided. Greater system control flexibility may also be achieved.

Thermal coefficient of performance can be expected to rise with hot water supply temperatures, but at a decreasing rate, until it remains relatively constant at temperatures above 82 C. However, no discernable maximum in COP as a function of hot water supply temperatures, $T_{g,i}$, was found.

The second law of thermodynamics places a theoretical limit on chiller COP. A Carnot refrigerator driven by a Carnot heat engine would achieve that theoretical limit. Wilbur and Karaki [13] describe such a system and given the COP as:

$$COP_{carnot} = \frac{1 - \frac{T_{rej}}{T_{heat\ source}}}{\frac{T_{rej}}{T_{evap}} - 1} \qquad (9\text{-}1)$$

where

T_{rej} = ambient temperature to which heat is being rejected

$T_{heat\ source}$ = temperature at which heat is supplied to the heat engine

T_{evap} = temperature of the space heating cooled.

Equation (9-1) can be approximated by substitution of the operating temperatures in Equation (9-2)

$$COP_{carnot} = \frac{1-T_{wb}/T_{g,i}}{T_{wb}/T_{cw,o}-1} \qquad (9\text{-}2)$$

From (9-1), COP is zero when T_{rej} is equal to $T_{heat\ source}$. In the actual chiller, COP is zero when the input energy rate, Q_g, is just below that level required for generation of internal pressures sufficient to drive the absorption cycle. A maximum COP as a function of $T_{g,l}$ does not exist in theory, and none was found in practice.

In a particular chiller-cooling coil system, a maximum COP may exist at some specific level of $T_{g,l}$. Above that temperature, a decline in COP with rising $T_{g,l}$ is probably due to the direct "spilling" of liquid refrigerant off evaporator tubes into the absorbent pool in the bottom of the absorber. This situation can arise if the cooling coil is unable to remove heat from the room air at a rate which is equal to full chiller capacity at the prevailing operating conditions. The enthalpy of the cold water returning to the chiller will not be sufficient to boil all of the refrigerant produced in the generator. Thus, increasing hot water supply temperature will result in more "spilling" in the evaporator and further reduction in COP.

This performance penalty emphasizes the importance of sizing (or slightly oversizing) the water-to-air heat exchanger (cooling coil). Ample exchanger capacity is particularly important in dry climates where latent cooling load is small. Rates of air flow to the heat exchanger should also be somewhat higher than normal (1500-2000 SCFM for Solar House III and the chiller-coil used in 1982).

The effect of start-up transients in reducing thermal COP is mitigated to a large extent by spin-down operation. Based on the results of cold start-ups (unit at ambient temperature) and normal shut-downs, the average COP over those transient periods was approximately

90 percent of the steady-state values. In several cases, chiller capacity did not decline significantly over the entire spin-down period. This observation suggests that the spin-down time might be extended. Capacity did decline sharply during spin-down if the condenser fan cycled off and on more than once. This decrease is caused by a rise in evaporator temperature and pressure resulting from interruption of air flow and reduced heat rejection from absorber and condenser. Heat rejection from the absorber should continue during spin-down and should be interrupted only at the condenser if the condenser temperature falls below acceptable levels. That strategy was used in Solar House I during the summer of 1981. In that operation, cooling water flow to the condenser was occasionally interrupted while the heat rejection fan continued to operate and the absorber continued to be evaporatively cooled. It should be noted that the effect of spin-down is small (< 4 percent increase in COP) for duty cycles of two or more hours.

10.0 CONCLUSIONS

A solar space cooling system was installed and instrumented in CSU Solar House III. The system consisted of an array of low cost plastic collectors developed at Brookhaven National Laboratory (BNL), 4500 ℓ water thermal storage tank, a 10.55 kW (3-ton) evaporatively cooled absorption chiller, a three-ton, air-to-air heat pump as an auxiliary air conditioner, and a microprocessor controller. Failure of the BNL collectors prevented solar operations of the system, but a detailed performance evaluation of the chiller was conducted. From this evaluation it is concluded that:

1. Capacities in excess of 10.55 kW (3-ton) can be achieved at hot water supply temperatures of 80 to 90 C, compatible with flat plate collectors of good performance characteristics ($F_R \tau\alpha \geq 0.7$ and $F_R U_L \leq 4.0$ W/m^{2}C).

2. The capacity of the chiller is affected by, in order of importance, hot water temperature, hot water flow rate, and ambient outdoor wet bulb temperature. Performance maps of capacity and energy into the generator have been developed for the following ranges of operating conditions:

hot water supply temperature	:	76-90 C [169-194 F]
hot water flow rate	:	880-2420 kg/hr [4-11gpm]
ambient outdoor wet bulb temperature	:	12-22 C [54-74 F]

3. The effect of hot water flow rate on chiller performance indicates that cooling capacity may be controlled by adjusting the flow rate in accordance with prevailing operating conditions.

4. The dependence of chiller performance on chilled water temperature and flow rate could not be established because of insufficient variation in this parameter.

5. Since chiller performance is directly affected by the capacity of the water-to-air heat exchanger, its proper sizing and adequate air flow rates are essential to utilization of full chiller capacity.

6. The coefficient of performance (COP) was generally above 0.7 (but rarely over 0.75) at hot water temperatures above 80 C. The major effect of increasing hot water temperatures is an increase in capacity.

7. The degrading effect of start up transients on the overall thermal COP have largely been mitigated by spin-down operation (allowing the unit to continue running for four minutes after hot water flow to the generator has stopped). Average COP during spin-up and spin-down periods is approximately 90 percent of the steady-state value.

8. COP during the start-up/shut-down period might be improved by extending the spin-down period and allowing continuous evaporative cooling of the absorber during spin-down. The effect of this improvement on chiller performance for duty cycles greater than 2 hours would be small.

9. A TRNSYS-compatible chiller model has been shown to agree well with measured data. The model incorporates steady-state performance relations as well as start-up, shut-down, and heat rejection fan cycling transients. Verification of the modeling of transient performance with measured data remains to be done.

10. Simulation results show that on hot sunny days in four types of summer climates (including Phoenix), a good quality 56 m^2 flat plate collector and the XWF-3600 chiller can provide 2 to 3 tons of cooling for 6 to 9 hours and maintain room temperatures below 25 C (27 in Phoenix) in the typical house used in the analysis.

11. Simulation computations show a maximum daily cooling delivery of 412 MJ (32 ton-hours), in Phoenix, representing 27 percent of incident solar radiation (overall conversion of solar energy to cooling), at ambient temperatures reaching 41.5 C (107 F) in mid-afternoon.

11.0 NOMENCLATURE

A_c	-	collector area
CAP	-	cooling capacity
CAPHSE	-	house capacitance
COP	-	coefficient of performance
C_p	-	constant pressure specific heat
e	-	microvolts corresponding to temperature on thermocouples conversion curve
Δe	-	thermopile output (microvolts)
F_{cw}	-	volumetric flow rate of chilled water
F_g	-	volumetric flow rate of hot water to generator
F_R	-	collector heat removal factor
H_T	-	incident radiation per unit area
ℓ_f	-	latent fraction of cooling load
$\dot{m}$	-	mass flow rate
$\dot{m}_a$	-	mass flow rate of air
$\dot{m}_{cw}$	-	mass flow rate of chilled water
$\dot{m}_g$	-	mass flow rate of hot water supplied to chiller generator
$\dot{m}_r$	-	mass flow rate of refrigerant
$\dot{m}_{rej}$	-	mass flow rate for heat rejection
$\dot{m}_s$	-	mass flow rate of solution
MODE	-	mode of operation used in TRNSYS chiller model
Q_{COOL}	-	negative of chiller capacity (used in simulation)
Q_g	-	heat supplied to generator
Q_{GAIN}	-	heat addition to conditioned space from internal generation

Q_L	-	heating and cooling load (negative for cooling)
Q_S	-	rate of sensible heat gain in building
Q_T	-	heat transferred at cooling coil
Q_u	-	useful energy collected
t	-	time
t_d	-	time delay between chiller start and production of cooling capacity
T	-	temperature
ΔT	-	temperature difference
T_a	-	ambient outdoor dry bulb temperature
$T_{a,i}$	-	air temperature upstream of cooling coil
$T_{a,o}$	-	air temperature downstream of cooling coil
$T_{cw,i}$	-	chilled water temperature into chiller
$T_{cw,o}$	-	chilled water temperature out of chiller
$T_{g,i}$	-	hot water supply temperature to chiller
$T_{g,o}$	-	hot water return temperature from chiller
T_i	-	fluid temperature at inlet to collector
T_o	-	fluid temperature out of collector
T_R	-	room temperature
T_{rej}	-	heat sink temperature for chiller
T_{wb}	-	ambient outdoor wet bulb temperature
U_L	-	collector thermal loss coefficient
α	-	absorptance
ε	-	effectiveness
η_c	-	collector efficiency
τ	-	transmittance

τ_{CAP} - time constant for start-up curve of chiller capacity

τ_{QG} - time constant for start-up curve of generator inflow

ϕ - relative humidity

12.0 REFERENCES

1. Doesken, N.J., McKee, T.B., Ebel, D.M., "Colorado Solar Radiation Data," Colorado Climate Center, Department of Atmospheric Science, Colorado State University, Fort Collins, CO, Climatology Report No. 82-2, August 1982.

2. Andrews, J.W. and Wilhelm, W.G., "Thin-Film Flat-Plate Solar Collectors for Low-Cost Manufacture and Installation," BNL 51124, March 1980.

3. Wilhelm, W.G., "Low-Cost Solar Collectors Using Thin-Film Plastic Absorbers and Glazings," Proc. Am. Sec. ISES Ann. Mtg., Phoenix, AZ, June 1980.

4. Sharp, M.K., "Thermal Stratification in Liquid Sensible Heat Storage," M.S. Thesis, Mechanical Engineering Department, Colorado State University, Fort Collins, CO, 1978.

5. Lof, G.O.G., Duff, W.S., Hancock, C.E., Swartz, D., "Performance of Eight Solar Heating and Cooling Systems in CSU Solar House I, 1980-1981," Final Report, No. COO-30122-27 and No. SAN-30569-14, Colorado State University, Solar Energy Applications Laboratory, Fort Collins, CO, June 1982.

6. ASHRAE Standard Measurement Guide, Section on Temperaure Measurements, ASHRAE No. 41.1-74, New York, March 1974.

7. Benedict, R.P., Fundamentals of Temperature Pressure and Flow Measurements, John Wiley and Sons, New York, 1977.

8. Thermocouple Reference Tables Based on IPTS-68, U.S. Department of Commerce, NBS Monograph 125, Washington, DC, March 1974.

9. Ward, D.S., Lof, G.O.G., Uesaki, T., "Cooling Subsystem Design in CSU Solar House III," Solar Energy, Vol. 20, pp. 119-126, Pergamon Press, 1978.

10. Merrick, R.H. and Murray, J.G., "Evaporatively Cooled Chiller for Solar Air Conditioning Systems Design and Field Test," Topical Report, DOE Contract #DE-AC03-77CS-34593, Arkla Industries, September 1983.

11. SOLMET, "Hourly Solar Radiation - Surface Meteorological Observation: Users Manual," National Climatic Center, Asheville, NC.

12. Liv, B.Y.H. and Jordan, R.C., "The Interrelationship and Characteristic of Direct, Diffuse and Total Solar Radiation," Solar Energy, Vol. VI, July 1960.

13. Wilbur, P.J. and Karaki, S., "Solar Cooling," The Franklin Institute Press, Philadelphia, PA, 1977.

14. "TRNSYS - A Transient Simulation Program," Solar Energy Laboratory, University of Wisconsin-Madison, Madison, WI, June 1979.

13.0 ACKNOWLEDGEMENTS

The project was financially supported by the Conservation and Solar Applications Division of the U.S. Department of Energy. The authors wish to express their appreciation to the personnel of Arkla Industries, Inc., especially Mr. Richard Merrick, Mr. Joe Murray, and Mr. Terry Ferguson for their technical assistance throughout the project; also to the personnel of Brookhaven National Laboratory, especially Mr. John Andrews, Mr. William Wilhelm, Mr. Paul LeDoux and Mr. David Hanson. Appreciation must also be expressed to members of the laboratory staff, technicians, graduate students and others for their assistance during the project and particularly to Ms. Jill Oesterle and Mrs. Wendy Asa and others in the preparation of this report.

APPENDIX A

CHILLER/COIL PERFORMANCE

APPENDIX A

Time Traces of Key Parameters of Chiller-Coil Performance

Typical chiller-cooling coil performance can be seen in the time traces of several key parameters in Figures A-1, A-2, and A-3. The time traces are based on measurements made every five minutes. The sensivity of system performance to hot water temperatures and flow rates, wet bulb temperature and cycling of the heat rejection fan can be seen. the nomenclature used in the figures and in the text of the report is the same and is repeated below for convenience.

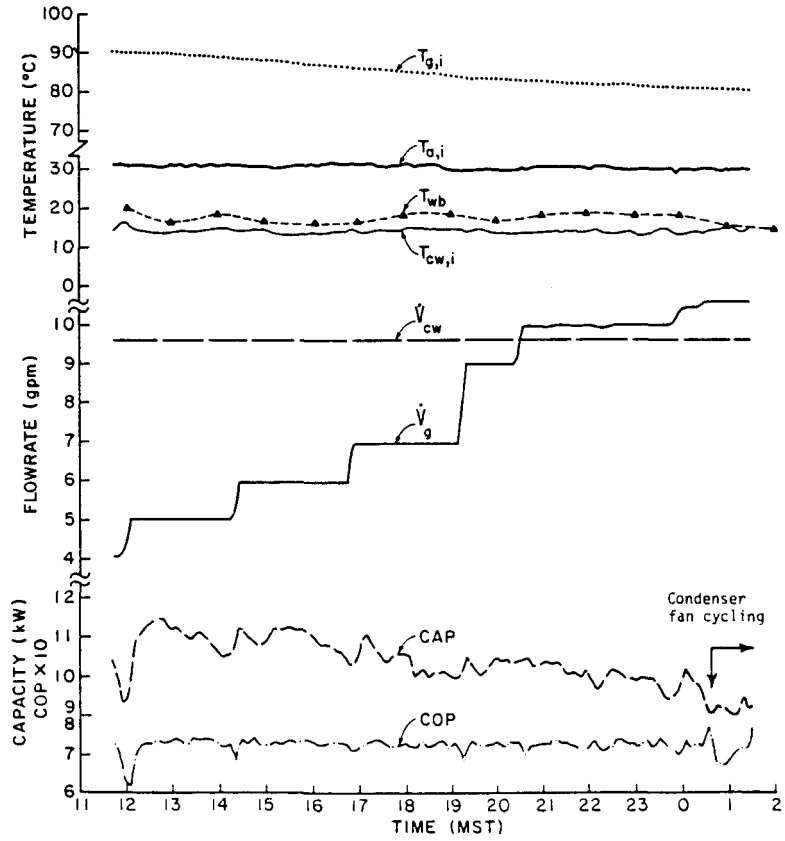

Figure A-1. Time trace of chiller-cooling coil performance and key operating parameters for August 10, 1982.

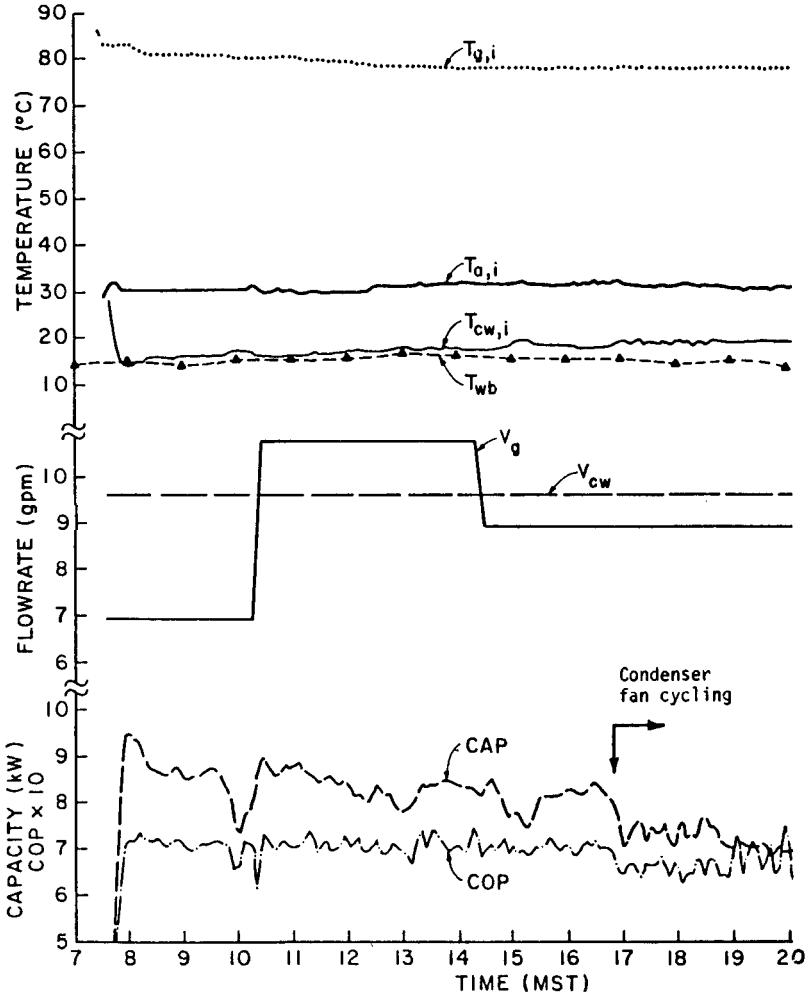

Figure A-2. Time trace of chiller-cooling coil performance and key operating parameters for August 12, 1982.

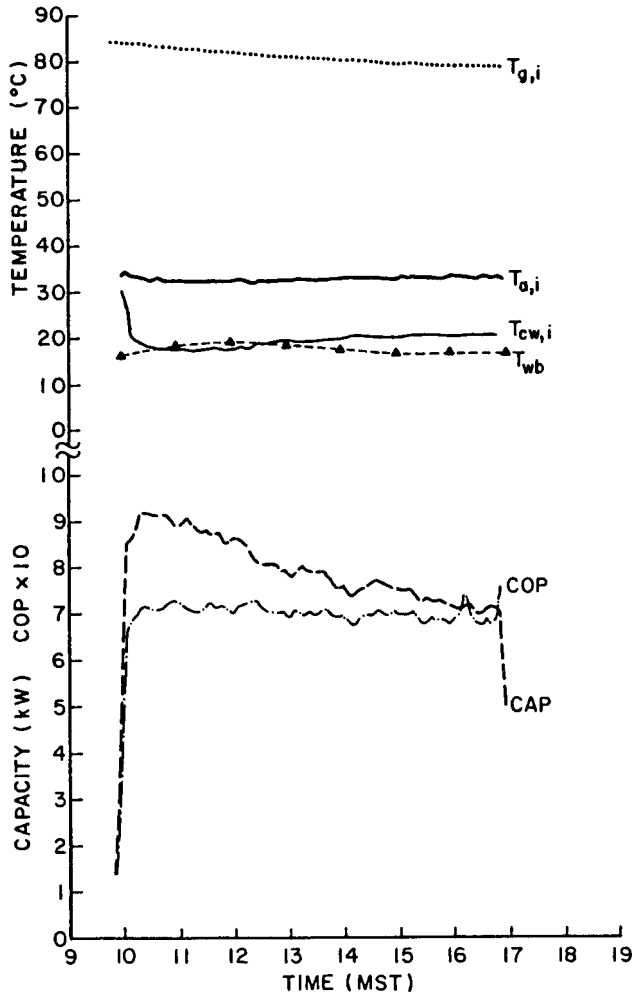

Figure A-3. Time trace of chiller-cooling coil performance and key operating parameters for August 15, 1982.

CAP	-	cooling capacity of the chiller (kW)
COP	-	thermal coefficient of performance
F_{cw}	-	volumetric flow rate of chilled water (gmp)
F_g	-	volumetric flow rate of hot water (gmp)
$T_{a,i}$	-	air temperature upstream of the cooling coils (C)
$T_{cw,i}$	-	chilled water temperature into the chiller (C)
$T_{g,i}$	-	hot water supply temperature (C)
T_{wb}	-	ambient outdoorwet bulb temperaure (C)

APPENDIX B

TRNSYS SIMULATIONS

Nomenclature

CAP	-	chiller cooling capacity
CAP_{ss}	-	steady-state cooling capacity
Q_g	-	energy inflow to the generator
$Q_{g,ss}$	-	steady-state generator inflow of energy
$\dot{m}_g$	-	mass flow rate of hot water to the generator
$T_{g,i}$	-	temperature of hot water supply to the generator
$T_{g,o}$	-	temperature of hot water return from the chiller
T_{wb}	-	ambient outdoor wet bulb temperature
t	-	time the chiller has been on
t_d	-	time between chiller start and production of significant cooling capacity
τ_{CAP}	-	time constant for cooling capacity start-up curve
τ_{QG}	-	time constant for generator inflow start-up curve
t_{OFF}	-	percent of time heat rejection fan is off during the time step
ε_{CAP}	-	correction for cooling capacity due to cycling of the heat rejection fan
ε_{QG}	-	correction for generator inflow energy due to cycling of the heat rejection fan
γ_{ON}	-	on/off cooling signal

Mathematical Description

Chiller cooling capacity and generator energy inflow are functions of $T_{g,i}$, T_{wb}, and $\dot{m}_g$. The following steady-state relations were empirically derived from operational data:

$$CAP_{ss} = 6.13 - 0.0218*(T_{g,i}-78.)^2 + 0.639*(T_{g,i}-78) - 0.149*(T_{wb}-16.) + 0.0013*(\dot{m}_g-881.) \quad \text{(B-1)}$$

$$Q_{g,ss} = 9.30 - 0.0217*(T_{g,i}-78.)^2 + 0.74*(T_{g,i}-78.) - 0.177*(T_{wb}-16.) + 0.0014*(\dot{m}_g-881.) \quad \text{(B-2)}$$

At chiller start-up, generator energy inflow begins immediately and rises exponentially according to:

$$\frac{Q_g}{Q_{g,ss}} = 1 - \exp\ (-t/\tau_{Q_g} \quad \text{(B-3)}$$

Cooling capacity is not produced in significant quantity during a brief period followed by an exponential rise described by:

$$\frac{CAP}{CAP_{ss}} = 1 - \exp\left[\min\begin{pmatrix} 0 \\ -(t-t_d)/\tau_{CAP} \end{pmatrix}\right] \quad \text{(B-4)}$$

where t_d is typically three and one-half minutes.

When the chiller is turned off by stopping hot water supply, it continues to operate for about four minutes at the steady-state cooling capacity for the prevailing operating conditions.

The heat rejection fan turns off when the condenser temperature falls below 27 C. This may occur when ambient wet bulb temperature is low and when hot water temperature and flow rate are low. The percent

of time the heat rejection fan is off during the timestep is determined by the following equation.

$$t_{OFF} = 0.235 - 0.109*(T_{g,i}-78.)-0.0115*(T_{wb}-16)^2 \\ -0.126*(T_{wb}-16.)-0.000104*(\dot{m}_g-881.) \\ (0 \leq t_{OFF} \leq .60) \tag{B-5}$$

The correction factors for CAP and Q_g are defined as follows:

$$\varepsilon Q_g = 1 - \frac{Q_g \text{ corrected}}{Q_g} \text{ and } \varepsilon_{CAP} = 1 - \frac{CAP_{corrected}}{CAP} \tag{B-6}$$

and are related to t_{OFF} by:

$$\varepsilon_{Q_g} = 0.712*t_{OFF} \tag{B-7}$$

$$\varepsilon_{CAP} = 0.00922*t_{OFF}^2 + 0.6238*t_{OFF} \tag{B-8}$$

TRNSYS Component Configuration

Parameter No.	Description
1	MODE - 1 - steady-state relations only 2 - transient start-up and shut-down
2	τ_{Q_g} - time constant of start-up curve for Q_g*
3	τ_{CAP} - time constant for start-up curve for CAP*
4	t_d - time delay before significant cooling capacity is produced.

*If τ_{Q_g}, CAP or t_d is less than zero then the measured value for the Arkla XWF-3600 is used. These are $\tau_{QG} = 0.05$, $\tau_{CAP} = 0.0888$, and $t_d = 0.0583$ hours.

Input No.	Description
1	$T_{g,i}$ - hot water supply temperature to the chiller (C)
2	$\dot{m}_g$ - mass flow rate of hot water (kg/hr)
3	T_{wb} - ambient outdoor wet bulb temperature (C)
4	γ_{ON} - chiller on/off signal

Output No.	Description
1	$T_{g,o}$ - hot water return temperature (C)
2	$\dot{m}_g$ - mass flow rate of hot water (kg/hr)
3	CAP - rate of cooling provided (kJ/hr)
4	Q_g - heat flow to generator (kJ/hr)
5	t_{OFF} - time heat rejection fan was off during timestep (hr).

Information Flow Diagram

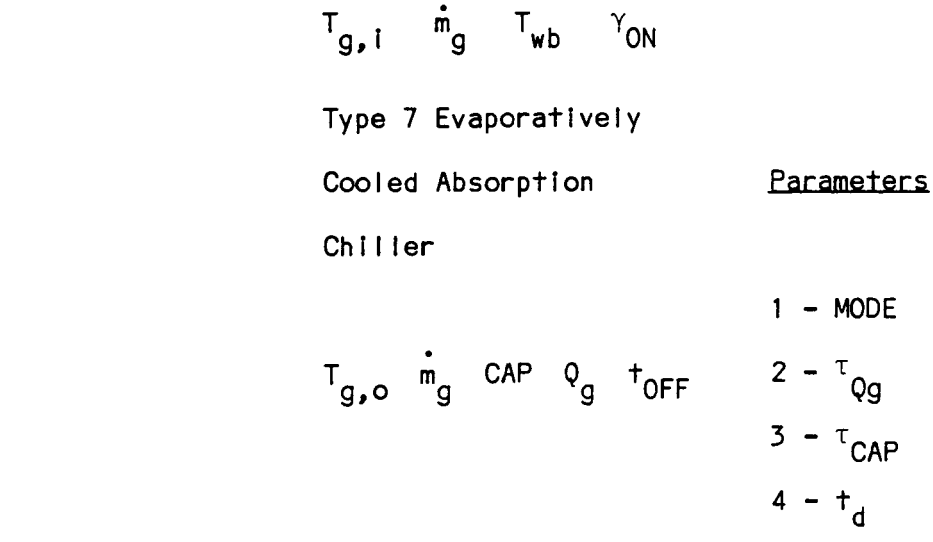

B-2. Validation of the Subroutine

To validate the model, the performance of the TRNSYS component was compared to that of the actual device. A simulation was run centered on the chiller. In the program, the temperatures and mass flow rates to the chiller were set to those measured in the performance of the actual system. The capacity and COP of the TRNSYS model were then compared to the measured capacity and COP.

The program was run with 1 hour time steps. The results are presented in Figures B-1 through B-4. The simulated performance compares to measured performance within about 1 kJ/hr for capacity and 0.01 for COP. Only periods of continuous operation were used for comparison with the internal controls of the chiller at nominal settings.

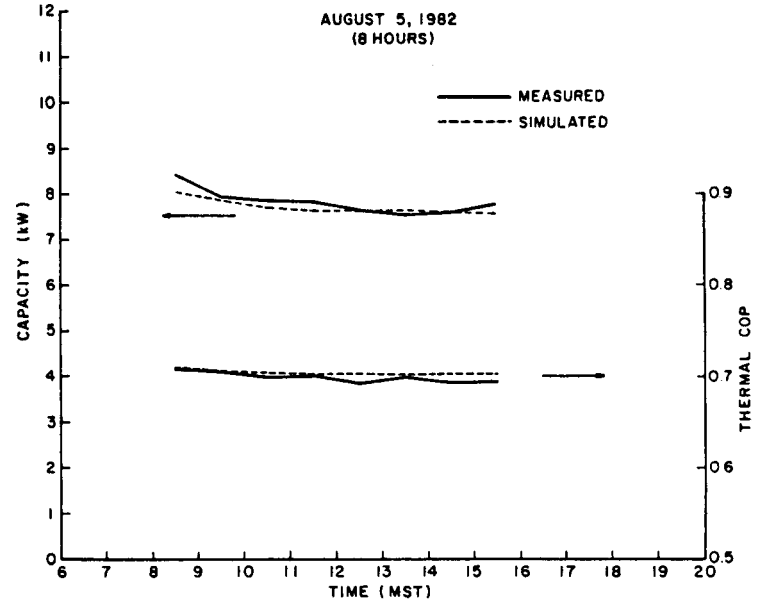

Figure B-1. Comparison of simulated and measured capacity and COP of the Arkla chiller.

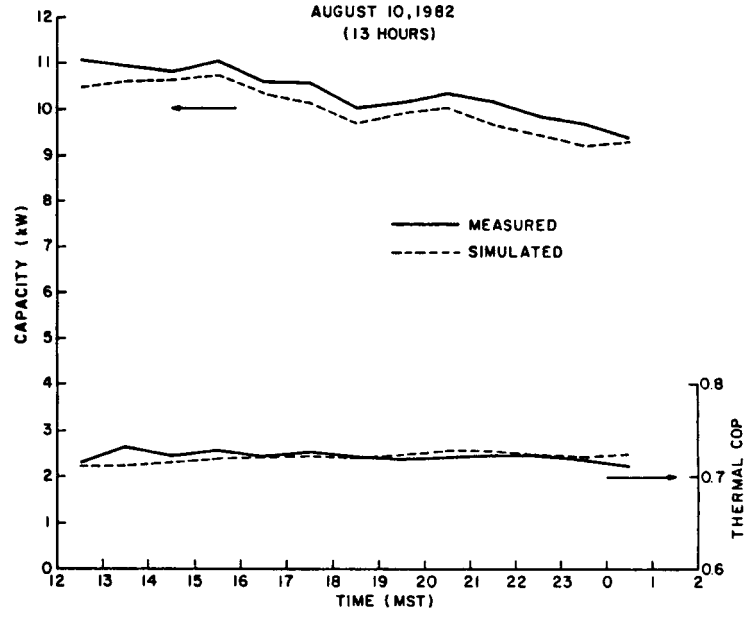

Figure B-2. Comparison of simulated and measured capacity and COP of the Arkla chiller.

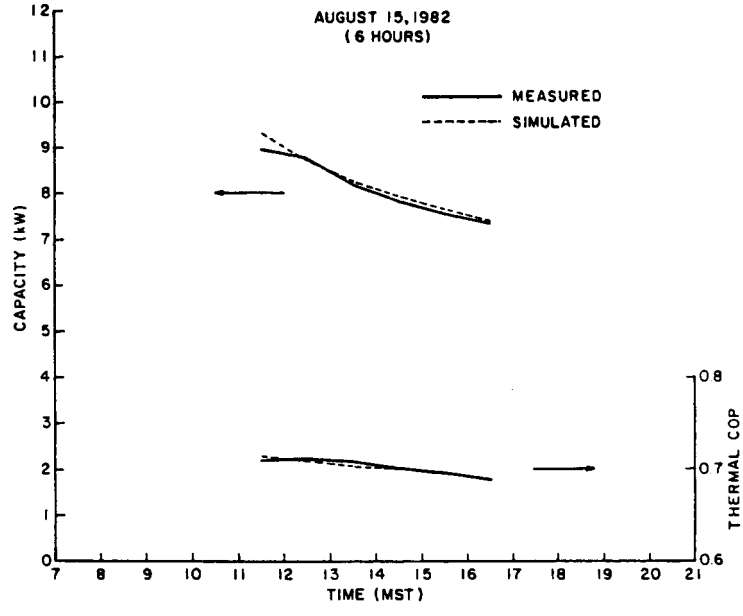

Figure B-3. Comparison of simulated and measured capacity and COP of the Arkla chiller.

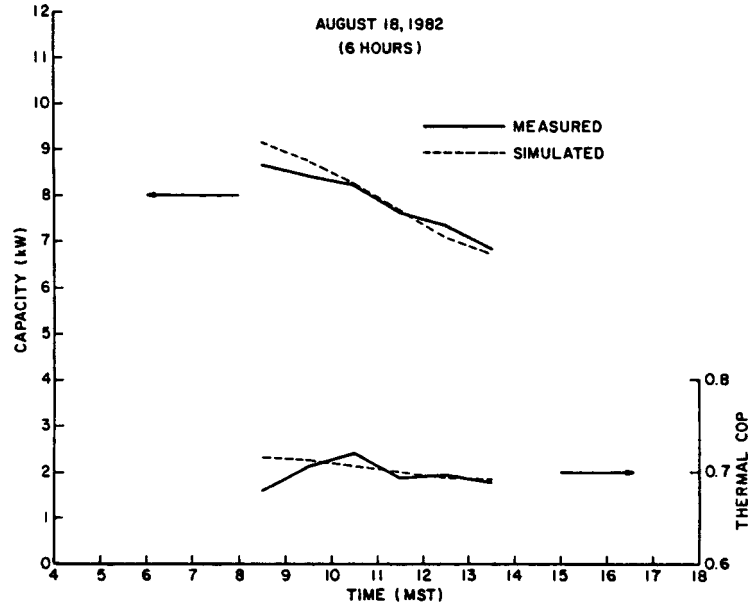

Figure B-4. Comparison of simulated and measured capacity and COP of the Arkla chiller.

Statistical displays of differences between measured and simulated chiller performance are shown on Figures B-5 and B-7 for energy flow to the generator, capacity and COP. The mean of the differences for capacity is 0.14 kJ/hr, standard deviation 1.03 kJ/hr with skewness slightly to the right. For Q_g the mean of the differences is -0.10 kJ/hr, standard deviation 1.21 kJ/hr with nearly normal distribution. The mean of the differences for COP is 0.008, standard deviation of 0.045 with skewness slightly to the left. The differences are considered small, and the simulation model is valid when compared to measured data.

The modeling of the transient performance of the chiller is presented in Section 7. There were insufficient data to perform an

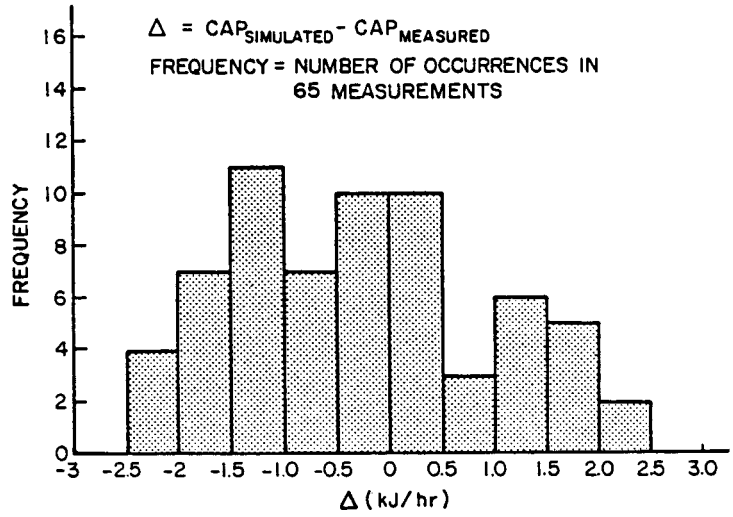

Figure B-5. Statistical distribution of differences between simulated and measured chiller capacities.

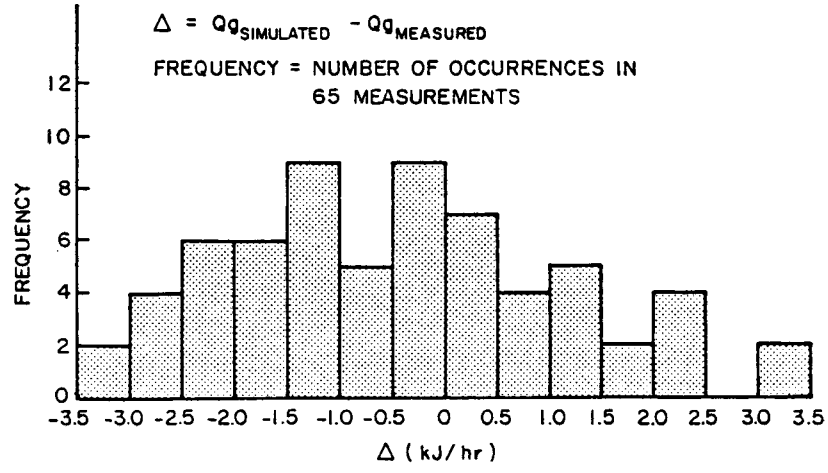

Figure B-6. Statistical distribution of differences between simulated and measured energy flows to the generator.

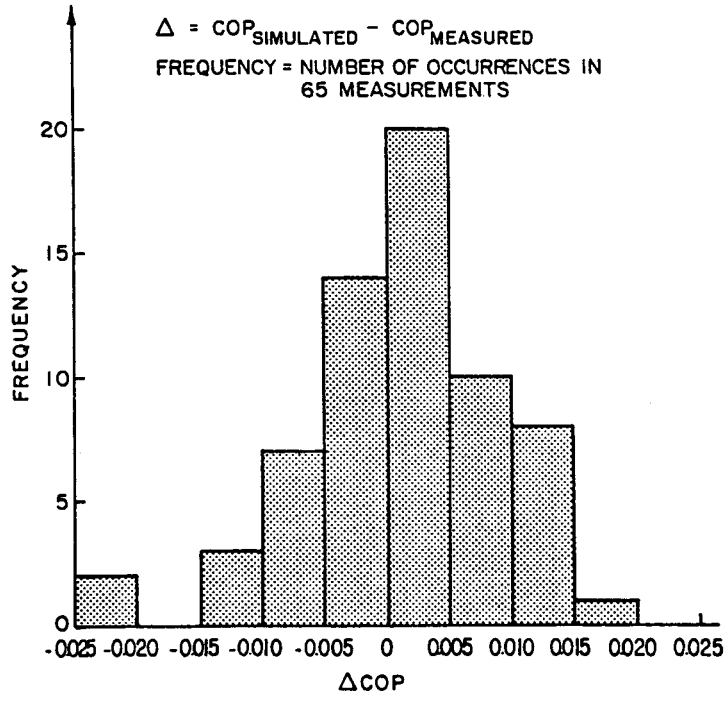

Figure B-7. Statistical distribution of differences between simulations and measurements for COP.

adequate comparison between simulated and measured results. Therefore, the chiller model is validated only for steady-state operations (MODE = 1).

B-3. Simulation Results of System Performance

The TMY data for the selected days of simulation for the four cities are provided in Tables B-1 through B-4. Mnemonics used for table headings are explained below:

Mnemonic	Description	Units
STATION	Weather station identification number	
MON	Month of year	
DAY	Day of month	
TIME	Solar time	
HRAD	Total radiation on horizontal	KJ/m^2
	("Standard year" corrected)	
TAMB	Ambient dry bulb temperature	C
TDP	Dew point temperature	C

Detailed results of TRNSYS simulations for Denver, CO, Phoenix, AZ, Washington, DC, and Miami, FL, appear in Tables B-5 through B-8. Mnemonics used for headings in those tables are listed below:

MNEMONICS

```
HT    -INSOLATION ON A TILTED SURFACE     (MJ/M2)
QU    -USEFUL ENERGY COLLECTED              (MJ)
QLD   -ENERGY SUPPLIED TO LOAD FROM STORAGE (MJ)
QTL   -ENERGY LOSSES FROM STORAGE           (MJ)
QDUMP-ENERGY DUMPED WHEN STO. IS AT 100 C   (MJ)
QCOOL-CHILLER CAPACITY                      (MJ)
QG    -ENERGY SUPPLIED TO CHILLER GENERATOR (MJ)
QSENS-SENSIBLE HEAT REMOVED FROM AIR        (MJ)
QLAT  -LATENT HEAD REMOVED FROM AIR         (MJ)
TAMB  -AMBIENT DRY BULB TEMPERATURE          (C)
TWB   -AMBIENT WET BULB TEMPERATURE          (C)
TSTO  -STORAGE TANK TEMPERATURE              (C)
TGI   -INLET TEMP. TO CHILLER GENERATOR      (C)
TGO   -OUTLET TEMP. FROM CHILLER GENERATOR   (C)
TSR   -RETURN TEMPERATURE CHILLER TO STORAGE (C)
TBP   -TEMP. OF WATER BYPASSED TO MIX VALVE  (C)
TRM   -ROOM TEMPERATURE                      (C)
DE    -CUMULATIVE CHANGE IN STORED ENERGY    (MJ)
MG    -MASS FLOW TO CHILLER GENERATOR     (KG/HR)
MSR   -MASS FLOW OF RETURN TO STORAGE     (KG/HR)
MB    -MASS FLOW BYPASSED TO MIXING VALVE(KG/HR)
GAM   -ON/OFF CONTROL FUNCTION TO CHILLER
CEFF  -COLLECTOR EFFICIENCY
COP   -THERMAL COEF. OF PERFORMANCE OF CHILLER
```

Table B-1. TMY Data for Denver, CO.

STATION	MON	DAY	TIME	HRAD	TAMB	TDP
23062	7	10	100	0.	22.2	6.1
23062	7	10	200	0.	20.6	6.7
23062	7	10	300	0.	20.6	6.1
23062	7	10	400	0.	19.4	5.6
23062	7	10	500	4.	18.3	6.7
23062	7	10	600	312.	20.0	6.7
23062	7	10	700	1035.	22.2	8.3
23062	7	10	800	1800.	25.0	8.3
23062	7	10	900	2434.	27.2	9.4
23062	7	10	1000	2979.	30.0	5.0
23062	7	10	1100	3284.	31.7	3.3
23062	7	10	1200	3407.	33.3	3.3
23062	7	10	1300	3242.	33.9	2.2
23062	7	10	1400	2353.	30.6	6.1
23062	7	10	1500	2102.	31.1	5.0
23062	7	10	1600	1385.	30.6	4.4
23062	7	10	1700	678.	26.7	7.2
23062	7	10	1800	389.	25.6	7.2
23062	7	10	1900	175.	25.6	7.8
23062	7	10	2000	2.	25.0	7.2
23062	7	10	2100	0.	23.9	8.9
23062	7	10	2200	0.	22.2	10.0
23062	7	10	2300	0.	21.1	10.6
23062	7	10	2400	0.	21.1	10.6

Table B-2. TMY Data for Phoenix, AZ.

STATION	MON	DAY	TIME	HRAD	TAMB	TDP
23183	7	1	100	0.	31.2	12.1
23183	7	1	200	0.	31.1	11.6
23183	7	1	300	0.	31.1	11.4
23183	7	1	400	0.	31.1	11.3
23183	7	1	500	0.	31.2	11.3
23183	7	1	600	68.	31.4	11.6
23183	7	1	700	633.	31.8	12.2
23183	7	1	800	1793.	32.2	12.8
23183	7	1	900	2571.	33.7	12.8
23183	7	1	1000	3171.	35.2	12.8
23183	7	1	1100	3553.	36.7	12.8
23183	7	1	1200	3731.	38.0	13.0
23183	7	1	1300	3738.	39.3	13.1
23183	7	1	1400	3559.	40.6	13.3
23183	7	1	1500	3174.	41.0	12.2
23183	7	1	1600	2569.	41.3	11.1
23183	7	1	1700	1786.	41.7	10.0
23183	7	1	1800	628.	40.4	8.3
23183	7	1	1900	71.	39.1	6.7
23183	7	1	2000	0.	37.8	5.0
23183	7	1	2100	0.	35.8	4.6
23183	7	1	2200	0.	33.7	4.3
23183	7	1	2300	0.	31.7	3.9
23183	7	1	2400	0.	30.9	4.6

Table B-3. TMY Data for Washington, DC.

STATION	MON	DAY	TIME	HRAD	TAMB	TDP
93734	7	3	100	0.	22.2	21.1
93734	7	3	200	0.	22.0	20.9
93734	7	3	300	0.	21.9	20.8
93734	7	3	400	0.	21.7	20.6
93734	7	3	500	0.	22.2	21.1
93734	7	3	600	81.	22.8	21.7
93734	7	3	700	323.	23.3	22.2
93734	7	3	800	672.	24.4	22.6
93734	7	3	900	1073.	25.6	22.9
93734	7	3	1000	1475.	26.7	23.3
93734	7	3	1100	2026.	28.4	23.3
93734	7	3	1200	2520.	30.0	23.3
93734	7	3	1300	2929.	31.7	23.3
93734	7	3	1400	2783.	31.7	22.9
93734	7	3	1500	2479.	31.7	22.6
93734	7	3	1600	2012.	31.7	22.2
93734	7	3	1700	1416.	29.7	22.4
93734	7	3	1800	773.	27.6	22.6
93734	7	3	1900	198.	25.6	22.8
93734	7	3	2000	0.	24.3	22.1
93734	7	3	2100	0.	23.0	21.3
93734	7	3	2200	0.	21.7	20.6
93734	7	3	2300	0.	21.5	20.4
93734	7	3	2400	0.	21.3	20.2

Table B-4. TMY Data for Miami, FL.

STATION	MON	DAY	TIME	HRAD	TAMB	TDP
12839	7	5	100	0.	23.9	22.8
12839	7	5	200	0.	23.3	22.8
12839	7	5	300	0.	23.3	22.8
12839	7	5	400	0.	23.3	22.8
12839	7	5	500	0.	22.8	22.2
12839	7	5	600	4.	23.3	22.8
12839	7	5	700	536.	25.6	23.3
12839	7	5	800	1341.	27.8	22.8
12839	7	5	900	1982.	28.3	22.8
12839	7	5	1000	2624.	29.4	22.8
12839	7	5	1100	3034.	30.0	22.8
12839	7	5	1200	3243.	30.0	23.3
12839	7	5	1300	3243.	31.7	20.6
12839	7	5	1400	2945.	31.7	20.6
12839	7	5	1500	2547.	31.7	21.1
12839	7	5	1600	1904.	31.7	21.7
12839	7	5	1700	1251.	31.1	22.2
12839	7	5	1800	607.	31.1	20.6
12839	7	5	1900	4.	29.4	22.8
12839	7	5	2000	0.	27.8	22.2
12839	7	5	2100	0.	26.7	22.2
12839	7	5	2200	0.	26.1	22.2
12839	7	5	2300	0.	25.0	22.8
12839	7	5	2400	0.	25.0	22.8

Table B-5. Detailed TRNSYS Results for Denver, CO.

HEAT FLOW AND TEMPERATURE SUMMARY

HOUR	HT	QU	QLD	QTL	QDUMP	QCOOL	QG	QSENS	QLAT	TAMB	TWB	TSTO	TGI	TGO	TSR	TRP	TRM
0.	0.00	0.00	0.00	2.35	0.00	0.00	0.00	0.00	0.00	23.0	13.3	75.0	0.0	0.0	0.0	0.0	23.5
1.	0.00	0.00	0.00	2.42	0.00	0.00	0.00	0.00	0.00	21.4	12.9	74.9	0.0	0.0	0.0	0.0	23.5
2.	0.00	0.00	0.00	2.45	0.00	0.00	0.00	0.00	0.00	20.6	12.6	74.8	0.0	0.0	0.0	0.0	23.6
3.	0.00	0.00	0.00	2.48	0.00	0.00	0.00	0.00	0.00	20.0	12.1	74.7	0.0	0.0	0.0	0.0	23.6
4.	0.00	0.00	0.00	2.52	0.00	0.00	0.00	0.00	0.00	18.9	11.8	74.5	0.0	0.0	0.0	0.0	23.6
5.	.05	0.00	0.00	2.50	0.00	0.00	0.00	0.00	0.00	19.2	12.1	74.4	0.0	0.0	0.0	0.0	23.6
6.	.18	0.00	0.00	2.41	0.00	0.00	0.00	0.00	0.00	21.1	13.2	74.3	0.0	0.0	0.0	0.0	23.6
7.	.28	0.00	0.00	2.29	0.00	0.00	0.00	0.00	0.00	23.6	14.5	74.2	0.0	0.0	0.0	0.0	23.7
8.	1.77	31.40	0.00	2.21	0.00	0.00	0.00	0.00	0.00	26.1	15.7	74.9	0.0	0.0	0.0	0.0	23.9
9.	2.56	67.79	38.39	2.17	0.00	-25.09	36.44	-20.07	-5.02	28.6	15.9	76.5	76.3	72.7	72.7	72.7	23.7
10.	3.04	89.82	44.57	2.15	0.00	-29.65	41.68	-23.72	-5.93	30.9	15.6	78.4	78.1	74.0	74.0	74.0	23.1
11.	3.27	99.69	51.01	2.18	0.00	-34.31	47.14	-27.44	-6.86	32.5	15.9	80.7	80.4	75.7	75.7	75.7	22.3
12.	3.16	92.31	0.00	2.29	0.00	0.00	0.00	0.00	0.00	33.6	16.1	84.3	0.0	0.0	0.0	0.0	22.2
13.	2.25	46.79	0.00	2.51	0.00	0.00	0.00	0.00	0.00	32.3	16.1	87.8	0.0	0.0	0.0	0.0	22.8
14.	1.98	31.02	0.00	2.66	0.00	0.00	0.00	0.00	0.00	30.9	16.1	89.7	0.0	0.0	0.0	0.0	23.4
15.	1.27	0.00	0.00	2.70	0.00	0.00	0.00	0.00	0.00	30.9	15.8	90.4	0.0	0.0	0.0	0.0	23.8
16.	.61	0.00	61.60	2.71	0.00	-44.03	59.39	-35.22	-8.81	28.7	15.4	88.5	87.1	81.2	81.2	81.2	23.4
17.	.35	0.00	0.00	2.75	0.00	0.00	0.00	0.00	0.00	26.2	15.0	86.8	0.0	0.0	0.0	0.0	22.8
18.	.16	0.00	0.00	2.77	0.00	0.00	0.00	0.00	0.00	25.6	14.9	86.7	0.0	0.0	0.0	0.0	23.1
19.	.00	0.00	0.00	2.77	0.00	0.00	0.00	0.00	0.00	25.3	14.8	86.5	0.0	0.0	0.0	0.0	23.4
20.	0.00	0.00	0.00	2.80	0.00	0.00	0.00	0.00	0.00	24.5	14.7	86.4	0.0	0.0	0.0	0.0	23.6
21.	0.00	0.00	0.00	2.86	0.00	0.00	0.00	0.00	0.00	23.1	14.8	86.2	0.0	0.0	0.0	0.0	23.7
22.	0.00	0.00	0.00	2.92	0.00	0.00	0.00	0.00	0.00	21.7	14.7	86.1	0.0	0.0	0.0	0.0	23.8
23.	0.00	0.00	0.00	2.93	0.00	0.00	0.00	0.00	0.00	21.1	14.7	85.9	0.0	0.0	0.0	0.0	23.9
24.	0.00	0.00	0.00	2.93	0.00	0.00	0.00	0.00	0.00	21.1	14.7	85.8	0.0	0.0	0.0	0.0	24.0
DAY	21.42	458.52	195.57	63.73	0.00	-133.08	184.65	-104.45	-26.62	25.2	14.5	81.5	80.4	75.9	75.9	75.9	23.4

CHANGE IN STORED ENERGY-FLOW RATES AND CONTROL FUNCTION

HOUR	DE	MG	MSR	MB	GAM
0	0.00	0.	0.	0.	0.
1.	-2.42	0.	0.	0.	0.
2.	-4.88	0.	0.	0.	0.
3.	-7.35	0.	0.	0.	0.
4.	-9.87	0.	0.	0.	0.
5.	-12.37	0.	0.	0.	0.
6.	-14.78	0.	0.	0.	0.
7.	-17.07	0.	0.	0.	0.
8.	-19.49	0.	0.	0.	0.
9.	39.54	2423.	2423.	0.	1.
10.	82.67	2423.	2423.	0.	1.
11.	129.20	2423.	2423.	0.	1.
12.	219.20	0.	0.	0.	0.
13.	241.00	0.	0.	0.	0.
14.	291.40	0.	0.	0.	0.
15.	288.60	0.	0.	0.	0.
16.	224.60	2423.	2032.	391.	1.
17.	221.60	0.	0.	0.	0.
18.	210.80	0.	0.	0.	0.
19.	216.00	0.	0.	0.	0.
20.	213.20	0.	0.	0.	0.
21.	210.40	0.	0.	0.	0.
22.	207.40	0.	0.	0.	0.
23.	204.60	0.	0.	0.	0.
24.	201.60	0.	0.	0.	0.

Table B-6. Detailed TRNSYS Results for Phoenix, AZ.

HEAT FLOW AND TEMPERATURE SUMMARY

HOUR	HT	QU	QLB	QTI	QDUMP	QCOOL	QG	QSENS	QLAT	TAMB	TWB	TSTO	TGI	TGO	TSR	TRP	TRM
0.	0.00	0.00	0.00	1.98	0.00	0.00	0.00	0.00	0.00	31.3	18.9	75.0	0.0	0.0	0.0	0.0	23.5
1.	0.00	0.00	0.00	1.98	0.00	0.00	0.00	0.00	0.00	31.2	18.7	75.0	0.0	0.0	0.0	0.0	23.7
2.	0.00	0.00	0.00	1.98	0.00	0.00	0.00	0.00	0.00	31.1	18.5	74.8	0.0	0.0	0.0	0.0	24.2
3.	0.00	0.00	0.00	1.98	0.00	0.00	0.00	0.00	0.00	31.1	18.4	74.7	0.0	0.0	0.0	0.0	24.6
4.	0.00	0.00	0.00	1.97	0.00	0.00	0.00	0.00	0.00	31.2	18.4	74.6	0.0	0.0	0.0	0.0	25.1
5.	0.00	0.00	0.00	1.96	0.00	0.00	0.00	0.00	0.00	31.3	18.5	74.5	0.0	0.0	0.0	0.0	25.5
6.	.11	0.00	0.00	1.94	0.00	0.00	0.00	0.00	0.00	31.6	18.8	74.4	0.0	0.0	0.0	0.0	25.9
7.	.80	0.00	0.00	1.92	0.00	0.00	0.00	0.00	0.00	32.0	19.2	74.3	0.0	0.0	0.0	0.0	26.3
8.	1.89	43.10	0.00	1.92	0.00	0.00	0.00	0.00	0.00	33.0	19.7	75.4	0.0	0.0	0.0	0.0	26.7
9.	3.49	78.41	39.85	1.95	0.00	-25.14	38.40	-20.11	-5.03	34.5	20.1	77.5	77.2	73.6	73.6	73.6	26.6
10.	4.21	101.10	46.25	1.99	0.00	-30.20	47.27	-24.16	-6.04	36.0	20.5	79.9	79.5	75.4	75.4	75.4	26.1
11.	3.48	111.90	53.14	2.06	0.00	-35.14	48.19	-28.11	-7.03	37.4	21.0	82.9	82.4	77.6	77.6	77.6	25.4
12.	3.54	112.80	58.18	2.13	0.00	-38.87	52.93	-31.10	-7.77	38.7	21.4	85.7	85.2	80.0	80.0	80.0	24.6
13.	3.37	104.00	54.49	2.19	0.00	-41.07	56.01	-32.86	-8.22	40.0	21.9	88.4	87.7	82.2	82.2	82.2	23.8
14.	2.97	84.68	50.00	2.25	0.00	-40.81	55.64	-32.65	-8.16	40.8	21.9	90.4	87.4	81.9	81.9	81.9	23.0
15.	2.34	55.84	51.98	2.27	0.00	-41.00	55.86	-32.80	-8.20	41.2	21.5	91.3	87.4	81.9	81.9	81.9	22.3
16.	1.52	20.87	0.00	2.28	0.00	0.00	0.00	0.00	0.00	41.5	21.2	91.8	0.0	0.0	0.0	0.0	22.5
17.	.54	0.00	0.00	2.32	0.00	0.00	0.00	0.00	0.00	41.1	20.6	92.2	0.0	0.0	0.0	0.0	23.4
18.	.07	0.00	55.81	2.30	0.00	-41.65	56.54	-33.32	-8.33	39.8	19.6	90.6	86.3	81.4	81.4	81.4	23.4
19.	0.00	0.00	63.30	2.21	0.00	-41.58	56.34	-33.27	-8.32	38.5	18.7	87.2	86.3	80.8	80.8	80.8	22.6
20.	0.00	0.00	0.00	2.21	0.00	0.00	0.00	0.00	0.00	36.8	17.8	85.6	0.0	0.0	0.0	0.0	22.6
21.	0.00	0.00	0.00	2.29	0.00	0.00	0.00	0.00	0.00	34.8	17.0	85.4	0.0	0.0	0.0	0.0	23.3
22.	0.00	0.00	0.00	2.38	0.00	0.00	0.00	0.00	0.00	32.7	16.2	85.3	0.0	0.0	0.0	0.0	23.8
23.	0.00	0.00	50.76	2.37	0.00	-40.50	54.72	-32.40	-8.10	31.3	15.8	83.7	83.7	78.7	78.7	78.7	23.5
24.	0.00	0.00	44.96	2.25	0.00	-36.56	49.84	-29.25	-7.31	31.3	15.8	81.1	81.5	76.6	76.6	76.6	22.5
DAY	26.59	712.72	568.72	53.06	0.00	-412.52	564.74	-330.03	-82.51	35.2	19.2	82.1	84.1	79.1	79.1	79.1	24.3

CHANGE IN STORED ENERGY,FLOW RATES AND CONTROL FUNCTION

HOUR	DE	MG	MSR	MR	GAM
0.	0.00	0.	0.	0.	0.
1.	1.98	0.	0.	0.	0.
2.	-3.76	0.	0.	0.	0.
3.	-5.94	0.	0.	0.	0.
4.	-7.91	0.	0.	0.	0.
5.	-9.86	0.	0.	0.	0.
6.	-11.80	0.	0.	0.	0.
7.	14.72	0.	0.	0.	0.
8.	27.45	0.	0.	0.	0.
9.	64.07	2423.	2423.	0.	1.
10.	117.00	2423.	2423.	0.	1.
11.	174.60	2423.	2423.	0.	1.
12.	226.10	2423.	2423.	0.	1.
13.	273.40	2423.	2114.	309.	1.
14.	305.90	2423.	1408.	1015.	1.
15.	307.50	2423.	1327.	1096.	1.
16.	226.10	0.	0.	0.	0.
17.	225.70	0.	0.	0.	0.
18.	265.40	2423.	1455.	968.	1.
19.	200.10	2423.	2361.	62.	1.
20.	192.90	0.	0.	0.	0.
21.	195.60	0.	0.	0.	0.
22.	193.20	0.	0.	0.	0.
23.	140.10	2423.	2423.	0.	1.
24.	91.90	2423.	2423.	0.	1.

Table B-7. Detailed TRNSYS Results for Washington, DC.

HEAT FLOW AND TEMPERATURE SUMMARY

HOUR	HT	QU	QLD	QTL	QDUMP	QCOOL	QG	QSENS	QLAT	TAMB	TWB	TSTO	TGI	TGO	TSP	TRP	TRM
0.	0.00	0.00	0.00	2.39	0.00	0.00	0.00	0.00	0.00	22.3	21.4	75.0	0.0	0.0	0.0	0.0	23.5
1.	0.00	0.00	0.00	2.39	0.00	0.00	0.00	0.00	0.00	22.1	21.2	74.9	0.0	0.0	0.0	0.0	23.6
2.	0.00	0.00	0.00	2.39	0.00	0.00	0.00	0.00	0.00	22.0	21.0	74.8	0.0	0.0	0.0	0.0	23.7
3.	0.00	0.00	0.00	2.39	0.00	0.00	0.00	0.00	0.00	21.8	20.9	74.7	0.0	0.0	0.0	0.0	23.7
4.	0.00	0.00	0.00	2.38	0.00	0.00	0.00	0.00	0.00	22.0	21.0	74.6	0.0	0.0	0.0	0.0	23.8
5.	.03	0.00	0.00	2.35	0.00	0.00	0.00	0.00	0.00	22.5	21.6	74.4	0.0	0.0	0.0	0.0	23.9
6.	.15	0.00	0.00	2.32	0.00	0.00	0.00	0.00	0.00	23.1	22.1	74.3	0.0	0.0	0.0	0.0	24.0
7.	.45	0.00	0.00	2.28	0.00	0.00	0.00	0.00	0.00	23.9	22.6	74.2	0.0	0.0	0.0	0.0	24.2
8.	.87	0.00	0.00	2.22	0.00	0.00	0.00	0.00	0.00	25.0	23.2	74.1	0.0	0.0	0.0	0.0	24.3
9.	1.29	10.64	0.00	2.18	0.00	0.00	0.00	0.00	0.00	26.2	23.8	74.2	0.0	0.0	0.0	0.0	24.5
10.	1.85	36.11	0.00	2.16	0.00	0.00	0.00	0.00	0.00	27.6	24.3	75.4	0.0	0.0	0.0	0.0	24.8
11.	2.37	59.72	34.64	2.16	0.00	-21.41	32.02	-14.99	-6.42	29.2	24.7	76.9	76.7	73.5	73.5	73.5	24.7
12.	2.81	79.36	39.01	2.16	0.00	-25.12	36.28	-17.58	-7.54	30.9	25.1	78.6	78.3	74.7	74.7	74.7	24.3
13.	3.64	71.97	43.21	2.20	0.00	-28.63	40.40	-20.04	-8.59	31.7	25.2	80.3	80.0	76.0	76.0	76.0	23.8
14.	2.34	56.55	50.72	2.24	0.00	-28.76	40.55	-20.13	-8.63	31.7	24.9	81.0	80.0	76.0	76.0	76.0	23.3
15.	1.85	34.75	47.36	2.22	0.00	-28.88	40.70	-20.22	-8.67	31.7	24.7	80.7	80.0	76.0	76.0	76.0	22.8
16.	1.25	8.23	35.26	2.21	0.00	-29.05	40.90	-20.34	-8.72	30.7	24.4	79.5	80.0	76.0	76.0	76.0	22.4
17.	.67	0.00	0.00	2.27	0.00	0.00	0.00	0.00	0.00	28.7	24.0	78.7	0.0	0.0	0.0	0.0	22.3
18.	.18	0.00	0.00	2.35	0.00	0.00	0.00	0.00	0.00	26.6	23.6	78.6	0.0	0.0	0.0	0.0	22.7
19.	0.00	0.00	0.00	2.42	0.00	0.00	0.00	0.00	0.00	25.0	23.0	78.5	0.0	0.0	0.0	0.0	23.0
20.	0.00	0.00	0.00	2.48	0.00	0.00	0.00	0.00	0.00	23.7	22.1	78.3	0.0	0.0	0.0	0.0	23.2
21.	0.00	0.00	0.00	2.53	0.00	0.00	0.00	0.00	0.00	22.4	21.2	78.2	0.0	0.0	0.0	0.0	23.3
22.	0.00	0.00	0.00	2.56	0.00	0.00	0.00	0.00	0.00	21.6	20.7	78.1	0.0	0.0	0.0	0.0	23.4
23.	0.00	0.00	0.00	2.56	0.00	0.00	0.00	0.00	0.00	21.4	20.5	77.9	0.0	0.0	0.0	0.0	23.5
24.	0.00	0.00	0.00	2.55	0.00	0.00	0.00	0.00	0.00	21.4	20.5	77.8	0.0	0.0	0.0	0.0	23.6
DAY	18.74	357.33	250.20	58.34	0.00	-161.85	230.85	-113.30	-48.56	25.4	22.7	76.9	79.2	75.4	75.4	75.4	23.6

CHANGE IN STORED ENERGY,FLOW RATES AND CONTROL FUNCTION

HOUR	DE	MG	MSR	MB	GAM
0.	0.00	0.	0.	0.	0.
1.	-2.39	0.	0.	0.	0.
2.	-4.79	0.	0.	0.	0.
3.	-7.18	0.	0.	0.	0.
4.	-9.56	0.	0.	0.	0.
5.	-11.91	0.	0.	0.	0.
6.	-14.23	0.	0.	0.	0.
7.	-16.51	0.	0.	0.	0.
8.	-18.73	0.	0.	0.	0.
9.	-10.27	0.	0.	0.	0.
10.	23.62	0.	0.	0.	0.
11.	46.59	2423.	2423.	0.	1.
12.	84.78	2423.	2423.	0.	1.
13.	111.30	2423.	2423.	0.	1.
14.	114.90	2423.	2423.	0.	1.
15.	100.10	2423.	2423.	0.	1.
16.	70.86	2423.	2423.	0.	1.
17.	48.60	0.	0.	0.	0.
18.	66.25	0.	0.	0.	0.
19.	63.82	0.	0.	0.	0.
20.	61.35	0.	0.	0.	0.
21.	58.82	0.	0.	0.	0.
22.	56.22	0.	0.	0.	0.
23.	53.71	0.	0.	0.	0.
24.	51.16	0.	0.	0.	0.

Table B-8. Detailed TRNSYS Results for Miami, FL.

HEAT FLOW AND TEMPERATURE SUMMARY

HOUR	HT	QU	QLD	QTL	QDUMP	QCOOL	QG	QSENS	QLAT	TAMB	TWB	TSTO	TGI	TGO	TGR	TRF	TEM
0.	0.00	0.00	0.00	2.30	0.00	0.00	0.00	0.00	0.00	24.2	21.0	75.0	0.0	0.0	0.0	0.0	24.5
1.	0.00	0.00	0.00	2.32	0.00	0.00	0.00	0.00	0.00	23.6	22.9	74.9	0.0	0.0	0.0	0.0	24.6
2.	0.00	0.00	0.00	2.33	0.00	0.00	0.00	0.00	0.00	23.3	22.8	74.8	0.0	0.0	0.0	0.0	24.7
3.	0.00	0.00	0.00	2.33	0.00	0.00	0.00	0.00	0.00	23.3	22.8	74.7	0.0	0.0	0.0	0.0	24.9
4.	0.00	0.00	0.00	2.33	0.00	0.00	0.00	0.00	0.00	23.1	22.5	74.6	0.0	0.0	0.0	0.0	24.0
5.	0.00	0.00	0.00	2.33	0.00	0.00	0.00	0.00	0.00	23.1	22.5	74.4	0.0	0.0	0.0	0.0	24.1
6.	.09	0.00	0.00	2.26	0.00	0.00	0.00	0.00	0.00	24.5	23.3	74.3	0.0	0.0	0.0	0.0	24.3
7.	.67	0.00	0.00	2.15	0.00	0.00	0.00	0.00	0.00	26.7	23.9	74.2	0.0	0.0	0.0	0.0	24.5
8.	1.51	21.94	0.00	2.11	0.00	0.00	0.00	0.00	0.00	28.1	24.0	74.7	0.0	0.0	0.0	0.0	24.8
9.	2.25	54.14	0.00	2.16	0.00	0.00	0.00	0.00	0.00	28.9	24.2	76.6	0.0	0.0	0.0	0.0	25.1
10.	2.74	74.77	42.03	2.23	0.00	-25.47	36.70	-17.83	-7.64	29.7	24.5	78.9	78.3	74.7	74.7	74.7	25.0
11.	3.00	85.15	44.93	2.29	0.00	-29.56	41.50	-20.69	-8.87	30.0	24.7	80.7	80.3	76.3	76.3	76.3	24.4
12.	3.04	85.77	49.21	2.34	0.00	-33.26	45.96	-23.28	-9.98	30.9	24.2	82.6	82.3	77.7	77.7	77.7	23.7
13.	2.77	73.04	51.56	2.37	0.00	-35.81	49.10	-25.07	-10.74	31.7	23.5	84.0	83.7	78.9	78.9	78.9	23.0
14.	2.48	55.26	55.44	2.38	0.00	-35.72	49.00	-25.01	-10.72	31.7	23.7	84.3	83.7	78.9	78.9	78.9	22.3
15.	1.77	26.93	0.00	2.41	0.00	0.00	0.00	0.00	0.00	31.7	24.0	84.9	0.0	0.0	0.0	0.0	22.2
16.	1.15	0.00	0.00	2.45	0.00	0.00	0.00	0.00	0.00	31.4	24.3	85.5	0.0	0.0	0.0	0.0	22.8
17.	.56	0.00	0.00	2.46	0.00	0.00	0.00	0.00	0.00	31.1	23.9	85.4	0.0	0.0	0.0	0.0	23.3
18.	.00	0.00	0.00	2.49	0.00	0.00	0.00	0.00	0.00	30.3	23.9	85.3	0.0	0.0	0.0	0.0	23.7
19.	0.00	0.00	47.08	2.50	0.00	-35.93	49.27	-25.15	-10.78	28.6	24.0	83.8	83.8	79.1	79.1	79.1	23.5
20.	0.00	0.00	41.00	2.45	0.00	-32.78	45.36	-22.95	-9.84	27.3	23.4	81.3	81.7	77.3	77.3	77.3	22.7
21.	0.00	0.00	0.00	2.44	0.00	0.00	0.00	0.00	0.00	26.4	23.2	80.2	0.0	0.0	0.0	0.0	22.4
22.	0.00	0.00	0.00	2.47	0.00	0.00	0.00	0.00	0.00	25.6	23.2	80.1	0.0	0.0	0.0	0.0	22.7
23.	0.00	0.00	0.00	2.49	0.00	0.00	0.00	0.00	0.00	25.0	23.2	79.9	0.0	0.0	0.0	0.0	23.0
24.	0.00	0.00	0.00	2.48	0.00	0.00	0.00	0.00	0.00	25.0	23.2	79.8	0.0	0.0	0.0	0.0	23.2
DAY	21.93	476.99	331.25	58.85	0.00	-228.53	316.89	-159.98	-68.56	27.4	23.5	79.4	82.0	77.6	77.6	77.6	23.6

CHANGE IN STORED ENERGY+FLOW RATES AND CONTROL FUNCTION

HOUR	DE	MG	MSR	MU	GAM
0.	0.00	0.	0.	0.	0.
1.	-2.32	0.	0.	0.	0.
2.	-4.66	0.	0.	0.	0.
3.	-6.98	0.	0.	0.	0.
4.	-9.31	0.	0.	0.	0.
5.	-11.64	0.	0.	0.	0.
6.	-14.90	0.	0.	0.	0.
7.	-16.05	0.	0.	0.	0.
8.	3.78	0.	0.	0.	0.
9.	55.25	0.	0.	0.	0.
10.	86.27	2423.	2423.	0.	1.
11.	124.70	2423.	2423.	0.	1.
12.	158.40	2423.	2423.	0.	1.
13.	177.50	2423.	2423.	0.	1.
14.	174.90	2423.	2423.	0.	1.
15.	199.50	0.	0.	0.	0.
16.	197.00	0.	0.	0.	0.
17.	194.60	0.	0.	0.	0.
18.	192.10	0.	0.	0.	0.
19.	142.50	2423.	2423.	0.	1.
20.	99.05	2423.	2423.	0.	1.
21.	96.62	0.	0.	0.	0.
22.	94.15	0.	0.	0.	0.
23.	91.66	0.	0.	0.	0.
24.	89.18	0.	0.	0.	0.